2022

The Impact of Formation and Fracture Properties Alternations on the Productivity of the Multi-stage Fractured Marcellus Shale Horizontal Wells.

Dalal Aldbayan
da0036@mix.wvu.edu

The Impact of Formation and Fracture Properties Alternations on the Productivity of the Multi-stage Fractured Marcellus Shale Horizontal Wells.

Dalal Aldbayan

Thesis submitted to the

Benjamin M. Statler College of Engineering and Mineral Resources at

West Virginia University

In partial fulfillment of the requirements for the degree of

Master of Science

In

Petroleum and Natural Gas Engineering

Mohamed El Sgher, Ph.D., Chair

Kashy Aminian, Ph.D.

Samuel Ameri, Ph.D.

Department of Petroleum and Natural Gas Engineering

Morgantown, West Virginia

November 22nd, 2022

Keywords: Marcellus Shale, Gas Production, Compaction, Natural Fractures, Hydraulic Fracture

ABSTRACT

The Impact of Formation and Fracture Properties Alternations on the Productivity of the Multi-stage Fractured Marcellus Shale Horizontal Wells

Dalal Aldbayan

As the reservoir deplete, the pore pressure decreases and the effective stress increases. The increase in the effective stress results in the formation compaction which can alter the formation and hydraulic fracture properties. This is particularly significant for a Marcellus shale horizontal well with multi-stage hydraulic fracture due to low Young's modulus and moderate Poisson's ratio of the Marcellus shale. The degree of the effective stress increase depends on the initial productivity of the well, which is influenced by the hydraulic fracture properties, formation properties, as well as the operating conditions. Therefore, it is necessary to couple the geomechanical and fluid flow simulations to accurately predict the gas production from a horizontal Marcellus Shale well with multi-stage fractures. The objective of this study was to investigate the impact of the formation mechanical properties (Young's modulus and Poisson's ratio), the hydraulic fracture properties (half-length, initial conductivity, and spacing), as well as operating conditions (wellbore pressure) on the productivity of a horizontal Marcellus Shale well with multi-stage fractures.

The advanced technical information available from the Marcellus Shale horizontal wells located at the Marcellus Shale Energy and Environment Laboratory (MSEEL) site provided an opportunity to investigate the impact of the shale compressibility on gas production. The core, well log, well test, completion, stimulation, and production data from the wells at the MSEEL site were utilized to estimate the shale mechanical and petrophysical properties as well as the hydraulic fracture characteristics. The results of the data analysis were then utilized to develop a reservoir model for a horizontal well completed in Marcellus Shale with multi-stage hydraulic fractures. A geomechanical (Mohr-Coulomb) module was coupled with reservoir model to determine the effective stress distribution and the formation compaction and its impact on the shale porosity. The impact of the shale compaction on the permeability for both matrix and fissure, and the conductivity of the hydraulic fractures were determined from the Marcellus shale core plug

analysis as well as the published measurements on the propped fracture conductivity in Marcellus shale and were incorporated in the reservoir model.

The inclusion of the compressibility impacts in the reservoir model provided a more realistic simulated production profile. The gas recovery was found to be negatively impacted by the formation compaction due to the increase in the effective stress. The reduction in the conductivity of the hydraulic fractures due to the compressibility impact was found to have the most adverse effect on the gas recovery. The compressibility impacts were found to be more severe during the early production due to higher production rates. Finally, the model was employed to investigate the impact of the formation's mechanical properties, hydraulic fracture properties, and the operating conditions on the gas recovery. The higher values of Young's modulus and Poisson's ratio can mitigate the compressibility impacts and lead to higher recovery. Conversely, the higher values of the fracture half-length as well as the closer fracture spacing will amplify the adverse impacts of the compressibility on the early gas recovery. However, the adverse impacts diminishes with time. The higher values of the initial hydraulic fracture conductivity can also mitigate the compressibility impacts

DEDICATION

"To my mother, father, sister, and brothers"

ACKNOWLEDGEMENTS

First and foremost, I would like to express my genuine gratitude and appreciation to my research advisor, and committee chair, ***Dr. Mohamed El Sgher***. He was dedicated to the great potential he saw within me and kept pushing me towards success, always. The guidance of *Dr. El Sgher* developed my character to become a better student, researcher, engineer, and a professional in the oil and gas industry from his passion to research and education. Throughout the consistent and priceless guidance, he ensured that I was on the right track, always. It was an honor working with him and grow under his supervision towards the completion of this thesis and the opportunities that opened to me.

I am delighted to express my sincere gratitude to ***Dr. Kashy Aminian***, the program coordinator for his valuable support throughout this journey which aided in improving the quality of this thesis and my performance as a graduate student. With the guidance, feedback, and knowledge I gained from Dr. Aminian in writing this thesis, it shaped me of who I am as a person dedicated to research today. In addition, my special gratitude toward ***Dr. Samuel Ameri*** who was the father-figure and his doors were always open to welcome me. I would like to thank the Department of Petroleum and Natural Gas engineering from my fellow graduate students and faculty for supporting me throughout this wonderful journey.

Lastly, special appreciation, gratitude, and thanks to my backbone, ***my family***. The unconditional support and love of my parents is what endured me to succeed and preserve towards the completion of this thesis. Thankful for my siblings for the constant support through the good and bad times. To my beloved aunt, ***Moudhi AlSanousi,*** may her soul rest in peace, who shaped me to the person I am today and saw me pursuing this degree since I was a little kid. Forever grateful for the support of ***my friends*** which aid in succeeding in the completion of this thesis. *I aspire to improve, learn, and develop as a person, always. Thank you.*

LIST OF FIGURES

LIST OF TABLES

LIST OF SYMBOLS / NOMENCLATURE

k_f: $fracture\ \ permeability, mD$

k: $formation\ permeability,$ mD

Ww_f: $Fracture\ Width,$ ft

X_f: $Fracture\ Half-length,$ $ft.$

F_{CD}: $Fracture\ Conductivity,$ $md-ft$

V_p: $Pore\ Volume,$ ft^3

V_b: $Bulk\ Vlume,$ ft^3

V_{b^0}: $Initial\ Bulk\ Volume,$ ft^3

ϕ: Angle of internal friction and

c cohesive strength of the material

μ*: Coefficient of friction

ν: $Poisson's\ Ratio$

E: $Young's\ Modulus,$ psi

σ: $Stress,$ psi

ε: $Strain,$ psi

σ': $effective\ stress,$ psi

$\emptyset^*$: $porosity,$ %

β: $volumetric\ thermal\ expansion\ coeffcint\ of\ the\ formation,$ $(\frac{1}{C})$

c_b: $Bulk\ compressibility,$ psi^{-1}

σ_m: $Mean\ Total\ Stress,$ psi

ko: $Measured\ permeability\ at\ confining\ pressure\ Po,$ mD

Po: $Lowest\ Confining\ pressure\ (net\ stress),$ psi

P: $Confining\ pressure\ (net\ stress),$ psi

CHAPTER 1
INTRODUCTION

The largest natural gas producing country from the unconventional reservoirs worldwide is the United States according to the records in 2021 (N. Sönnichsen, 2021). Most of the prolific shale gas production is from Marcellus shale located in the Appalachian Basin in the Northeast region. The Marcellus shale formation is the largest shale gas play in the U.S (American Petroleum Institute, API). A fine-grained sedimentary rock, with low porosity and ultra-low permeability, is what defines shale. Additionally, shale acts as both source rock and reservoir rock due to the consolidated clay-sized particles.

The complexity of the natural fracture propagation of this formation limited the resources for development. Recent studies showed that the application of horizontal drilling and hydraulic fracturing has enhanced the productivity of the reservoir to enhance production. The extraction of shale gas can be challenging due to the tight pore space. There are two states of gas storage in the formation. The free state of the gas is when it is stored in these pore spaces, whereas it reaches the adsorbed state when the organic material is stored.

The Marcellus shale represents a significant resource for the U.S. natural gas industry. Based on the studies and analyses, the global shale gas market is expecting a $68.61 billion growth (Shale Gas Global Market Report, 2022). The production from Marcellus shale causes the reservoir to undergo compaction. At the early stages of the production, significant drop in pressure occurs resulting in increase in the effective stress. The increase in the effective stress s results in a decrease in porosity and permeability both in the formation and hydraulic fracture.

Reservoir simulation and modeling has been the focus in the industry for the development of the unconventional reservoirs. . Most reservoir simulators lack the geomechanical component to account for the reservoir compaction accompanied by the changes in the effective stress (Settari, 2002). Furthermore, the impact the of the formation and fracture properties on the formation and fracture compressibility due to increased effective stress has not been fully investigated.. Coupling a reservoir simulator with a geomechanical module can provided the insights into the reservoir compaction and subsidence mechanism (Settari and Sen, 2008). This study focuses on evaluating the impact of the formation and fracture properties on the productivity of the multistage fractured Marcellus shale horizontal wells impacted by the formation and fracture compressibility due to increased effective stress.

(El Sgher et al., 2022) used the iterative geomechanical coupling to investigate the impact of effective stress increase on the productivity of the multistage fractured Marcellus shale horizontal wells. However, the previous studies did not focus on the impact of hydraulic fracture properties and stage spacing on the effective stress changes. It is therefore, important to evaluate how the formation mechanical properties (Young's modulus and Poisson's ratio), hydraulic fracture properties (half-length, initial conductivity, and stage spacing), and operating conditions (wellbore pressure) impact the magnitude of effective stress increase. As a result, evaluating the effective stress changes could lead to accurate prediction of the gas recovery from the Marcellus shale. Therefore, it is essential to couple the reservoir simulator with a geomechanics module to predict the productivity of the unconventional well.

CHAPTER 2
LITERATURE REVIEW

2.1 UNCONVENTIONAL RESERVOIRS

The United States of America is the world's largest leading producer of natural gas as of 2022, with a production rate of 934 billion cubic meters (Sönnichsen, 2022). In 1821, the first extraction of natural gas took place in Fredonia, New York, by William Hart (American Public Gas Association, n.d.). Unconventional reservoirs refer to as ultra-light source rock containing high organic matter reaching thermal maturity without migration (SEG wiki, 2018).

Over the past decades, the exploration of unconventional reservoirs has been enhanced by the application of several techniques such as directional drilling which is the most applicable for shale formations as well as hydraulic fracturing. In fact, (Figure 1) illustrates the consumption of natural gas in the U.S. as well as dry production which is the highest with the net import declining due to the pandemic in 2020 (EIA reports, 2022).

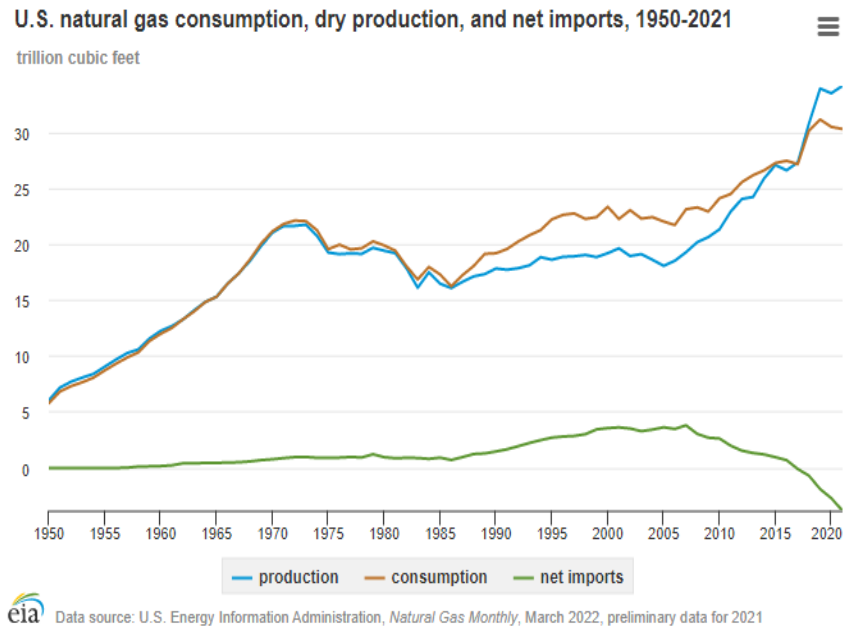

Figure 1: U.S natural gas consumption, production, and net imports 1950-2021 (EIA reports, 2022)

Production from shale gas formations has been increasing dramatically over the decades and will continue due to the availability of modern technologies and techniques to enhance the exploration of natural gas. The below figure (Figure 2) illustrates that the production of shale gas

accounts for 70% of the total U.S. production which enhanced the natural gas industry's economy by 9% until this day (EIA reports, 2019).

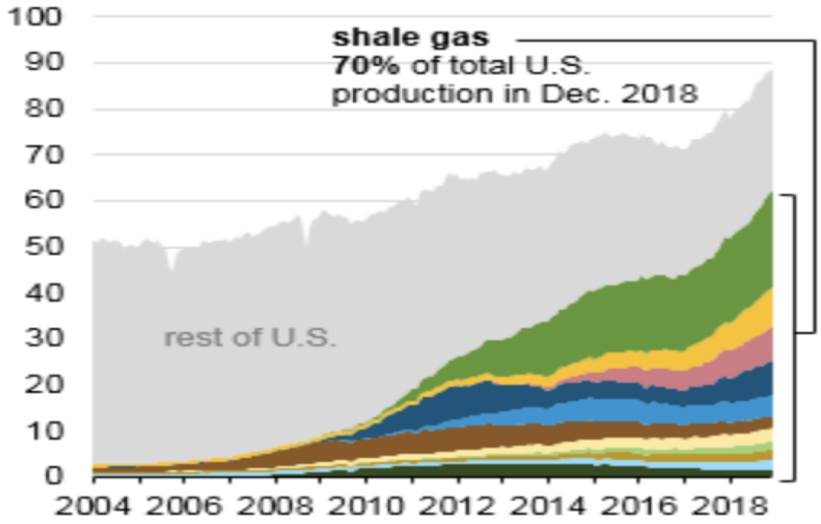

Figure 2: The production of shale gas in the U.S. (EIA reports, 2019)

2.2 MARCELLUS SHALE

In the United States, the largest shale play is Marcellus shale covering a total geologic area of 95,000 square miles (American Petroleum Institute, API). shale plays which are known as the largest deposits of natural gas in the U.S. are present in the Permian Basin. The largest natural gas-producing play in the U.S. is the Marcellus Shale which is located in the Appalachian Basin. The Marcellus shale formation extends to six states including New York, Pennsylvania, Ohio, West Virginia, Maryland, and Virginia (Institute of Energy Research, n.d.). Marcellus shale is often referred to as an abundant fine-grained sedimentary rock created by compaction of both silt and clay-size mineral particles with the flexibility of folding into thin layers (King, n.d.). The figure below (Figure 3) shows the Marcellus shale formation on the U.S. map extending from New York to West Virginia.

Figure 3: Marcellus Shale formation location on the map (Bentek, 2015)

In fact, the 400-year-old Marcellus shale formation is one of the largest nationwide, yet it represents the highest producing fields of natural gas in the United States. In December 2021, the natural gas production in the US has increased to 118.8 billion cubic feet where the Appalachia region recorded the highest percentage of 31% from the total of 41% share of the US (EIA reports, 2022). With modern techniques used in the exploration of natural gas i.e., hydraulic fracturing and horizontal drilling, Marcellus shale contains roughly 400 trillion cubic feet of gas which shifted the focus of the oil and gas industry in the US on this formation (EIA reports, 2021). Marcellus shale has specific characteristics from the Middle Devonian age that is black, with low density, less than 10% porosity, and ultra-low permeability. It is a type of sedimentary rock which act as both source rock and reservoir rock. Since the first well was drilled in Marcellus shale in 2003 (Institute of Energy Research, n.d.), the production has increased rapidly over the years with a natural gas extraction of over 6 billion cubic feet per day (Worldwide power products, n.d.)

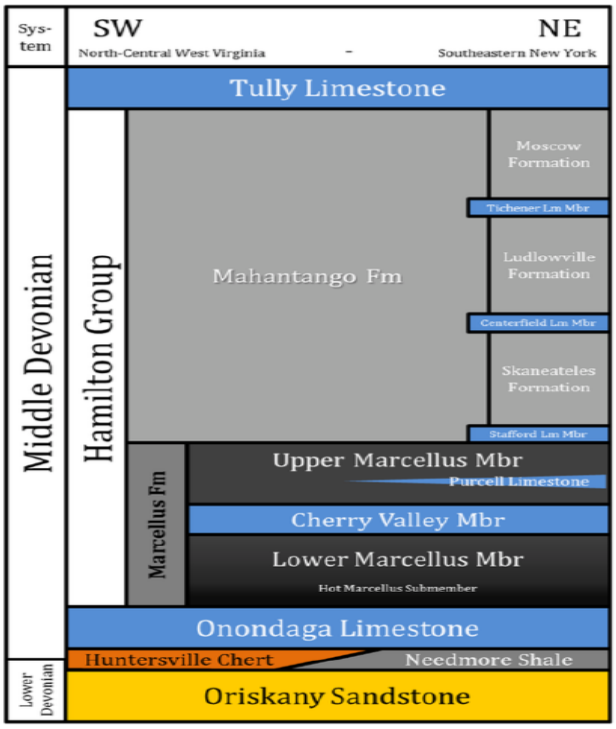

Figure 4: A stratigraphy of the Marcellus shale extending from North-Central West Virginia to Southeastern New York (Modified from Carter et al., 2011 and Zagorski et al., 2012).

The above figure (Figure 4), illustrates the formations present in the Middle Devonian located in the Appalachian Basin. The lower part of the Hamilton group consists of the Marcellus formation. The upper Marcellus Oatka Creek shale contains Purcell limestone and is bounded by the Mahantango formation. Additionally, the lower Marcellus Spring shale is thicker and bounded by the Onondaga limestone. Cherry Valley slightly separates the two members of the Marcellus shale formation i.e. upper and lower.

2.3 HYDRAULIC FRACTURING

One of the most important techniques for the exploration of natural gas in the industry is hydraulic fracturing. Hydraulic fracturing is used to optimize production with being cost-efficient and safe for the environment. In March 1949, the first application of a commercial hydraulic fracturing job on an oil well took place in Duncan, Oklahoma (wells, n.d.). The job was operated by experts from a collaboration of production petroleum teams. Additionally, leading companies i.e. Halliburton and Stanolind, which are operating companies fractured the second well in Holliday, Texas (wells, n.d.). The figure below (Figure 5) shows the first hydraulic fracturing job in the U.S. which took place in 1949.

Figure 5: The first commercial Hydraulic fracturing job on an oil well, 1949, (wells, n.d.)

Hydraulic fracturing has been applied for decades ago specifically on both oil and gas wells in unconventional reservoirs. These reservoirs are low in permeability and porosity which limits the fluid flow through the formation. This technique requires fluids to be pumped at very high pressures into the reservoir. Additionally, it targets the existing natural fractures to be enhanced to create more fractures in the formation. The fluid being pumped consists of water, acids, and proppant which varies in size depending on the formation characteristics. Having the fluid present in the fracture help keep it open until the treatment is completed. As a result, the net stress increases which leads to compaction in the reservoir to produce from the formation. The application hydraulic fracturing technique for shale gas reservoirs occurs in multiple phases represented by the figure below (Figure 6).

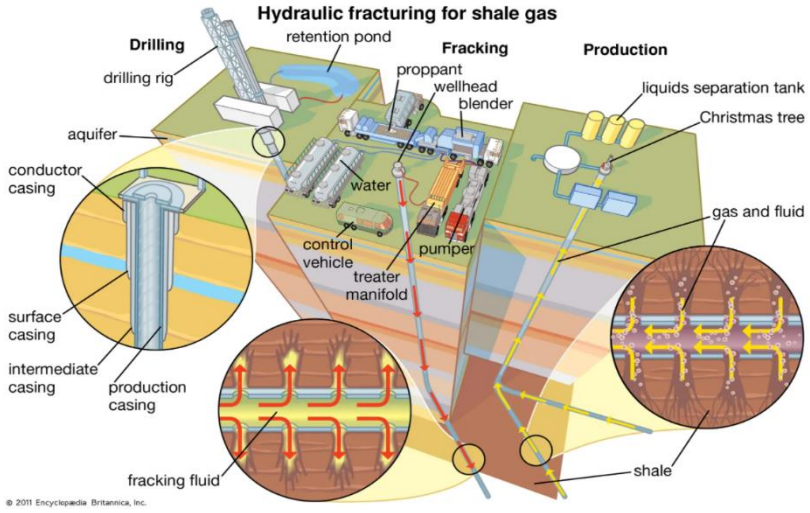

Figure 6: Hydraulic fracturing stages for a shale gas reservoir, (fracking | Definition, Environmental Concerns, & Facts, n.d.)

The evolution of technology-enhanced the application of hydraulic fracturing in the US. This led researchers to improve their studies on reservoir simulation modeling techniques. The development of Hydraulic fracturing depends on understanding the reservoir characteristics and studying the geomechanical effect with a higher impact on the formation. Predicting the production of a Marcellus shale well requires parametric studies and an enhanced understanding of the reservoir fluid flow to optimize productivity. (El Sgher et al., 2022) states that with the increase of compaction and subsidence, the length of hydraulic fractures increases. One of the limitations of the hydraulic fracturing process is the complexity of fracture network propagation. As a result, a correlation between firsthand pumping schedule data and reservoir performance is coupled to incorporate the fracking process (Zhan et al., 2016). Additionally, the application of this technique requires domain expertise in reservoir engineering. Despite the main aim of using hydraulic fracturing i.e. extracting unconventional oil and gas. It aids in increasing the injection rates during the sequestration of CO2, stimulates groundwater wells, and generates electricity in the geothermal systems (Hydraulic fracturing - Wikipedia, n.d.).

2.4 PRINCIPAL STRESSES IN THE FORMATION

Subsurface stresses include minimum horizontal stress, maximum horizontal stress, and overburden stress. Stresses acting horizontally perpendicular to the overburden stress are known as minimum horizontal stress and maximum horizontal stress. Fracture propagation and orientation are controlled by these three principal stresses. The greatest, intermediate, and least stresses are defined as σ1, σ2, and σ3, respectively. Due to historical tectonic movements, the three principal stresses are not always aligned in the same direction. Normal faults, strike-slip faults, and thrust faults are illustrated in (Figure 7). When it comes to normal faults, the vertical stress is the highest, when it comes to strike-slip faults, it is the most intermediate, while when it comes to thrust faults, and it is the lowest.

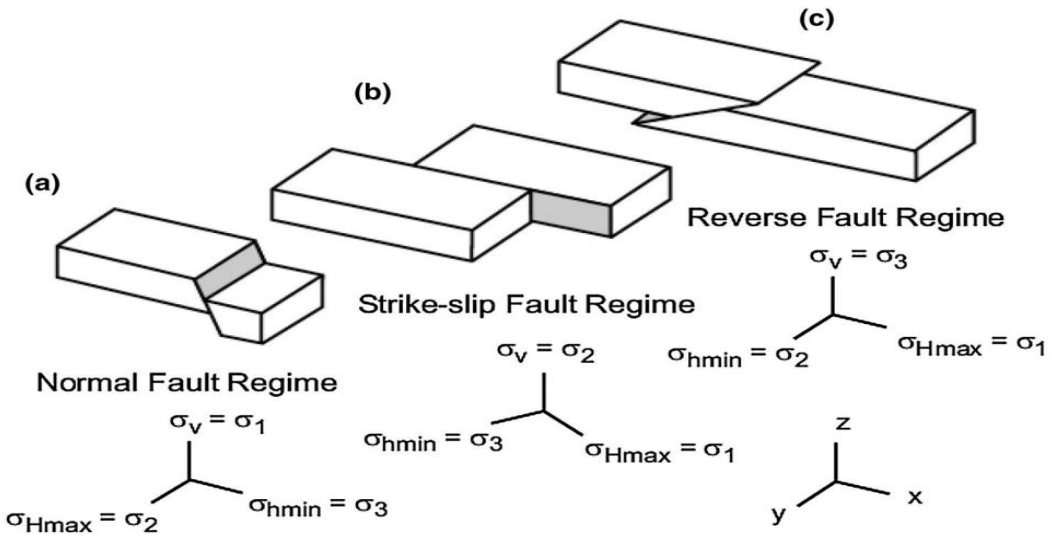

Figure 7: Different types of faults due to stress orientations (Jalili et al., 2017)

Understanding the relationship between principal stress and the lateral direction can optimize productivity, reserves, and economics for horizontal wells (Yang et al., 2016). The figure above (Figure 7) illustrates how stress can occur in different directions. Both horizontal stresses are occurring in opposite directions whilst the overburden stress is applied vertically above them. Furthermore, when stress is present in the formation it could lead to major fractures paired with stress correlation. Longitudinal fractures occur when the wellbore is drilled parallel with the horizontal maximum stress $\sigma_{h,max}$. On the other hand, transverse fractures occur when the wellbore is drilled perpendicular to the horizontal minimum stress$\sigma_{h,min}$.

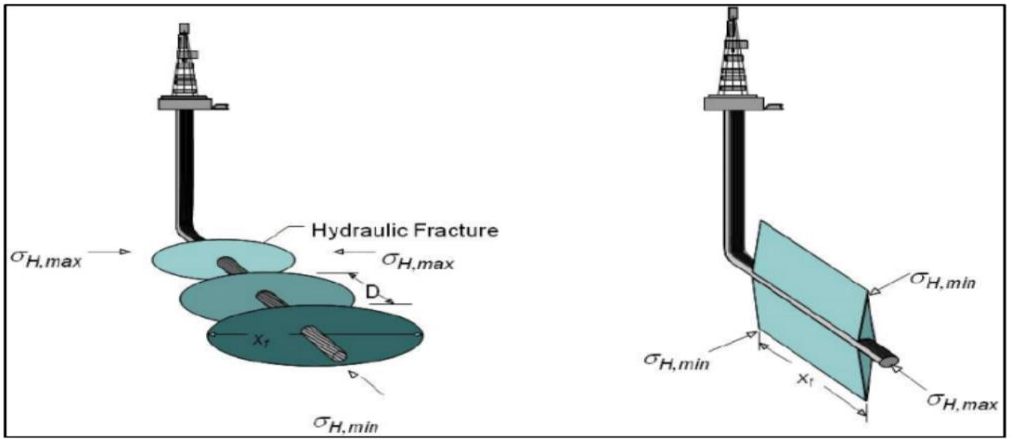

Figure 8: Longitudinal and transverse fracture overview (M.J. Economides, 2010)

2.5 RESERVOIR COMPACTION AND SUBSIDENCE

In the field of reservoir engineering, it has been highlighted that the act of compaction and subsidence are crucial phenomena for reservoir development. Reservoir compaction can induce the gas recovery from wells and indicate multiple field operational problems such as well failure. During reservoir compaction, pressure depletes causing an increase in the effective stress in the formation. Under these conditions, pore pressure decreases causing the overburden pressure to remain constant. As a result, a reduction in both porosity and permeability occurs leading the fluid to flow through the formation to produce (El Sgher et al., 2022).

Reservoir Compaction is often accompanied by the understanding of the main reservoir characteristics which are the foundation of reservoir engineering. Compaction depends on the depletion, reservoir thickness, and compaction coefficient (Settari, 2002). As a result, further analysis, prediction of production, and reservoir numerical modeling can be identified (Settari, 2002). The inclusion of parametric studies and research on the geomechanical impact on the productivity of the wells is led by compaction. The main drive of energy of the reservoir whether it was in the stimulated reservoir volume (SRV) or outside is the compaction which takes accountability for roughly 50-80% of the total energy (Settari, 2002). Furthermore, compaction occurs when the overall rock compressive strength exceeds the ability. Thus, it causes plastic deformation which is one of the important mechanical rock properties that is irreversible leading to again, the reduction of permeability and porosity due to these volumetric behaviors. The figure below (Figure 9) provides an overview of the reservoir during compaction.

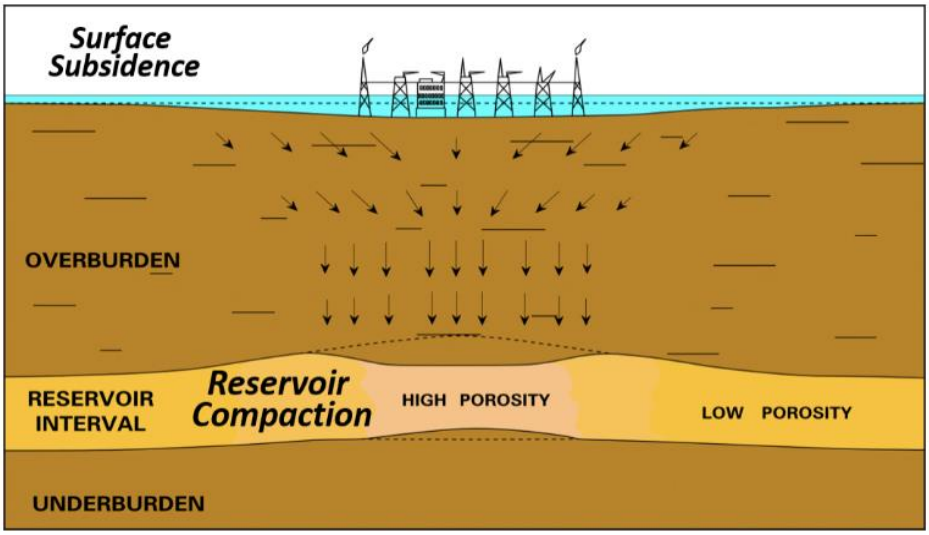

Figure 9: Reservoir compaction mechanism in the reservoir (Reservoir Compaction & Subsidence, n.d.)

On the other hand, reservoir compaction can increase the development costs of a certain project which leads to barriers to acceptance by the field development team. Also, over-estimation or under-estimation could lead to uncertainties. Thus, there is always a need to monitor, engineer, and screen for the pressure draw-down test which often occurs during the early life of the well when drilling starts (A. Settari, 2002). Besides having this phenomenon enhance the productivity of the well, providing the overall total energy in the reservoir, and most importantly, improving the reservoir gas recovery it could extend to potential critical problems such as well failure. Subsidence is a vertical downward movement in the reservoir due to the changes occurring to the formation mainly the deformation of the rocks during compaction.

Subsidence is a vertical downward movement in the reservoir due to the changes occurring to the formation mainly the deformation of the rocks during compaction. One of the major well failure problems that occurred due to subsidence was for the Wilmington oil field in California as well as the Ekofisk field in the North Sea (Wilmington Oil Field – Wikipedia, n.d.). Mainly, large volumes of oil leaked caused a pressure drop, and subsidence occurred at a depth of 9 meters. Ekofisk field sank by 1984 by more than a total of 3.5 meters resulting in extensive repairs and work to overcome in the Long Beach region. Financial risks of $1 billion resulted in almost losing the third largest oil field in the U.S. with cumulative production of 2,750 million barrels per day in 2008 (Wilmington Oil Field – Wikipedia, n.d.). After these incidents have occurred in both fields, researchers in the industry have been focusing more on the impact of geomechanical effects as well as parametric studies on the reservoir characteristics by focusing on the understanding of deformations. As a result, a dramatic decrease in limiting well failure led to an increase the field development management, consequently, observing better results of the reservoir modeling and improving other technologies associated with this matter for a better environment. The figure below (Figure 10) shows the remedial work done to overcome the damages done by subsidence in Long Beach, CA.

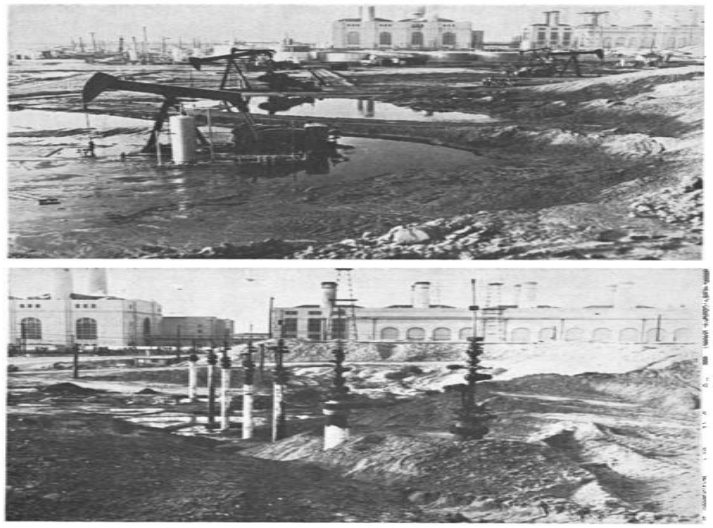

Figure 10: Remedial work near the Long Beach, CA area, (Pierce, 1970).

2.6 FORMATION (ROCK) MECHANICAL PROPERTIES

2.6.1 YOUNG's MODULUS

One of the important rock mechanical properties is acknowledging the importance of geomechanical impacts and how it would react in response to the changes being applied to it. The Young's Modulus is an elastic constant that represents the ratio between two measurements, the longitudinal stress to the strain which is usually a theoretical approach to predict the mechanical properties of the reservoir. This constant (E) is named after Thomas Young who is a British scientist who specialized in many fields such as solid mechanics, light, and energy (Thomas Young, Wikipedia, n.d.). Researchers have shown years ago, methods to optimize fracture design treatments by differentiating between elastic and dynamic testing. (Lacy, 1997) suggested that the stiffness ratio of the rock should be estimated. Additionally, his study conducted an approach to reduce 60 to 80% of the total time to contribute toward the effectiveness of the optimization process by using dynamic testing instead of static testing. The figure below (Figure 11) illustrates the relationship between the stress and strain changes which aid in the calculation of Young's modulus.

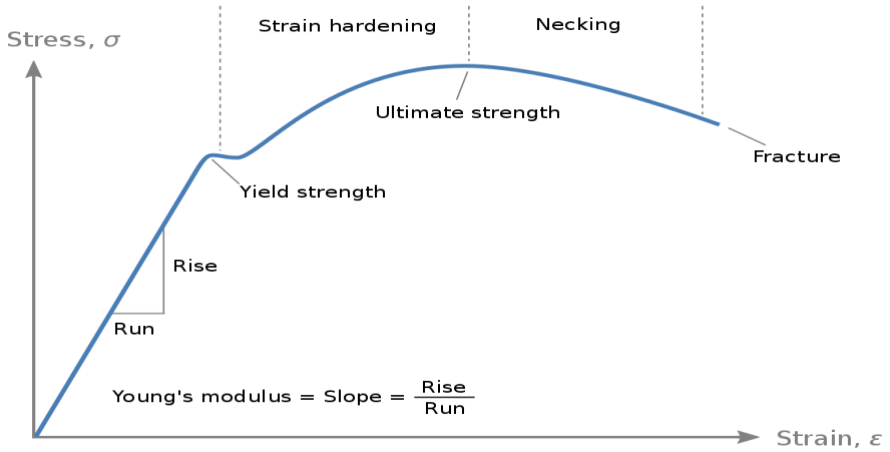

Figure 11: Relationship between stress and strain, (Stress-strain curve - Nicoguaro, n.d.)

Mathematically, Young's modulus can be represented by the following formula.

$$E = \frac{\sigma}{\varepsilon} = \frac{F/A}{\Delta L/L_0} \qquad Equation\ (1)$$

If Young's modulus is low, the solid is considered elastic whereas a stiff or inelastic material would have a high Young's modulus. Therefore, Young's modulus helps to differentiate the elasticity of the materials.

2.6.2 POISSON's RATIO

Poisson's ratio, introduced by a French mathematician (Simeon Poisson 1781-1840), is another major elastic constant that measures the compressibility of a specific material (Simeon Poisson, Wikipedia, n.d.). Poisson's ratio is defined as the ratio of the lateral strain to the longitudinal strain.

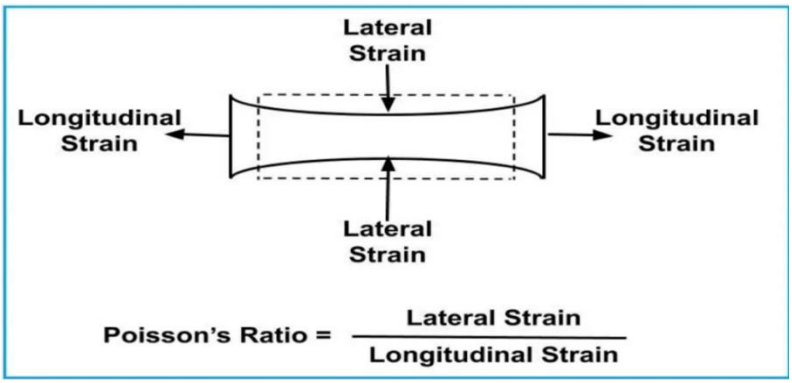

Figure 12: A schematic of the Poisson's ratio mechanism (Dey, n.d.)

The Poisson's ratio has been often accompanied by Young's modulus to represent the mechanical rock properties based on the stress applied as a force to cause the deformation. The equation below (Equation 2) illustrates the formula used for Poisson's ratio such that the axial (Longitudinal) strain is a function of change in length, whereas the lateral (Transverse) strain is a function of change in diameter.

$$\nu = \frac{\varepsilon_{lateral,x}}{\varepsilon_{longitudinal,y}} = \frac{\Delta D / D_o}{\Delta L / L_o} \qquad Equation\ (2)$$

In addition, the values of Poisson's ratio are generally ranging between 0.0 and 0.5 depending on the material's characteristics, if it was anisotropic, it would be greater than 1.0 (Dey, n.d.). The importance of Poisson's ratio relies on the impact of stress on a specific orientation of the rock. Such that, it could lead to permanent, irreversible, changes in the formation. Observing these changes can help with the design optimization of the pipes before drilling to limit the risks of well failure.

2.6.3 STRAIN AND DISPLACEMENT

In the field of reservoir engineering, the importance of understanding strain and displacement has been the main focus for well development. Such that, when the rock deforms due to compaction, both physical and chemical changes occur. Strain and displacement are key parameters used in iterative coupling which is a form of reservoir simulation modeling approach. Strain is observed when high stress is applied to a surface or material causing an irreversible, permanent, deformation. This external force applied leads to a reduction in the overall volume of the material (Strain – Schlumberger Oilfield Glossary, n.d.). In addition, the changes created by strain enhance the development of fractures to optimize the overall well performance. Furthermore, there are three main types of strain:

1- Brittle Deformation.
2- Ductile Deformation
3- Elastic Deformation.

In fact, Pressure, temperature, and mineral composition of the formation are key indicators of which type of deformation will occur based on the stress orientation and the rock's response (Stress and Strain – Rock Deformation, n.d.). The figure below (Figure 13) shows the

different types of deformation the rock undergoes. Firstly, brittle deformation occurs if the stress applied to the rock is greater than the rock's yield strength leads to creating a fracture in the rock. Secondly, ductile deformation occurs under high temperatures and in deep regions of the earth's surface. Since the temperature is high, it is possible to soften the rock and make it less brittle to respond to the stress. In this case, it could cause plastic deformation when the stress applied is greatly higher than the rock's yield strength which often causes the rock to flow. Lastly, elastic deformation occurs when the stress is less than the rock's yield strength, but it differs from the previous types because the deformation is reversible, not permanent.

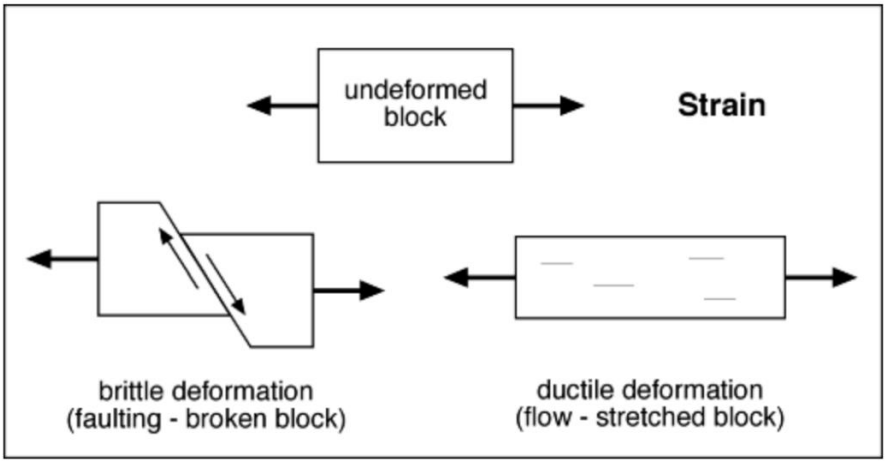

Figure 13: Deformation of the rock due to strain (Stress and Strain – Rock Deformation, n.d.)

Theoretically, strain is a function of the change in length of a block of solid material to the initial length of that block as shown in the equation below:

$$\varepsilon = \frac{\Delta L}{L_0} \qquad Equation\ (4)$$

The strain-displacement relationship is illustrated in the below schematic (Figure 14). From the figure, A and B can be assumed as vectors with stress being applied causing deformation to occur. The displacement from point A to B can be expressed as x to x + Δ x in the x-direction while leaving the y-direction constant (Kelly, PA). The displacement function can be expressed as normal strain (deformation of a line) in the equation below:

$$\varepsilon_{xx} = \frac{A'B^* - AB}{AB} = \frac{u_x(x + \Delta x, y) - u_x(x, y)}{\Delta x} \qquad Equation\ (5)$$

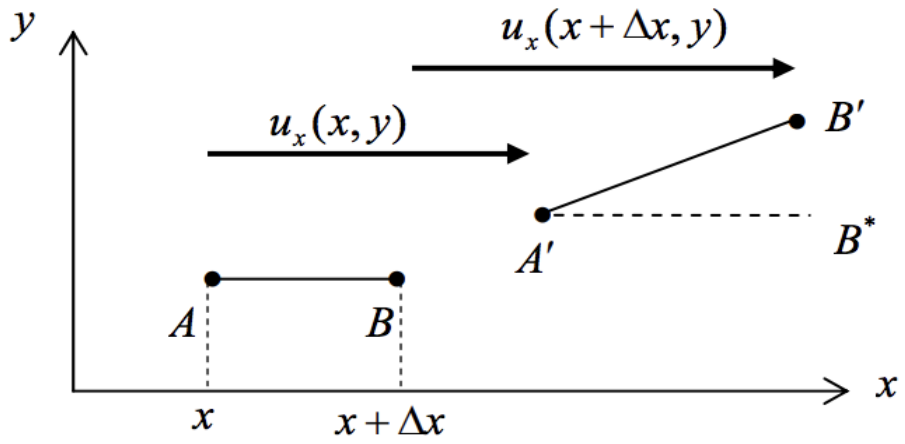

Figure 14: Schematic of the displacement function as a normal strain deformation, (Kelly, PA).

2.6.4 ROCK DEFORMATION

Generally, when any form of force is applied to a solid material such as a rock, the solid material would react based on the yield strength by deforming i.e., stretching or shrinking. Deformation is the act of change in the substance by an external force. In the reservoir, there are two main types of deformation which are dependent on the formation's yield strength in response to stress (Madhusha, 2018):

1- Elastic Deformation.
2- Plastic Deformation.

The occurrence of deformation could lead to both physical and chemical changes due To the main two factors of pressure and temperature during reservoir compaction. On one hand, Elastic deformation is a result of a reversible change when the external forces are removed from the material i.e., it goes back to the initial state. This change makes it non-permanent such that the existing chemical bonds stretch and bend but without the slippage of the atoms (Madhusha, 2018). On the other hand, an irreversible, plastic deformation is a permanent change as a result of applied external forces where the stress is greater than the rock's yield strength. Plasticity causes a noticeable physical change, without a fracture but a breakage occurs due to the atoms slipping on each other (Madhusha, 2018).

The stress-strain diagram below (Figure 15) represents how each region differentiates from the other. For instance, the elastic region starts at an early stage where the stress-strain values are not high and can be detected. Then, as soon as it passes the limit of that region, plasticity occurs. This means if the stress or strain values are significantly higher than the yield strength of the rock a fracture would occur (Madhusha, 2018). The importance of knowing the difference between these two deformations could help with the identification of well failure, the identification of the complex natural fracture as well as hydraulic fractures. Additionally, limiting well control problems means risks are reduced, and the formation of mechanical rock properties can be identified which would help with the overall understanding of the reservoir.

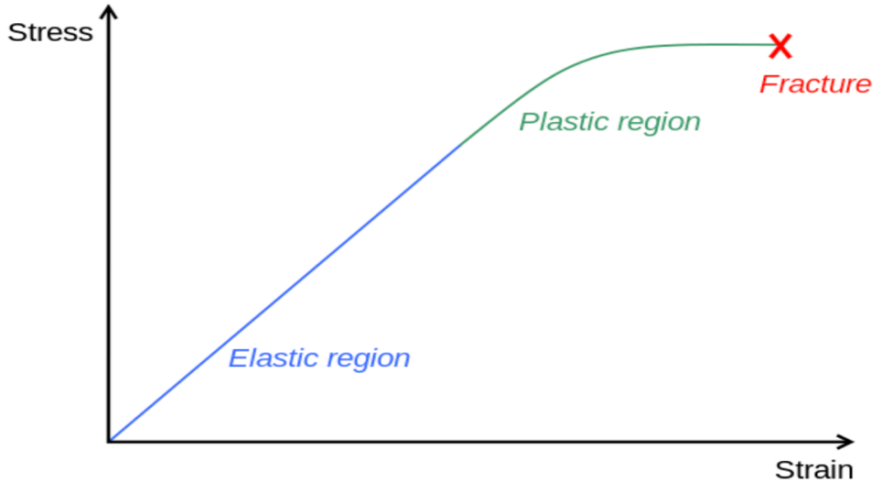

Figure 15: Stress-strain curve representing the elastic and plastic regions. (Madhusha, 2018)

2.6.5 FRACTURE CONDUCTIVITY

One of the important aspects of hydraulic fracture properties is the fracture conductivity of the formation. Generally, during the reservoir compaction, the effective stress increases on the stimulated reservoir volume (SRV) region. In some cases, subsidence is often accompanied by compaction due to the sudden reservoir pressure drop. As a result, the fracture conductivity increases at the early stages of the production of the well. The figure below (Figure 16) represents the hydraulic fracture orientation on a stimulated reservoir volume.

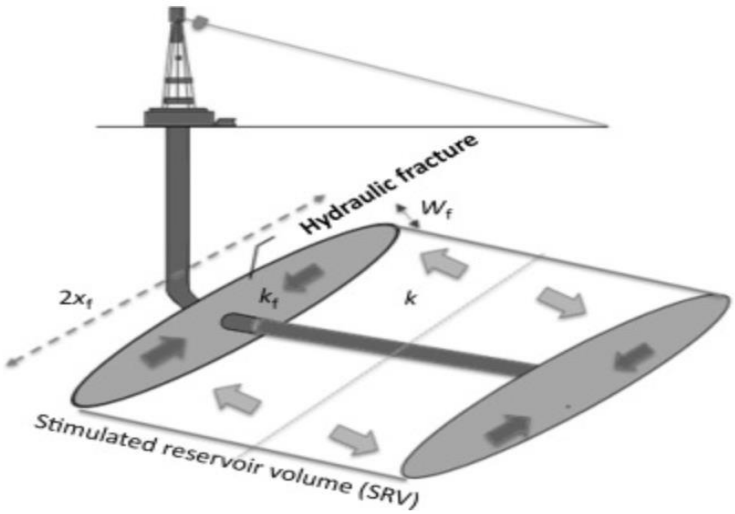

Figure 16: Propped hydraulic fracture conductivity in the SRV (Belyadi et al., 2019)

The dimensionless fracture conductivity is a parameter that is defined as shown in the equation below:

$$F_{CD} = \frac{Kk_f \times w_f}{Kk \times X_f} \qquad Equation\ (5)$$

The interpretation of the factors impacting the production performance of the reservoir to predict the overall well performance is crucial. As the reservoir depletes during compaction, it causes the cumulative gas production to increase which leads to a significant increase in the initial propped fracture conductivity of the wells in Marcellus shale specifically. Additionally, having this observation would result in enhancing the geomechanical effects on the formation (El Sgher et al., 2022). Since the fracture conductivity is highly dependent on the effective closure stress, empirical experiments should further assist instead of the theoretical approaches. As a result, drilling deep wells by the application of hydraulic fracturing with limited data requires a long time of measurements at reservoir temperature as a way to enhance the propped fracture conductivity (Roodhart et al., 1988). The emphasis of using the artificial proppants to be pumped into the fractures has to be considered. Moreover, the use of coarse proppant sand grades requires less energy to crush during the production stage i.e. lower closure stress with the aid of the hydraulic fracturing fluid to ease the process. The figure below (Figure 17) illustrates the performance of different proppant types such as ceramic, resin coated, and white sand associated with their grades.

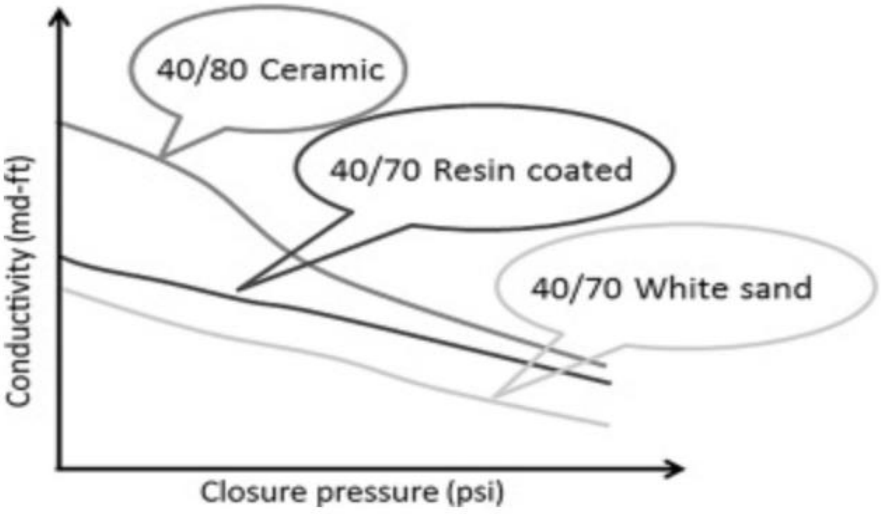

Figure 17: Proppant grades impact the conductivity versus the closure pressure (Belyadi et al., 2019)

Studies have shown the impact of the propped fracture conductivity has a greater impact on shale gas wells with multi-stage hydraulic fractures to enhance the production during the decline vicinity of the wells (El Sgher et al., 2018). (AlRamahi and Sundberg, 2012) took a step further to provide empirical laboratory experiments to observe the proppant embedment during the fracturing phase. The experiments were on hydraulic fracture conductivity in which they developed a relationship between the proppant embedment versus the fracture conductivity as a function of rock properties. Such that, the displacement of the hydraulic fracture conductivity could be a result of a variety of mechanisms, i.e. proppant crushing, diagenesis, and embedment. Since the study was conducted on an unconventional reservoir which means that it has a low young's modulus with a high clay content a correlation to predict the loss of the fracture conductivity between Young's modulus and the proppant embedment at specified stress measurements.

On the other hand, instead of the correlation of AlRamahi and Sundberg as a function of rock properties, (McGinley et al., 2015) developed experiments to observe the conductivity of the propped hydraulic fractures as a function of net stress. To come up with this correlation in the laboratory, core plug samples from Elimsport and Allenwood were collected as the main data to run the experiments from different locations. It is known that unconventional reservoirs have different orientations and deposits based on gravity. This is due to the abundance of clay minerals

i.e. anisotropic, these core plugs were cut both parallel and perpendicular to the planes to investigate the impact it has on the fracture conductivity.

Figures 18 and 19 illustrate the correlation developed between the fracture conductivity and the closure stress for both of the core samples, Allenwood and Elimsport, respectively.

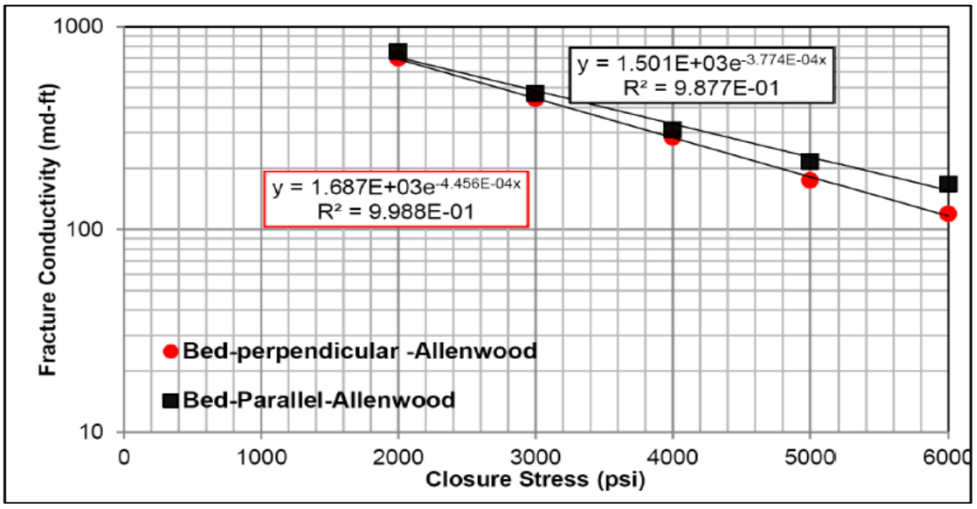

Figure 18: Propped hydraulic fracture conductivity versus closure stress for the Allenwood core plug sample (McGinley et al. 2015)

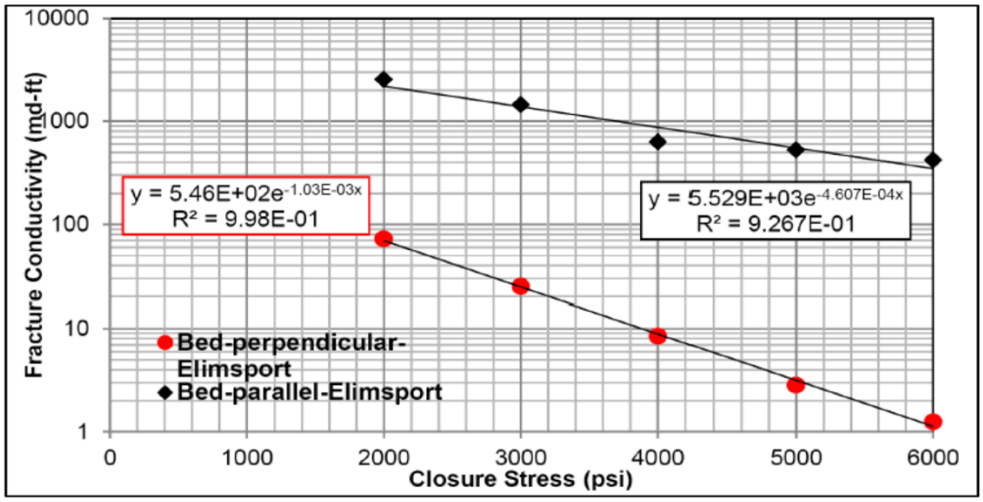

Figure 19: Propped hydraulic fracture conductivity versus closure stress for the Elimsport core plug sample (McGinley et al. 2015)

It was observed that both the bed-parallel and bed-perpendicular for the Allenwood sample were significantly lower than the Elimsport core plug which resulted in a fracture conductivity of $1.501 \times 10^{-3}\, psi^{-1}$ and $1.687 \times 10^{-4}\, psi^{-1}$, respectively. Likewise, the bed-parallel for Elimsport core plug was measured as $5.529 \times 10^{-4}\, psi^{-1}$ and the bed-perpendicular was lightly less than it with a measured fracture conductivity of $5.46 \times 10^{-4}\, psi^{-1}$. In conclusion,

McGinley's experiments were highly dependent mainly on the geomechanical impact of Young's modulus with a static behavior as well as the other reservoir characteristics during the development stage.

2.6.6. IMPACT OF STRESS ON THE MATRIX PERMEABILITY

A naturally fractured reservoir containing fractures and matrix systems is more sensitive to stress variations than a non-fractured reservoir (Lian et al., 2012). Heller et al. (2014) measured matrix permeability of shale as a function of net pressure under different pore pressures. Several core samples were analyzed by Heller et al. from the Marcellus, Barnett, Eagle Ford, and Montney formations.

Laboratory measurements on a Marcellus shale core plugs have been conducted to determine the petrophysical properties (Zamirian et al., 2015 and Elsaig et al., 2016). (Elsaig et al., 2016) measured the absolute permeability of the core plugs under four different pore pressures and seven different net stress values. A double slippage correction was applied to determine the absolute permeability at each net stress. These experiments revealed that the absolute permeability is affected by the net stress, as shown in Figure 20. As the net stress increases, the more stress-sensitive fissures close down first. The closure of the fissures leads to a significant reduction in the measured permeability of the core plug. Once all the fissures are closed, any further reduction in permeability is the result of matrix compression.

A linear trend is observed when $(k/ko)^{1/3}$ is plotted against ln P/Po if k is the permeability measured at a specific stress (P), and ko is the permeability measured at the lowest stress (Po) values (Walsh, 1981). An illustration of this plot is presented in Figure 21 for the above-mentioned Marcellus shale core plug (Elsaig et al., 2016). There are two straight lines on this plot as a result of the differences in compressibility between the fissures and the matrix. Fissure closure stress is determined by where these two lines intersect.

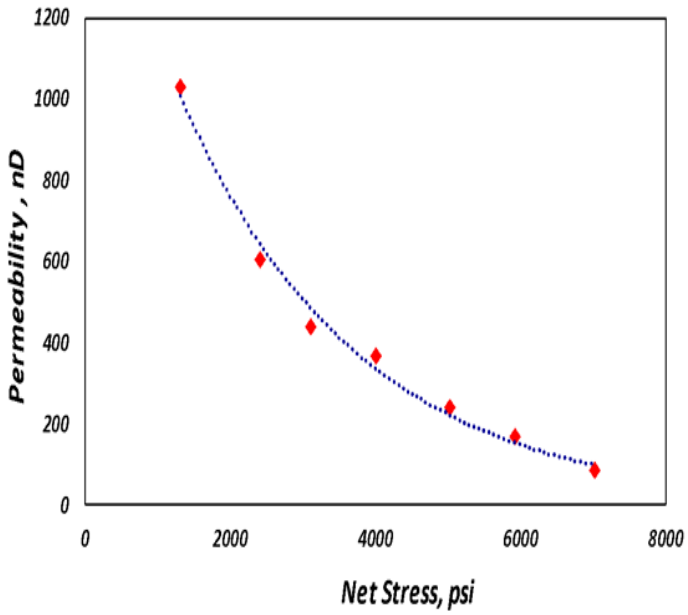

Figure 20: The Impact of Net Stress on the Absolute Permeability of the Marcellus Shale (After ElSaig et al., 2016)

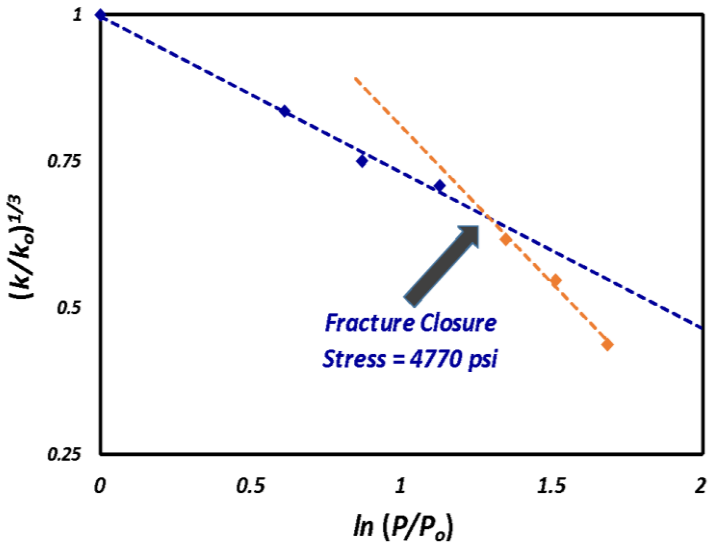

Figure 21: Evaluation of Fissure Closure Stress (after ElSaig et al., 2016).

2.8 CONSTITUTIVE LAWS

Over the past decade, reservoir simulation modeling techniques to optimize the reservoir performance have significantly improved leading to improvements in the ultimate gas recovery and reservoir productivity. Expertise in reservoir engineering is needed to understand reservoir characteristics such as the pre-existing natural fractures and the complexity of the fracture network.

Recent studies showed that commercial reservoir simulation models can be coupled with modules to help enhance the predictions. One of the modules is known as the Mohr-Coulomb model which is crucial for the identification of well failure. The flow diagram below (Figure 22) illustrates the main constitutive laws used in the industry for reservoir simulation modeling.

In addition, constitutive laws are divided into several categories but, in this research, the main focus will be on linear elasticity and elastoplasticity. These two categories branch into multiple models i.e., the Mohr-Coulomb and the Drucker-Prager model. Moreover, while the rock undergoes deformation, it can be categorized as elastic which follows the linear-elastic constitutive law. On the other hand, plastic deformation is associated with the elastoplasticity constitutive law such that the change is irreversible. When more force is applied it can create a fracture in the formation. This concludes the importance of understanding these laws to further predict the changes occurring during the compaction of the reservoir i.e., prediction of the production phase.

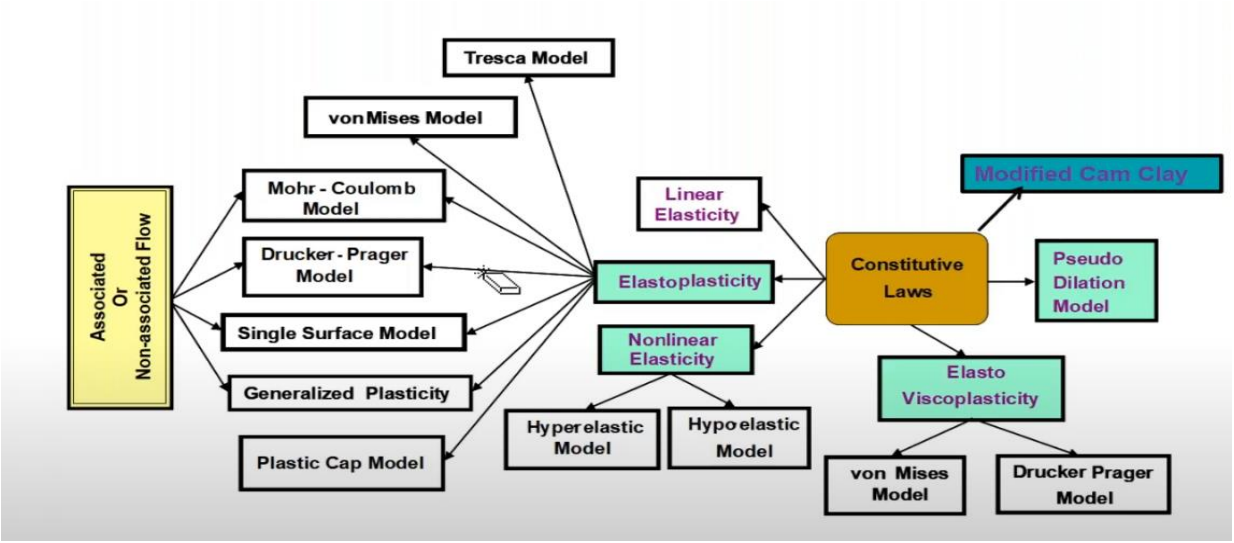

Figure 22: CMG's Geomechanics module with the available constitutive laws, (CMG, 2020).

2.8.1 MOHR-COULOMB MODEL

Coupled geomechanical modeling methods have been developed in the field of reservoir simulation engineering to further enhance different types of models. The Mohr-Coulomb model is specified for linear constitutive law. Mohr circles are used to graphically represent shear and normal stress components on arbitrary planes with maximum (σ_1)and minimum (σ_3) stresses provided. It describes stress in two dimensions. Coulomb's criterion is the simplest and most commonly used failure criterion, in which failure takes place along a plane caused by shear stress

acting in that direction. As can be seen in Figure 23, the horizontal stress minimum and maximum intersect the Mohr's envelope (envelope)

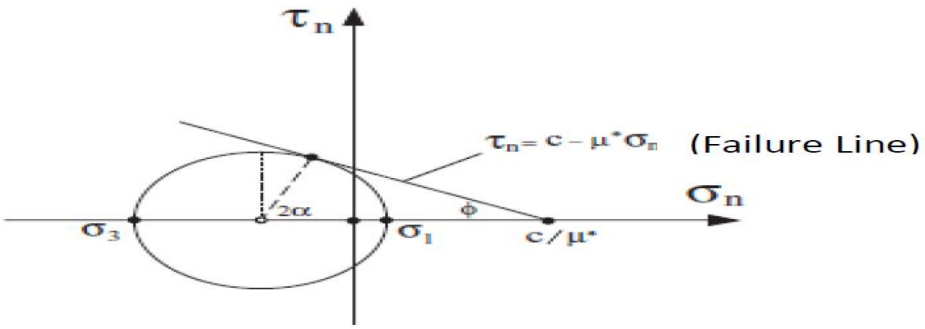

Figure 23: Mohr-Coulomb diagram for a sedimentary rock during the compaction stage of the reservoir. (Temizel et al., 2016)

$$\tau_n = \tau_f + c\,,\ \tau_f\,(Frictional\ Stress) = -\mu^* \times \sigma_n$$

$$\mu^* = tan\emptyset\ ,$$

Where:

ϕ = Angle of internal friction and c is cohesive strength of the material.

μ* = Coefficient of friction.

The Mohr-Coulomb is often associated with engineering management project teams to limit or predict failures during the development phase of the well such that the yield strength line and the peak strength line are evaluated by the tangents of the Mohr-Circle (Markou and Papanastasiou, 2020). Additionally, the below equations represent the mathematical approach to understanding the failure curve as functions of mean stress and deviatoric stress, such that:

$$\sigma' = \frac{1}{2}(\sigma_1' + \sigma_3') \qquad Equation\ (7)$$

$$\varepsilon = \frac{1}{2}(\sigma_1' + \sigma_3') \qquad Equation\ (8)$$

In CMG, Young's Modulus, Poisson's Ratio, Cohesion Strength, and Friction Angle are all porosity-dependent parameters which change with stress.

2.9 COUPLED GEOMECHANICS RESERVOIR STIMULATION MODELING

Unconventional reservoirs are known for their complexity of natural fractures and the heterogeneous behavior of the formation. Coupled geomechanical modeling is crucial for the geological complex fields (A. Settari, 2002). Marcellus shale led scientists to improve their understanding of reservoir characteristics. For this instance, the application of commercial reservoir simulation has been used for further analysis and assistance. During compaction, geomechanical parameters are calculated by a reservoir simulator to interpret the changes. An advanced coupling method with a geomechanical module accompanied by a commercial reservoir simulator would enhance the understanding of reservoir development.

Four coupling methods are used in the oil and gas industry. First, full coupling or implicit coupling due to the system being discrete on one grid domain (Settari et al., 2002). Simultaneous calculations are conducted as three main unknown pressure, temperature, and displacement to observe the behavior of the fluid flow through porous media by the finite element method. Secondly, the iterative coupling is the most used method since it solves both rock deformation and reservoir fluid flow calculations independently. A driver connects the reservoir simulator and the geomechanics module to check for convergence which takes into consideration the pressure and stress changes by each iteration (Settari et al., 2002). The third weakest coupling method is known as one-way coupling or explicit coupling. The changes in pressure are only being enhanced by the changes in stress and strain and not the other way around, unlike the two-way coupling method (Settari et al., 2002). Lastly, the pseudo-coupling method uses simple calculations between two genres: porosity and vertical displacement (subsidence), and porosity and stress. This can mimic the response of the reservoir during the compaction stage as well as horizontal stress changes. An empirical model to calculate porosity often works with the presence of a table with porosity and permeability versus pressure data obtained during this phenomenon (Settari et al., 2002).

2.9.1 ITERATIVE COUPLING TECHNIQUE

The diversity of the coupling methods has evolved since most reservoir simulators lack the incorporation of the geomechanical aspects i.e. effective stress changes and mechanical rock properties such as the deformation during the reservoir compaction in response to the changes in temperature and pressure (Settari et al., 2002). Iterative coupling is categorized as the most flexible accompanied by highly successful practical rates. The approval of using this coupling method by

the reservoir management teams is very high among other engineering specialties (Jalali and Dusseault, 2008). Furthermore, (El Sgher, 2022) illustrated that in the two-way coupling method, a geomechanical model is mainly used to observe the calculation of the stress changes by evaluating the response that the rocks undergo. He then highlighted the disadvantage of this approach since it requires a long-time duration due to a large number of iterations to reach convergence.

Shale gas reservoirs have significantly ultra-low permeability, which makes it challenging to produce from these formations. The fluid flow through porous media led engineers to enhance the production by formulating the porosity function. This helped to further understand the mechanism of the reservoir in the development phase i.e. gas storage in shale reservoirs. The porosity function has been impacted by several studies such that it can be affected by three main parameters: pressure, temperature, and mean total stress. Further developments have been applied to it to be used in iterative coupling between the geomechanics module and the reservoir simulator.

The correlation between pressure, volume, and stress has been very crucial for the development and understanding of fluid compressibility in the porous medium. (Geerstma, 1957) Conducted the porosity as a function of volumetric strain. Years later, (Skempton, 1960) developed a correlation between the fluid pore pressure (known as Skempton A and P pore pressure parameters) and the total stress to develop a way to relate these parameters to the porosity function. (Biot and Terzaghi, 1936) studies developed the original concept of effective stress and pore pressure, relative to the coupling techniques and how would these two parameters take part in the development of a three-dimensional theory to accompany the principles of continuum mechanics. Furthermore, (Khaled et al., 1984) created further investigations towards the enhancement of Biot's theory by applying it to the dual-porosity media by using the finite element formulation.

Additionally, the true porosity function is the ratio between the pore volume to the bulk volume measured such that, it differentiates from the reservoir porosity by having the initial bulk as shown in the equations below, such that:

$$True\ porosity: \emptyset = \frac{V_p}{V_b} \qquad Equation\ (9)$$

$$Reservoir\ porosity: \emptyset^* = \frac{V_p}{V_{b^0}} \qquad Equation\ (10)$$

(Settari and Mourits, 1998) developed a correlation between the effective mean stress, temperature, and pressure as well as including the compressibility of solid grains when it came to

combining equation (9) and equation (10). When these two porosity equations are combined, it could be written as a function of volumetric strain as (Geertsma, 1957) showed which is also a parameter calculated during the two-way coupling method such that:

$$\emptyset^* = \emptyset(1 - \varepsilon_v) \qquad Equation\ (11)$$

Consequently, the reservoir strain is a function of three main parameters i.e. pressure, temperature, and stress this makes it possible to have the reservoir porosity written as a function of stress, pressure, and temperature as shown:

$$\emptyset^* = \emptyset^*(P, T, \sigma_m) \qquad Equation\ (12)$$

Since the iterative coupling uses strain, stress, and displacement, it has been observed that the below porosity function is used during the two-way coupling method. In addition, the main function is to calculate the porosity to be sent to the driver for further iterations until convergence is observed in modern reservoir simulation. *Equation (13)* represents the porosity formula developed by (Tran et al., 2002) for the estimation of the matrix porosity for this study.

$$\emptyset^{n+1} = \emptyset^n + (c_0 + c_2\alpha_1)(p - p^n) + (c_1 + c_2\alpha_2)(T - T^n) \qquad Equation\ (13)$$

$$a_1 = factor\left\{\frac{2E}{9(1-v)}\alpha c_b\right\} \quad Equation\ (14)$$

$$a_2 = factor\left\{\frac{2E}{9(1-v)}\beta\right\} \qquad Equation\ (15)$$

$$c_0 = \frac{1}{V_b^0}\{\frac{dV_P}{d_p} + V_b\alpha c_b\frac{d\sigma_m}{d_p} - V_p\beta\frac{dT}{d_p}\} \quad Equation\ (16)$$

$$c_1 = \frac{V_b}{V_b^0}\ \beta \quad Equation\ (17)$$

$$c_2 = \frac{V_b}{V_b^0}\ \alpha c_b \ \ Equation\ (18)$$

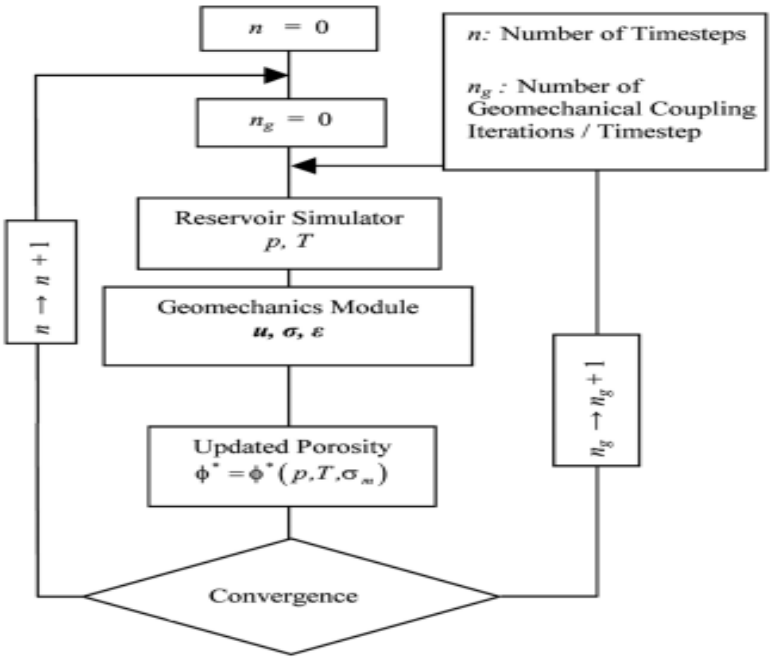

Figure 24: Iterative coupling flow chart, (Tran et al., 2002)

The iterative coupling has been one of the highlighted topics in reservoir engineering modeling approaches. The Figure above (Figure 24) illustrates a schematic of the two-way coupling method. Such that, engineers have been looking for new approaches to develop this technique to be further applicable. The mechanism of this method is not too complicated since it requires two types of variables: reservoir flow variables and geomechanics variables (Tran et al., 2002). These variables are fixed separately and sequentially by the main variables transferring energy called "the driving model" or "the coupled module". Additionally, the driving model allows the exchange of information between two main models: the reservoir simulator and the geomechanics module when the coupling iterations occur i.e., at each time step. It is controlled by the convergence criterion and is dependent on the pressure and stress changes in the last two iterations. During the iteration process, a better understanding of the rock deformation, as well as the reservoir flow in the formation, is observed.

The exchange of information allows the reservoir simulator to send pressure and temperature data to the driving model. Meanwhile, the geomechanics module responds with the updated porosity function to achieve convergence and proceed to the next iteration. The geomechanics module mechanism starts by accepting two external loads from the driver i.e., pressure and temperature. These two loads aid in the calculation of three parameters to develop

the porosity function, displacement, stress, and lastly strain, and each is computed by a specific method. Furthermore, the calculation of the displacement begins with an applied force first to allow the computation of strain by the strain-displacement relationship, then stress is obtained by the stress-strain constitutive relationship.

The below functions represent the cycle that occurs during the two-way coupling by an applied force to find displacement. Applying equation (19), proceeds to calculate the strain tensor by the tensor-displacement of equation (20), and finally, the effective stress tensor is calculated by the linear constitutive law from equation (21) as shown below (Joslin, Nguyen CMG, 2020).

$$\nabla\left[c{:}\frac{1}{2}(\nabla u + (\nabla u)^T)\right] = -\nabla[(\alpha p + \eta\Delta T]I + B \qquad Equation\ (19)$$

$$\varepsilon = \frac{1}{2}(\nabla u + (\nabla u)^T) \qquad Equation\ (20)$$

$$\sigma' = f(\varepsilon) \qquad Equation\ (21)$$

As soon as these three geomechanics variables are obtained they are updated to be included in the porosity function and are sent back to the coupled drive. Updated readings of both pressure and temperature are recorded, this process is repeated until convergence is achieved where the changes in pressure and stress are below tolerance.

CHAPTER 3
OBJECTIVES AND METHODOLOGY

3.1 OBJECTIVE

The main objective of this study was to investigate the influence of formation mechanical properties, including Young's modulus and Poisson's ratio, as well as hydraulic fracture properties, such as half-length, initial fracture conductivity, and spacing, as well as the operating conditions such as the wellbore pressure on the compressibility of the Marcellus Shale and therefore, on the productivity of horizontal Marcellus Shale wells with multi-stage fractures.

3.2 METHODOLOGY

In order to accomplish the objective of this study, a methodology consisting of the following steps was implemented:

1. Data collection and analysis
2. Development of a model, coupled with a geomechanical module, for a horizontal well with multi-stage hydraulic fractures
3. To evaluate the impact of the effective stress changes on the gas recovery
4. Parametric studies to investigate the impacts of the shale mechanical properties, Hydraulic fracture properties, as well as the operating conditions on the productivity of the horizontal Marcellus Shale.

The details on each step are provided in the following sections.

3.2.1 DATA COLLECTION AND ANALYSIS

In this study, data were collected from MSEEL, a Marcellus Shale field laboratory, which comprises two horizontal wells (MIP-4H and MIP-6H) that were drilled in 2011 and two horizontal wells (MIP-3H and MIP-5H) that were drilled in 2015, as well as a vertical observation well (MIP-SW) that was used to collect subsurface samples and monitor seismic activity. In addition to the results of the core plug analysis for well MIP-SW (Elsaig et al., 2016), completion and production records were collected for well MIP-6H. During the stimulation of well MIP-6H, eight fracture stages were performed over a lateral length of 2,380 feet. Approximately 3500 days of production were included in the production records.

The well logs for well MIP-6H were not available. In contrast, well logs and DFIT analysis from well MIP-3H located at the same site were used to estimate overburden pressures, closure

stress gradients, Young's Modulus, and Poisson's ratio (El Sgher et al., 2019). Additionally, the DFIT analysis was used to determine the colsure stress gradient. (El Sgher et al., 2019) predicted hydraulic fracture properties including fracture half-length, fracture height, and fracture conductivity based on fracture simulation models.

To account for gas desorption, the Langmuir pressure and volume were incorporated in the base model (Zamirian et al., 2015). By analyzing the core plugs and the measured propped fracture conductivity in Marcellus shale (McGinley et al., 2015), these multipliers were derived for the fissure permeability, matrix permeability, and hydraulic fracture properties conductivity as functions of effective stress (El Sgher et al., 2018).

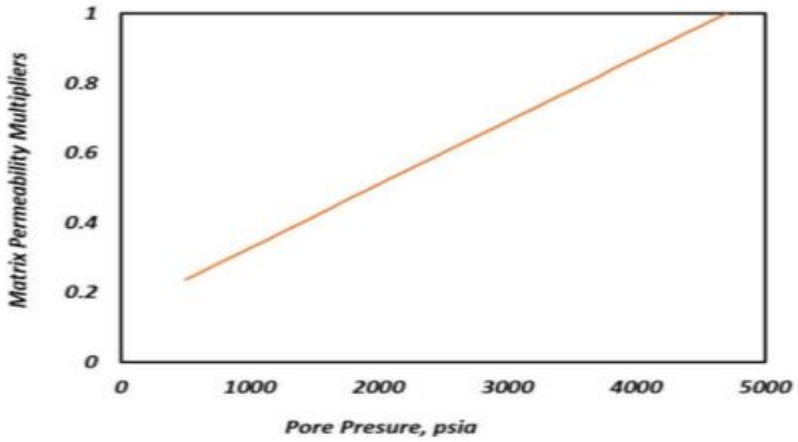

Figure 25: Matrix Permeability multiplier developed relative to the pore pressure for MIP-6H (El Sgher et al.., 2018)

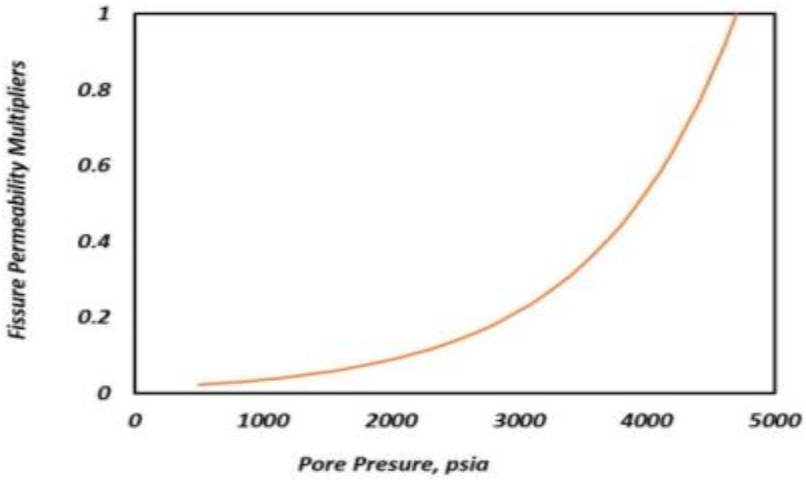

Figure 26: Fissure Permeability multiplier developed relative to the pore pressure for MIP-6H (El Sgher et al.., 2018)

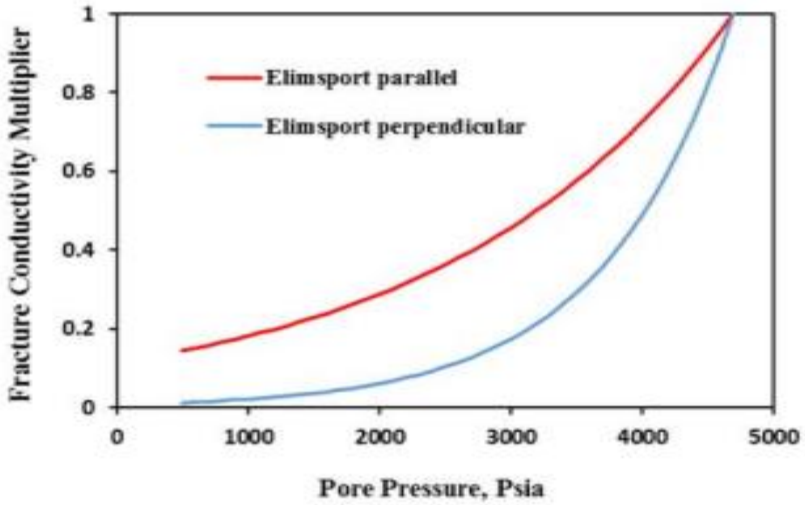

Figure 27: Fracture conductivity multiplier developed relative to the effective stress for the Elimsport core sample (El Sgher et al., 2018)

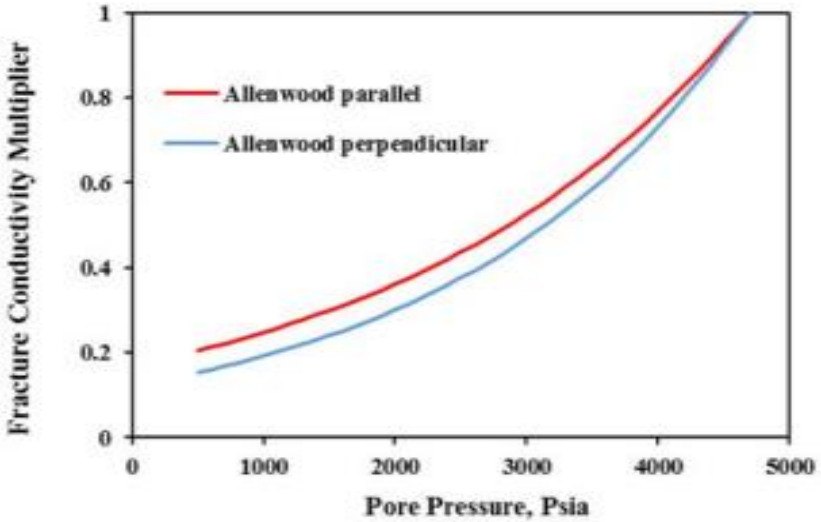

Figure 28: Fracture conductivity multiplier developed relative to the effective stress for the Allenwood core sample (El Sgher et al., 2018)

3.2.2 MODEL DEVELOPMENT

The reservoir base model for well MIP-6H was generated by using the reservoir simulation package of a commerical software (CMG-GEM, 2021). In order to build the reservoir model, the data collected and analyzed were imported into the software as shown in the table below *(Table 1)*, where it illustrated the base model parameters. A constraint for this model was the wellbore pressure being one of the operating conditions to investigate the impact of the compaction.

Iterative coupling or as known as “two-way coupling” was incorporated into the reservoir model with a linear elasto-plastic constitutive module referred to as Mohr-Coulomb. The Mohr-Coulomb module accompanied the effective stress alternations during the production of the well. The mechanism of the iterative coupling takes both pressure and temperature and send them to the geomechanics module where stress, strain, and displacement are calculated. Afterwards, both permeability and porosity are updated with the compressibility impacts and sent to the reservoir simulator to proceed with the next iteration.

The stress computed into the reservoir model is primarily used to determine the compaction occuring during the early stages and throughout the remaining life of the well. The compressibility factors which are the matrix porosity, matrix permeability, natural fractures (fissure) permeability, and the hydraulic fracture conductivity are directly related to the effective stress acting on the stimulated reservoir volume (SRV).

The matrix porosity determination was through the equation introduced by (Tran et al., 2002) in the liteature review of this study refered to as (Equation 13) which was then incorpoated into the generated reservoir model. Furthermore, both matrix and natural fracture (fissure) permeability, as well as the hydraulic fracture conductivty are depenednt on the initial values assigned based on the reservoir characteristcs as well as the developed multipliers for each of the parameters as discussed in data collection and analysis.

Figure 28 represent the 3-D model generated by the commerical reservoir simulation software (CMG-GEM, 2021) for well MIP-6H Figure 29 shows the eight hydraulic fractures assigned to the well over a lateral of 2,380 feet as a top grid view.

Table 1: The table below represent the Base Model Parameters for well MIP- 6H

MIP-6H Well information		
Reservoir Parameters	**Values**	**Units**
Model Dimensions (MIP-6H)	**4000(Length)×1000(Width) ×90(Height)**	**ft.**
Well Length (Horizontal)	**2380**	**ft.**
Initial Reservoir Pressure	**4800**	**psia.**
Overburden Pressure	**8800**	**psia**
Initial Fissure Porosity	**0.01**	**percent**
Initial Matrix Porosity	**3**	**percent**
Initial Fissure Permeability i, j, k	**360, 360, 36**	**nd**
Initial Matrix Permeability i, j, k	**340, 340, 34**	**nd**
HF Stage Spacing	**300**	**ft.**
Initial HF Conductivity	**20**	**md-ft**
Water Saturation	**0.15**	**Fraction**
Rock Density	**120**	**lb/ft^3**
Langmuir Pressure Constant	**0.00417**	**psi^{-1}**
Langmuir Volume Constant	**0.023**	**g-mol/lb**
Young's Modulus	**2×10^6**	**psi**
Poisson's Ratio	**0.2**	
Biot's Coefficient	**1**	
Wellbore Pressure	**400**	**psia**

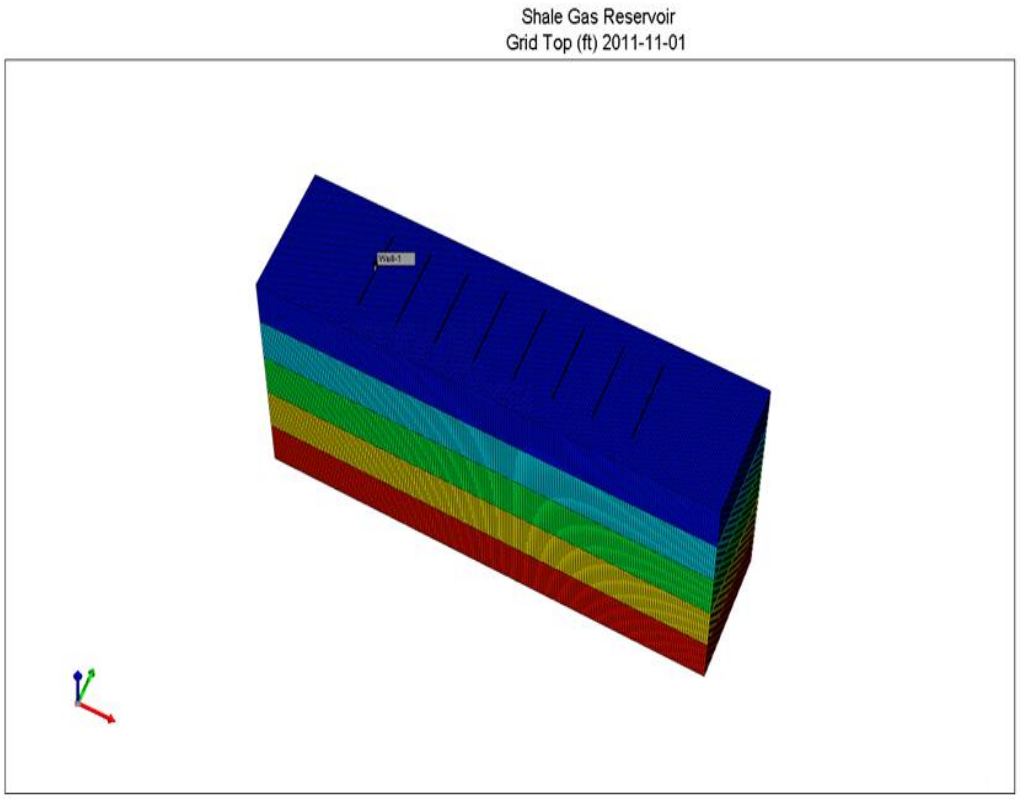

Figure 29: Shale gas reservoir base model in 3D using CMG reservoir simulation modeling software

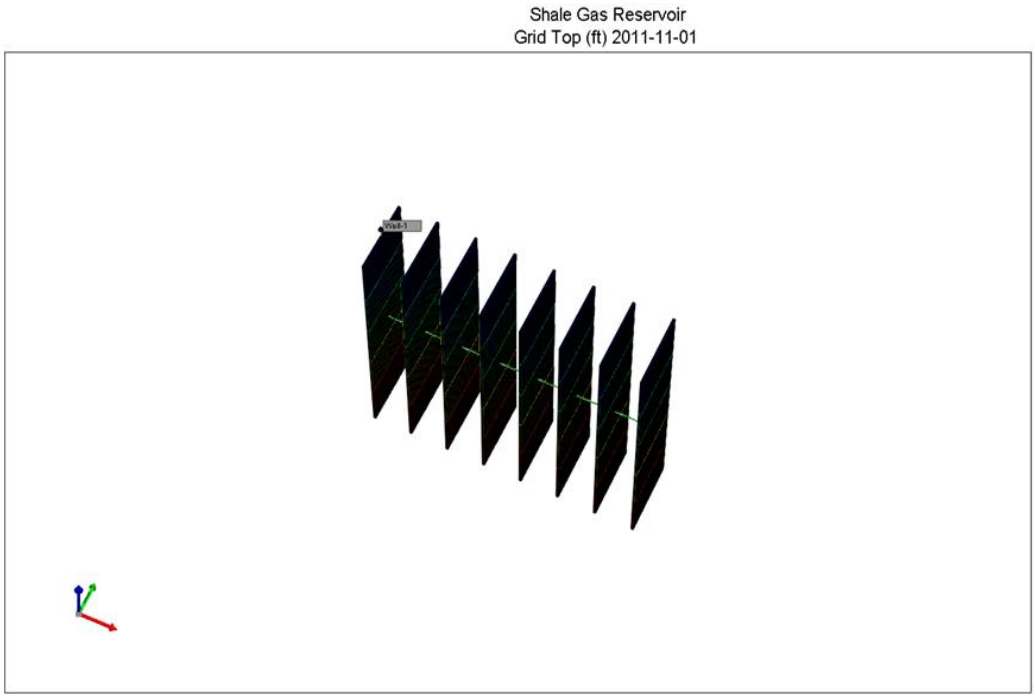

Figure 30: Shale gas reservoir base model illustrating the 8 fractures on a 2,380 ft. lateral in 3D using CMG reservoir simulation modeling software

3.2.3 THE IMPACT OF THE EFFECTIVE STRESS ON THE GAS RECOVERY

During the reservoir compaction, the effective stress increases over the stimulated reservoir volume which causes the pore pressure to decrease in relative to an increase in the gas production during the early-stages of the well MIP-6H. Additionally, this increase in the effective stress leads to a reduction in the primary reservoir characteristics in this study such as the matrix porosity, matrix permeability, natural fracture permeability and the hydraulic fracture conductivity. As discussed above, the effective stress plays an important role in affecting the gas production rates which is why the investigation was on this factor to predict and accurate gas recovery of the well.

For this reason, two production profiles were generated to observe the difference between the coupled model with the compressibility impact relative to the model excluded from these factors to limit the over-estimation of the gas production for the specified well MIP-6H with multi-stage fractures.

3.2.4 PARAMETRIC STUDIES

To investigate the impact of the increase in the effective stress on caused by the compaction of the stimulated reservoir volume on the gas recovery, parametric studies were conducted. These parametric studies included variety of values with different ranges based on the Marcellus shale formation for each compressibility factor category. The compressibility factors were divided into three categories such as the mechanical properties (Young's modulus & Poisson's ratio), hydraulic fracture properties (initial conductivity, half-length, and spacing), and lastly, operating conditions (wellbore pressure). In order to evaluate the impact on each parameter on the shale compaction during the production stage, the reservoir model was used to generate two production profile with inclusion and exclusion of the coupled model using iterative coupling. The table below (Table 2), illustrates the parameters used for the study along with the values chosen to investigate the compressibility impacts on the MIP-6H well with multi-stage hydraulic fractures.

Table 2: Parametric studies used for this study to investigate the compressibility impacts on the productivity of a Marcellus shale gas well MIP-6H

Parametric studies			
Parameters	**Base Model**	**Values**	**Unit**
Young's Modulus	**2 x 10^6**	**1 x 10^6 & 4 x 10^6**	**psi**
Poisson's Ratio	**0.2**	**0.1 & 0.4**	**-**
Half-length	**300**	**100, 200, & 400**	**ft.**
Initial Conductivity	**20**	**5, 10, 15, 25, 35, & 40**	**md-ft.**
Number of Stages	**8**	**12 & 16**	**-**
Wellbore Pressure	**400**	**600, 800, and 1000**	**psi**

CHAPTER 4

RESULTS AND DISCUSSION

The main objective of this study was to investigate the influence of formation mechanical properties, including Young's modulus and Poisson's ratio, as well as hydraulic fracture properties, such as half-length, initial fracture conductivity, and spacing, as well as the operating conditions such as the wellbore pressure on the compressibility of the Marcellus Shale and therefore, on the productivity of the well. In order to limit the over-estimation or under-estimation of the gas production for the well MIP-6H two stimulated production profiles were generated to visualize this approach.

Figure 30 represents the two stimulated production profiles including and excluding the compressibility impacts as well as the actual field data. The first stimulated production profile (line: Orange) was generated without coupling the reservoir model with a geomechanical module and ignoring the compressibility impacts. On the other hand, the second stimulated production profile (line: grey) was generated with the reservoir model iteratively coupled with a geomechanics module which accounts for the compressibility impacts. Additionally, the compressibility impacts include the matrix porosity, matrix permeability, natural fractures permeability, and the hydraulic fracture conductivity.

As can be observed, the second stimulated production profile with the coupled geomechanical module was in close agreement to the actual field data for well MIP-6H. Unlike the first production profile which illustrated an over-estimate of the reserves of the well MIP-6H which could affect the economic analysis further. As a result, the inclusion of the coupled reservoir model with the geomechanical module using the iterative coupling approach illustrated a more accurate prediction profile by matching the actual field data.

For this study, the compressibility impacts were investigated on different production profiles which include 1-year, 5-years, 10-years, and 15-years for further future production prediction. The figure below (Figure 31) illustrate the percent difference change in cumulative gas production based on the two generated stimulated production profiles in (Figure 30) due to the increase in the effective stress during compaction. The compressibility impacts diminish over time in response to the high gas production rates during the early production stages which promote the steep decline in pore pressure on the stimulated reservoir volume (SRV).

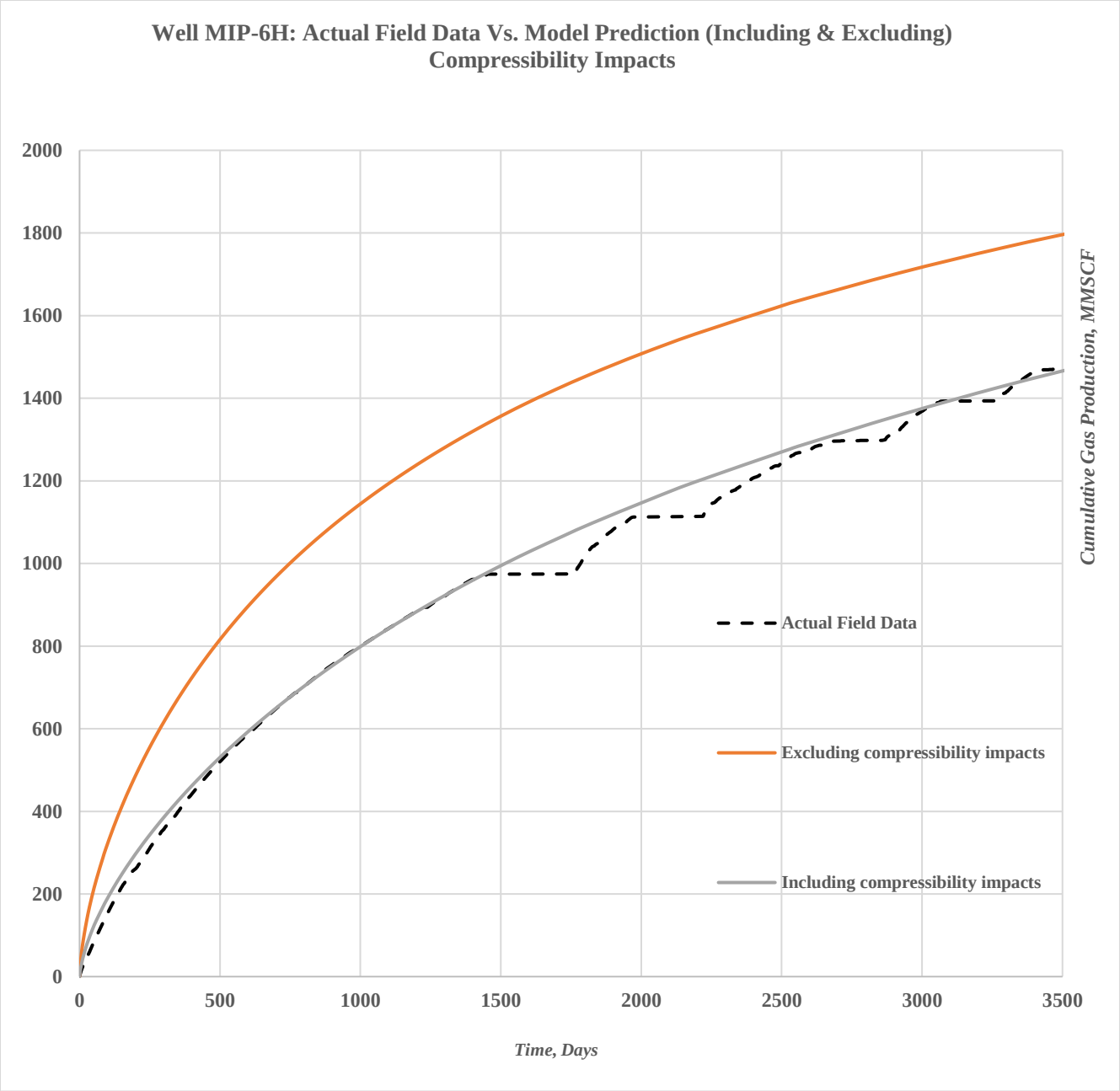

Figure 31: Well MIP-6H actual field data vs. model prediction (including & excluding) the compressibility impacts on the gas recovery.

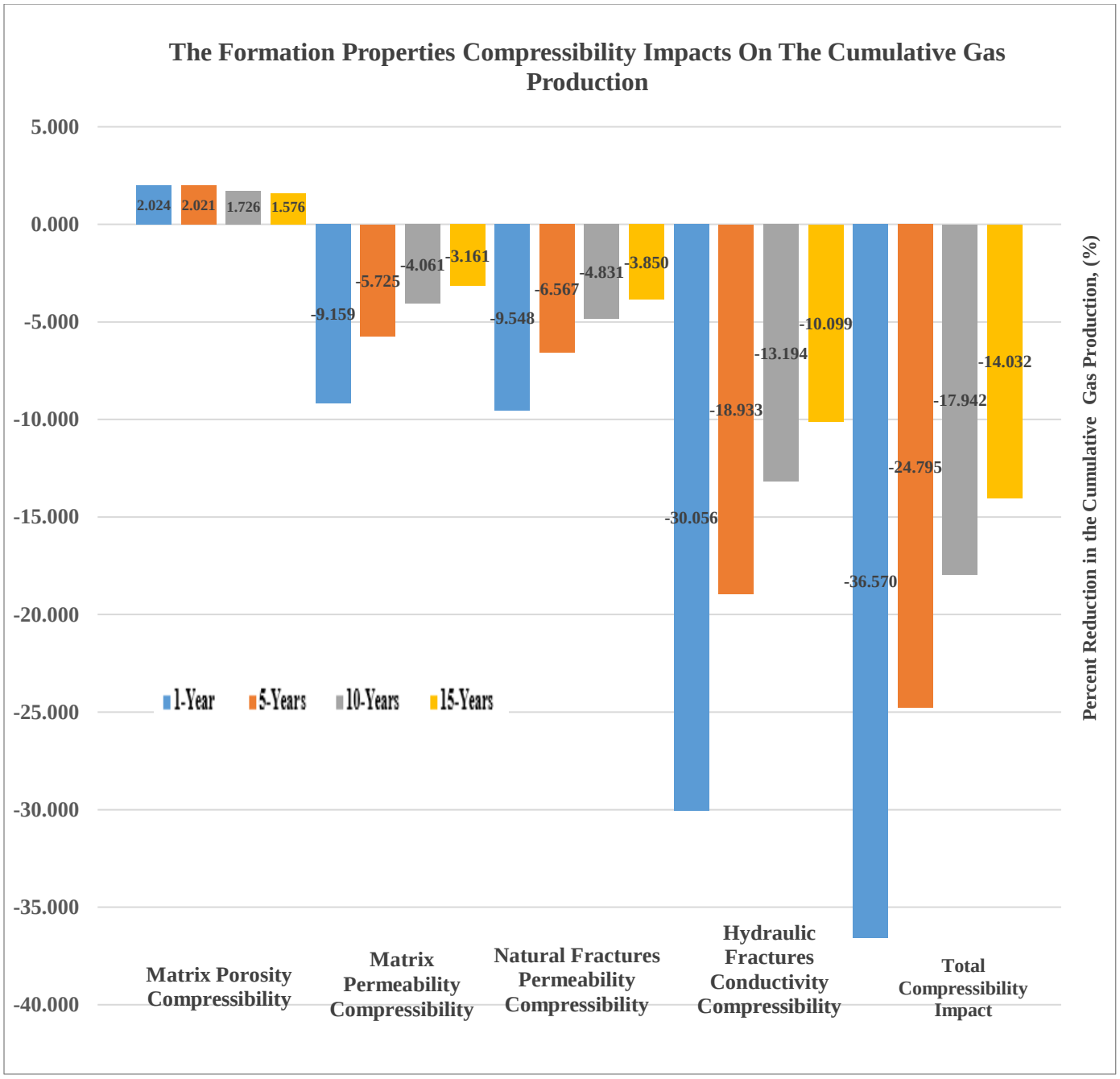

Figure 32: The formation properties compressibility impacts on the percent change in cumulative gas production for well MIP-6H

Additionally, the percent change in the cumulative gas production is affected by the different components of the compressibility impacts on the reservoir which are the matrix porosity, matrix permeability, natural fractures (fissure) permeability, and the hydraulic fracture properties. The constraint for the development of these production profiles for each compressibility factors is that each factor was individually observed by ignoring the other compressibility impacts in the

reservoir model. These constraints will be illustrated in the appendix for each compressibility factor.

In summary, the 1-year production profile (represented in blue) for all cases showed the most adverse impact on the percent reduction in the cumulative gas production for the MIP-6H well. The reason is due to the higher gas production rates during the early production stages which lead to a decline in the pore pressure in the formation while keeping the overburden pressure constant.

The most adverse yet negative impact from the compressibility factors was the hydraulic fracture conductivity followed by both natural fracture's permeability and matrix permeability. On the other hand, there was a slight positive reduction change in the matrix porosity on the gas recovery due to the matrix porosity acting as the driving force or "compaction drive" for the gas production. It was noted that the reduction in both matrix and natural fracture's permeability impact was almost identical due to the high initial effective stress in the reservoir model and relatively, low initial natural fracture permeability. Consequently, the impact of reduction in the natural fracture permeability on the gas production can be induced by the increase of the permeability or a lowered initial stress for a shale formation.

The sections below will discuss and analyze the formation mechanical properties (Young's modulus and Poisson's ratio), hydraulic fracture properties (initial fracture conductivity, half-length, and fracture spacing), and finally, operating conditions (wellbore pressure). Each of the above-mentioned properties had multiple values assigned for parametric studies based on the Marcellus shale formation characteristics as well as a special case study.

4.1 THE IMPACT OF THE FORMATION MECHANICAL PROPERTIES

In unconventional reservoirs, the basic reservoir understanding of the different rock characteristics is crucial. For this study, two main mechanical rock properties have been analyzed to investigate their impact on the productivity of the multi-stage fractured well. Additionally, the impact of such parameters was mainly on the stimulated reservoir volume (SRV) for well MIP-6H. The table below (Table 3) represent the parameters used aligned with the base model initial values in addition to the range of the values used for the parametric studies for both Young's modulus and Poisson's ratio for a Marcellus shale formation.

Table 3: The formation mechanical properties for well MIP-6H

Formation Mechanical Properties			
Parameters	**Base Model**	**Range Values**	**Unit**
Young's Modulus	**2 x 10^6**	**1 x 10^6 & 4 x 10^6**	**psi**
Poisson's Ratio	**0.2**	**0.1 & 0.4**	**-**

4.1.1 YOUNG's MODULUS AND POISSON's RATIO

For this parametric study, the focus will be on two main mechanical rock properties both Young's modulus and Poisson's ratio. In order to investigate the impact of the mechanical rock properties three case studies have been incorporated into the model. The table below (Table 4) illustrates the three different parametric studies along with their values. Recall that, the base model had a Young's modulus of $E = 2\ x\ 10^6$ and a Poisson's ratio of $v = 0.2$ per (Table 3). As a result, a lower value was chosen and a higher value with adjustments made later on based on the investigations on the formation compressibility.

Table 4: The % reduction change of the formation mechanical properties on the cumulative gas production rate for well MIP-6H

Mechanical Properties Values		Percent Reduction in Cumulative Gas Production
Young's Modulus	**Poisson's Ratio**	**%**
E = 1×10^6	**ν = 0.1**	**7.09**
E = 4×10^6	**ν = 0.4**	**-11.69**
E = 4×10^6	**ν = 0.4**	**17.35**

It was observed that for the case with the lower values of $E = 1\ x\ 10^6$ and $v = 0.1$ compared to the base case showed a higher reduction in the matrix porosity, matrix permeability,

natural fractures permeability, and the hydraulic fracture permeability due to the formation being more compressible under the compaction influence. Additionally, the brittleness of the Marcellus shale formation helped with the ease to compress the layers as well. Consequently, a slight positive enhancement was observed in the total percent reduction in gas recovery of 7.09 % for the lower Poisson's ratio and Young's modulus. Lastly, the increase in gas recovery was a result of the enhancement in the compaction drive due to the high reduction in the matrix porosity.

On the other hand, it was observed that for the case with the higher values of $E = 4\ x\ 10^6$ and $v = 0.4$ compared to the base case showed a lower reduction in the matrix porosity, matrix permeability, natural fractures permeability, and the hydraulic fracture permeability due to the formation being less compressible under the compaction influence. The higher the Young's Modulus and Poisson's ratio of the formation leads to a harder form of the rock to be compressed. Consequently, a negative trend in the total percent reduction in gas recovery of -11.96 % for the higher Poisson's ratio and Young's modulus. Additionally, a special case study was observed on the higher value of $E = 4\ x\ 10^6$ and $v = 0.4$ resulted in a positive improvement on the impact of the gas recovery with a 17.35 % in percent change in reduction will be discussed below.

The matrix porosity contributes to the compaction drive of the gas reservoir, such that it acts as the drive mechanism to initiate the fluid-flow in the porous medium. There is a direct relationship with the mechanical properties and the matrix porosity summarized in the porosity equation incorporated into the iterative coupled model. The equation below (Equation 13) will illustrate the porosity function and how it relates both Young's modulus and Poisson's ratio to have an impact on the productivity of the well.

$$\emptyset^{n+1} = \emptyset^n + (c_0 + c_2 a_1)(p - p^n) + (c_1 + c_2 a_2)(T - T^n) \qquad Equation\ (13)$$

Where both parameters of a_1 and a_2 represent the relationship as follows:

$$a_1 = factor\left\{\frac{2E}{9(1-v)}\alpha c_b\right\} \quad Equation\ (14)$$

$$a_2 = factor\left\{\frac{2E}{9(1-v)}\beta\right\} \qquad Equation\ (15)$$

For this study, the main multipliers incorporated were for the permeability and the hydraulic fracture conductivity for each of the three cases. Consequently, the permeability of both matrix and natural fractures (fissure) did not require significant alternations for the different values of the mechanical properties. However, the hydraulic fracture conductivity multiplier had to be adjusted for each case. For the case with the lower values of $E = 1\ x\ 10^6$ and$v = 0.1$, it was not

significantly different than the base case with $E = 2\ x\ 10^6$ and $v = 0.2$ so no further alternations were required since the percent reduction was positive. However, the case with the higher value of $E = 4\ x\ 10^6$ and $v = 0.4$ had a special case to be investigated.

The propped hydraulic fracture conductivity was adjusted for the higher values case from the available published data and measurements (McGinley et. al, 2015). Two core plug samples were taken from two different locations Elimsport and Allenwood and each had different mechanical rock properties. The Allenwood sample had similar characteristics of the second case with the higher value of Young's modulus $E = 4\ x\ 10^6$. As a result, a new adjusted multiplier was developed for that case and incorporated into the model to improve the production of the MIP-6H well. The table below (Table 5), illustrates the rock mechanical properties for both Elimsport and Allenwood core samples generated by McGinley before developing the study of the propped fracture conductivity.

Table 5: Summary of the rock mechanical properties for both the Elimsport and Allenwood samples (McGinley et. al, 2015)

Property	Allenwood	Elimsport
E_v	$4.41 \times 10^6\ psi$	$2.32 \times 10^6\ psi$
E_h	$3.99 \times 10^6\ psi$	$1.10 \times 10^6\ psi$
v_v	0.161	0.283
V_h	0.202	0.256

The figure below (Figure 33), shows the 5-year production profile for the three different cases of the mechanical properties compared to the base case. Additionally, the case with the higher Young's modulus and Poisson's ratio had two production profiles for comparison purposes due to the inclusion of the new hydraulic fracture conductivity multiplier to improve the gas recovery for well MIP-6H. The first production profile for f $E = 4\ x\ 10^6$ and $v = 0.4$ was simulated with the original hydraulic fracture conductivity multiplier. Whereas the second production profile for the same value was generated for the new hydraulic fracture conductivity multiplier using the Allenwood core sample from the published propped fracture conductivity measurement which showed an improvement on the gas recovery for well MIP-6H.

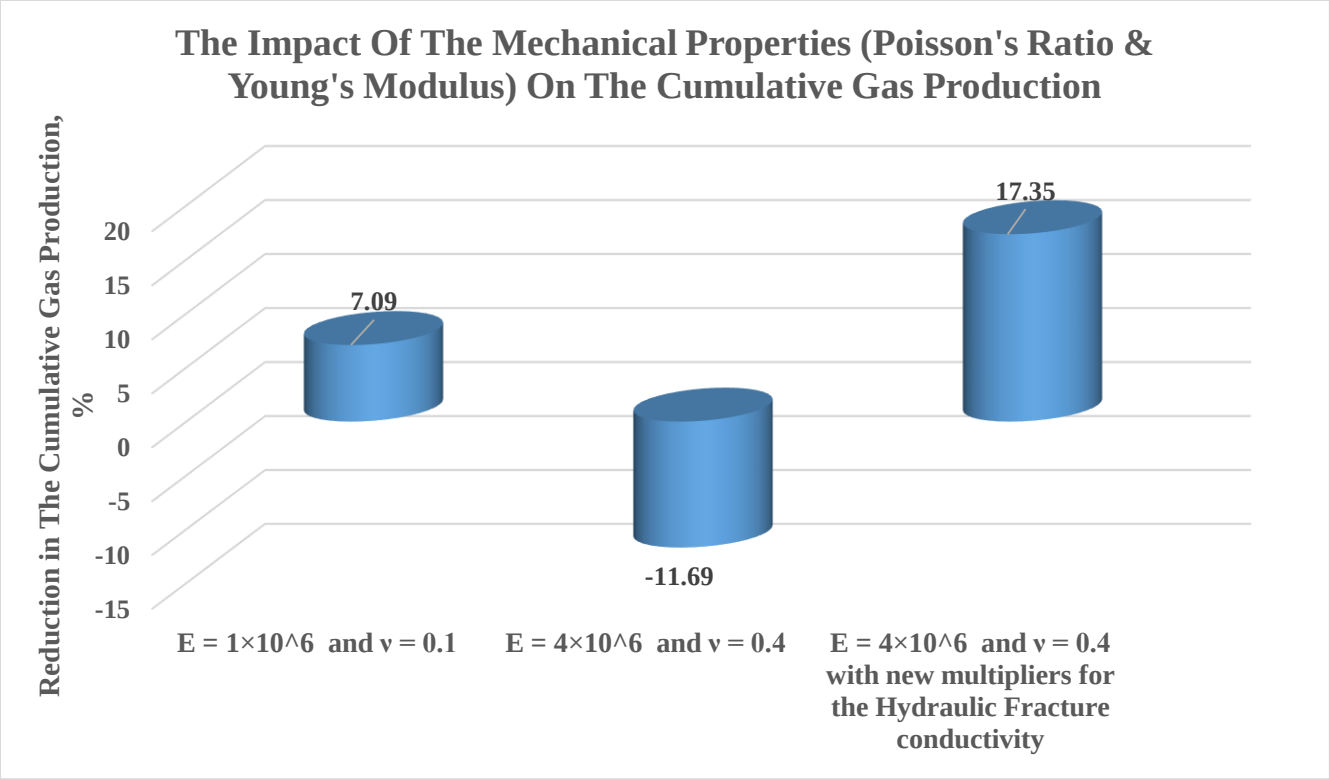

Figure 33: The impact of the formation mechanical properties (Young's modulus & Poisson's ratio) on the cumulative gas production rates of well MIP-6H

The reason behind the case with $E = 4\ x\ 10^6$ and $v = 0.4$ incorporated with the original hydraulic fracture multiplier showed a negative percent reduction change in the gas recovery was attributed to a lower reduction in the matrix porosity which lowered the compaction drive over time. On the other hand, the case with the new hydraulic fracture conductivity multiplier resulted in an increased percent reduction in the gas recovery which attributed towards less reduction in the hydraulic fracture conductivity. Consequently, the reduction of the hydraulic fracture conductivity on the productivity has a noticeable impact than the matrix porosity reduction. Such that, higher gas recovery is observed due to overcoming the reduction in production caused by the decreased compaction drive to keep the fracture open in the formation.

There was no direct impact or a noticeable impact on the effective stress but more on the hydraulic fracture conductivity since that was incorporated into the model to improve the production. In fact, both Young's Modulus and Poisson's Ratio are directly related to the porosity equation used for the iterative coupling which has a noticeable impact on the pore pressure as well.

4.2 THE IMPACT OF THE HYDRAULIC FRACTURE PROPERTIES

In unconventional reservoirs, the application of hydraulic fracturing has been heavily implemented in the oil and gas industry. For this study, three main hydraulic fracture properties have been analyzed to investigate their impact on the productivity of the multi-stage fractured well. Additionally, the impact of such parameters was mainly on the stimulated reservoir volume (SRV) for well MIP-6H. The table below (Table 6) represent the parameters used aligned with the base model initial values in addition to the range of the values used for the parametric studies. The range of the values have been selected per the Marcellus shale formation characteristics.

Table 6: The Hydraulic fracture properties for well MIP-6H

Hydraulic Fracture Properties			
Parameters	**Base Model**	**Range Values**	**Unit**
Half-length	**300**	**100, 200, & 400**	**ft**
Initial Conductivity	**20**	**5, 10, 15, 25, 35, & 40**	**md-ft**
Number of Stages	**8**	**12 & 16**	**-**

4.2.1 INITIAL FRACTURE CONDUCTIVITY

In order to investigate the impact of the initial fracture conductivity on the stimulated reservoir volume (SRV), two production profiles were generated for further analysis. The first production profile represents the early-production time of the well by selecting 1 year. On the other hand, the second production profile was chosen to be 5 years to investigate the effect over a longer period of production over time. Additionally, the compressibility impacts have been included to the model and act as a geomechanical barrier in comparison to the results with no compressibility impact. This approach was used in the study in order to provide a more realistic simulated production profile to reduce the over-estimation or under-estimation of the gas reserves production. The tables below (Table 7 and 8) illustrate the results obtained from the 1-year production profile including the compressibility impacts and without.

Table 7: fracture conductivity compressibility impact on the First Year cumulative gas production

Compressibility Impact	First-Year Production	
	Initial Fracture Conductivity	Cumulative Gas Production
	md-ft	SC (MMSCF)
	5	313
	10	376
	15	415
	20	437
	25	452
	35	468
	40	472

Table 8: First-Year cumulative gas production with no compressibility impacts

No Compressibility Impact	First-Year Production	
	Initial Fracture Conductivity	Cumulative Gas Production
	md-ft	SC (MMSCF)
	5	587
	10	648
	15	674
	20	689
	25	698
	35	712
	40	716

Table 9: First-Year cumulative gas production with compressibility impacts

% Reduction Change	1-Year Production Profile	
	Initial Fracture Conductivity	Total Reduction in Cumulative Gas Production
	md-ft	%
	5	46.6667
	10	42.0469
	15	38.4924
	20	36.5697
	25	35.3472
	35	34.2984
	40	34.0184

From the above tables, it can be seen that the cumulative gas production with the compressibility impacts is less than the cumulative gas production without the compressibility impacts. This is due to higher production rates during the early-production time. However, this can be better visualized in Figures 33 and 34 where each initial conductivity has its specific impact

over each gas production. As Figure 35 illustrates the percent difference of reduction in cumulative gas production for the 1-year production profile.

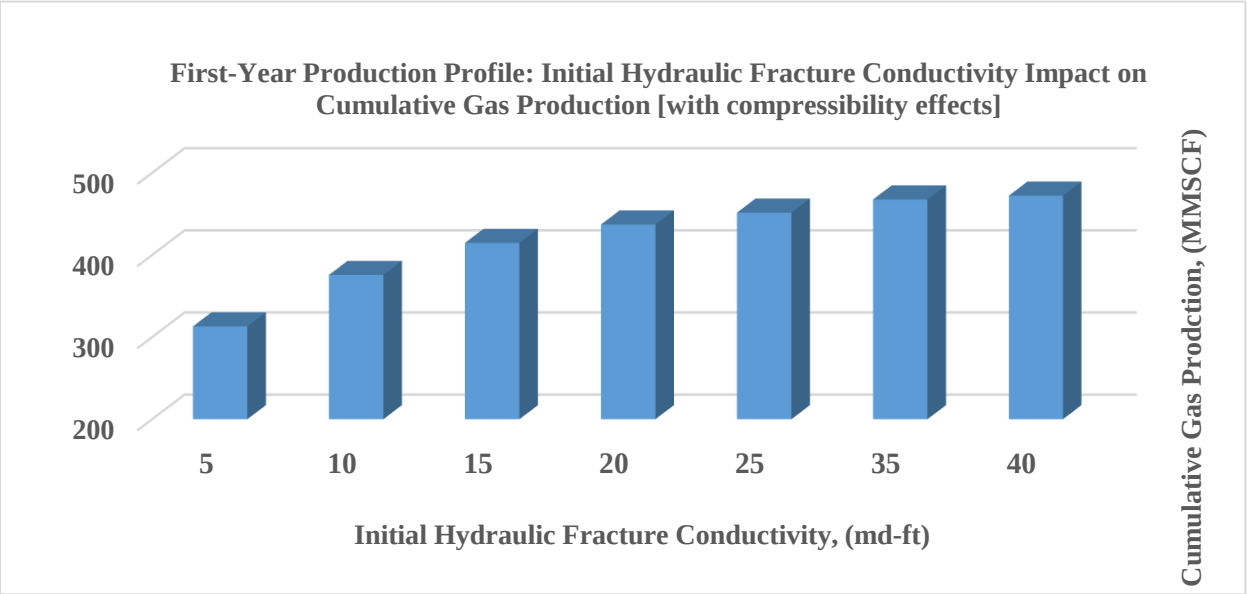

Figure 34: 1-Year Initial hydraulic fracture conductivity impact on the cumulative gas production (compressibility effects)

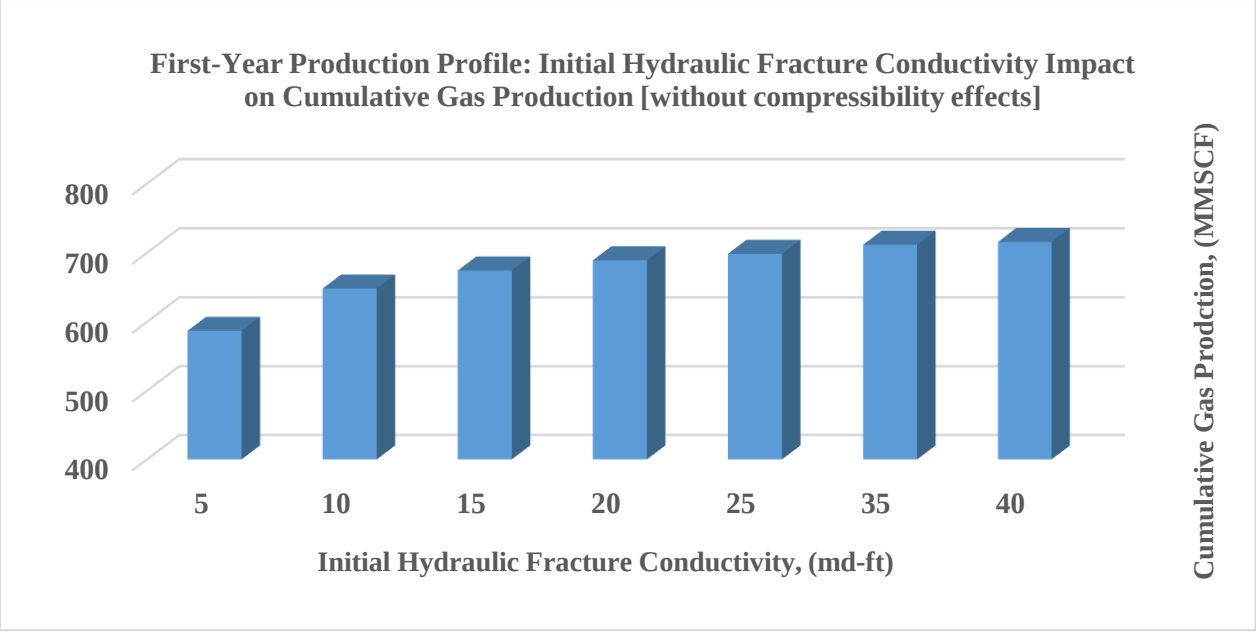

Figure 35: 1-Year Initial hydraulic fracture conductivity impact on the cumulative gas production (no compressibility effects)

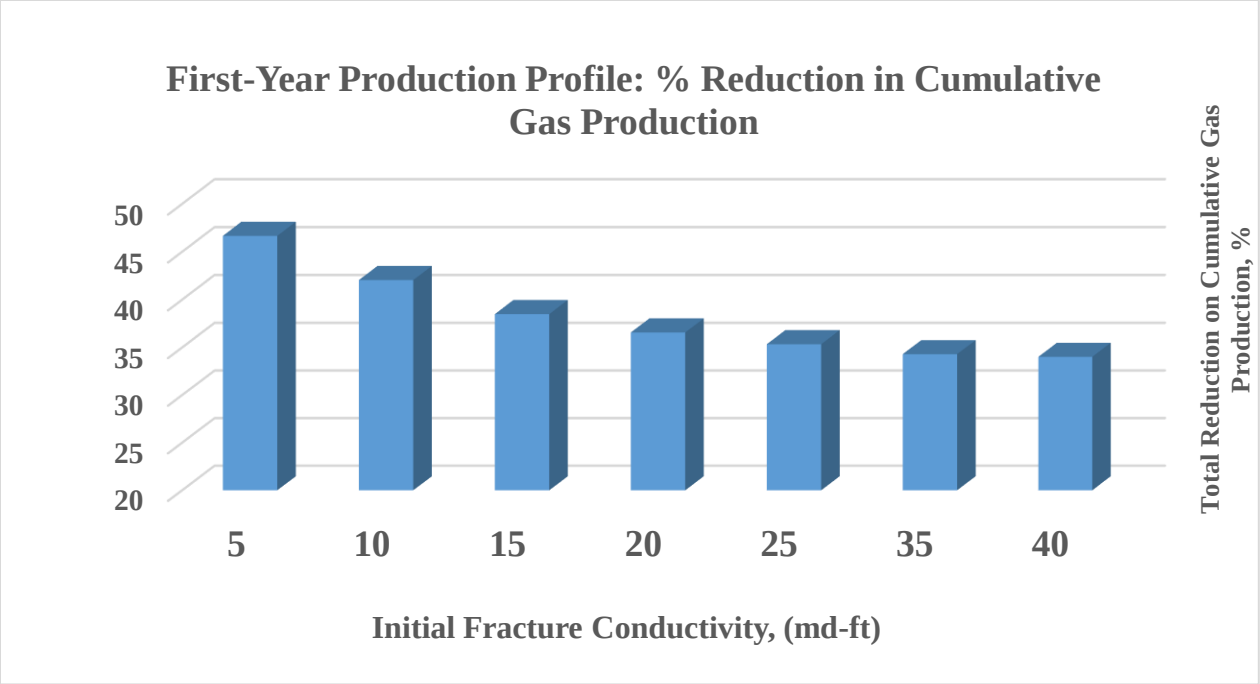

Figure 36: Percent Reduction in cumulative gas production for different values of the Initial hydraulic fracture conductivity.

From the figure above (Figure 36), it can be illustrated that the lowest initial fracture conductivity (5 md-ft) has the highest adverse impact on the percent reduction in gas recovery by 46.6%, whereas the highest fracture conductivity (40 md-ft) showed the least impact by roughly 34.0%. Similarly, the same approach has been applied but on a different production profile of 5 years to observe the impact on the gas recovery throughout the late life of the well. The tables below will illustrate the 5-year production profile, as well as the charts for each initial fracture conductivity.

Table 10: 5-Year Initial fracture conductivity on the cumulative gas production with no compressibility impacts

Compressibility Impact	5-Year Production Profile	
	Initial Fracture Conductivity	Cumulative Gas Production
	md-ft	SC (MMSCF)
	5	839
	10	986
	15	1059
	20	1098
	25	1124
	35	1153
	40	1162

Table 11: 5-Year Initial fracture conductivity on the cumulative gas production with no compressibility impacts

No Compressibility Impact	5-Year Production Profile	
	Initial Fracture Conductivity	Cumulative Gas Production
	md-ft	SC (MMSCF)
	5	1353
	10	1420
	15	1446
	20	1460
	25	1469
	35	1480
	40	1484

Table 12: 5-Year % reduction of Initial fracture conductivity on the cumulative gas production

% Reduction Change	5-Year Production Profile	
	Initial Fracture Conductivity	Total Reduction in Cumulative Gas Production
	md-ft	%
	5	37.9938
	10	30.5288
	15	26.7947
	20	24.7945
	25	23.5003
	35	22.1343
	40	21.7164

Generally, higher gas production rates are due to the increase in the initial fracture conductivity whether the impact of the compressibility and compaction was applied to that model, and this was showed for the different production profiles of 1-year and 5-year to demonstrate and emphasize the case study.

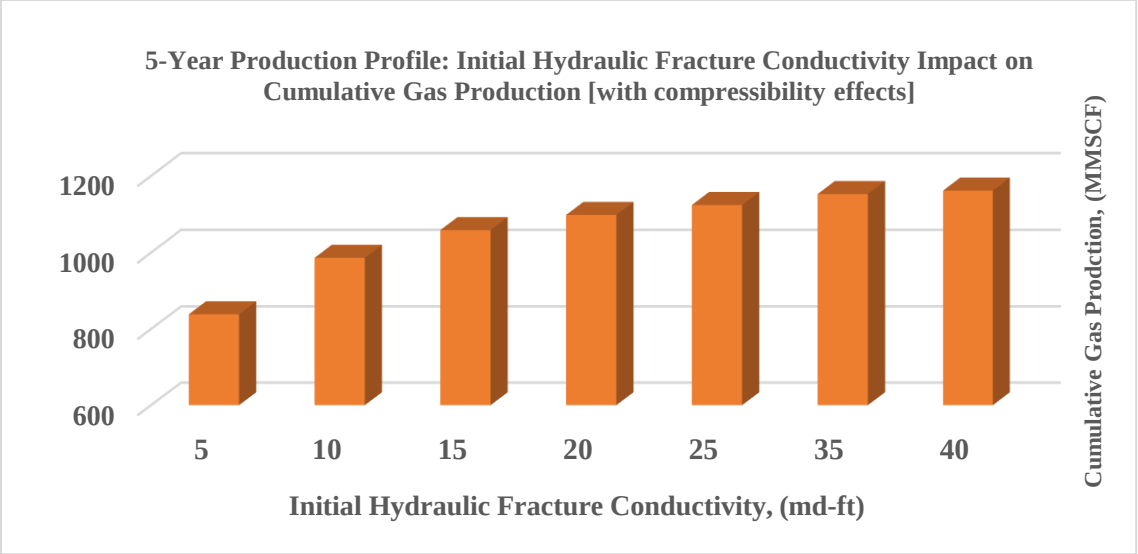

Figure 37: 5-Year Initial hydraulic fracture conductivity impact on the cumulative gas production (with compressibility effects)

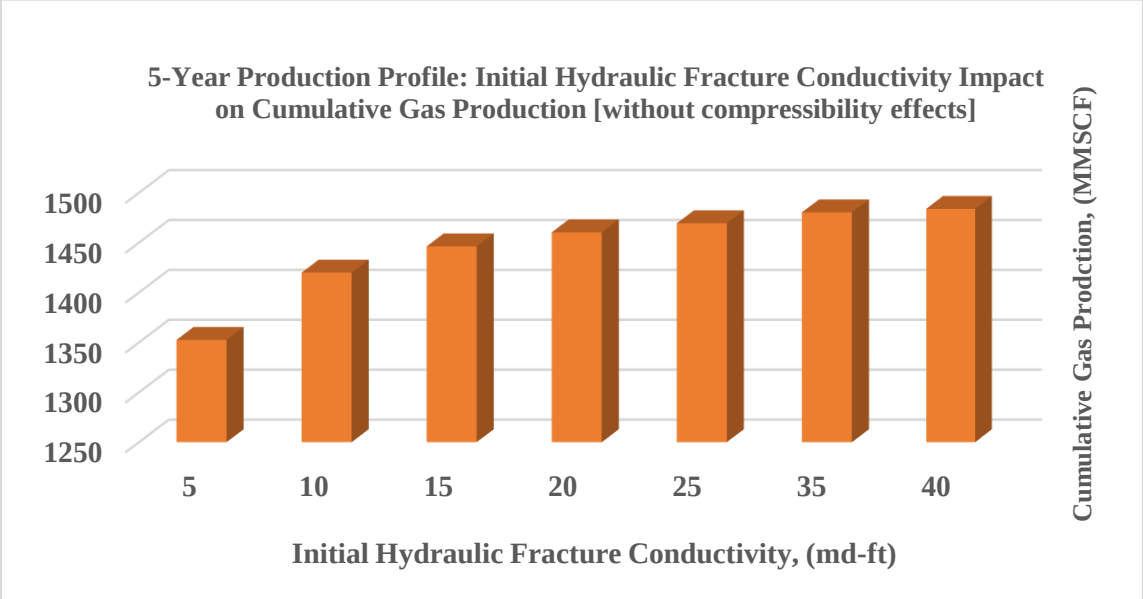

Figure 38: 5-Year Initial hydraulic fracture conductivity impact on the cumulative gas production (without compressibility effects)

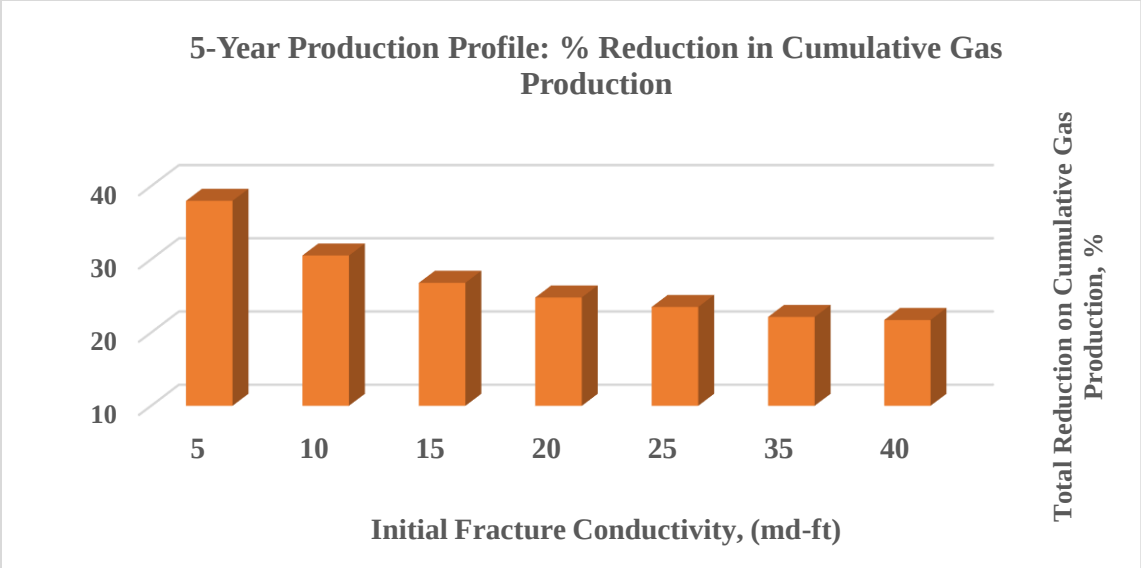

Figure 39: 5-Year percent Reduction in Initial hydraulic fracture conductivity impact on the cumulative gas production.

From the figure above (Figure 39), it can be illustrated that the lowest initial fracture conductivity (5 md-ft) has the highest adverse impact on the percent reduction in gas recovery by 37.9%, whereas the highest fracture conductivity (40 md-ft) showed the least impact on the percent reduction in gas recovery by roughly 21.7%.

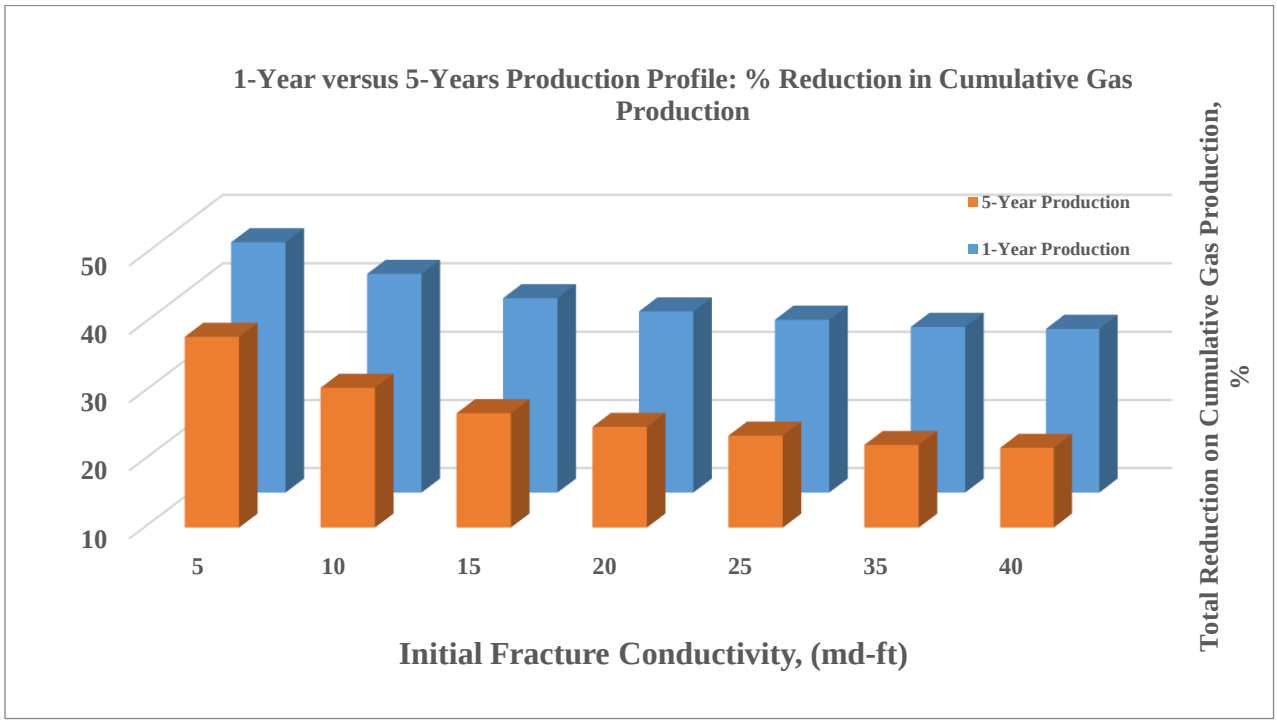

Figure 40: 5-Year percent Reduction in Initial hydraulic fracture conductivity impact on the cumulative gas production.

The figure above, (Figure 40) will illustrate the percent reduction in the cumulative gas production affected by the initial fracture conductivity for the different fracture conductivities, 5, 10, 15, 20, 25, 35, and 40 (md-ft) between the 1-year and the 5-year production profiles. As illustrated in the chart below (Figure 41), the initial fracture conductivities started to increase sharply from an effective of 4000 psi. During the early-production time, as the effective stress increases the initial fracture conductivity increases represented by a directly proportional relationship. However, this increasing effect diminishes over time as can be observed between the years 4 to 6 where the change is very slight due to a drop in the production rates.

For instance, the 1-year production profile for regarding the higher conductivities [25 md-ft and above] had a percent reduction in the cumulative gas production an average of 34.5%, whereas for the 5-year production profile the higher conductivities had an average of 22.45% which proves the early-production time has a higher impact on the percent reduction in gas recovery.

Lastly, the higher initial hydraulic fracture conductivity values ranging from 25 md-ft and above the reduction in the cumulative gas production was observed to be constant, and this was illustrated by observing the impact of it on the effective stress for the stimulated reservoir volume (SRV).

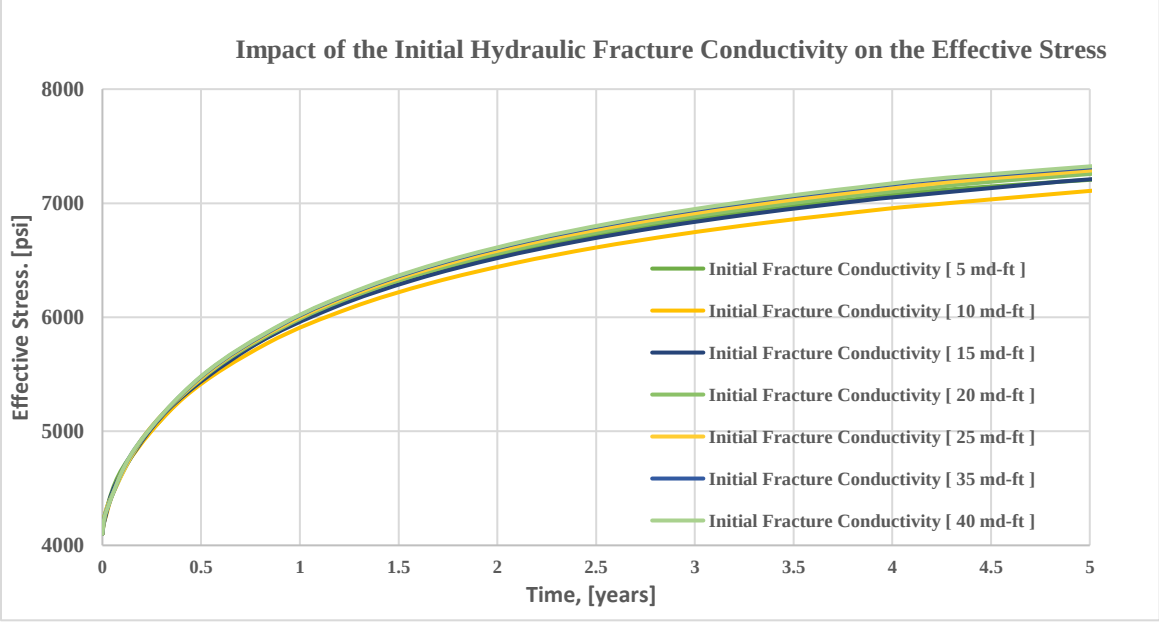

Figure 41: The impact of the initial fracture conductivity on the effective stress for well MIP-6H

On the other hand, (Figure 41) demonstrated how the wide range of initial fracture conductivities can contribute to impacting the effective stress, thus enhancing the productivity of the multi-stage fractured horizontal well. As can be observed, as the initial fracture conductivity increases, the effective stress acting on the stimulated reservoir volume (SRV) increases over time. Generally, during the hydraulic fracturing phase a proppant is injected into the fracture to keep it open. As a result, higher proppant into the fracture increases the conductivity whereas having less proppant in the fracture reduces the size of its which limits the stress to act on it. Higher production rates require high initial fracture conductivity to keep the fracture open leading to an increase in the effective stress.

The higher values of the initial fracture conductivity, [25, 35, 40 md-ft] showed a slight large impact on the effective stress. However, the smaller values of the initial fracture conductivity [5, 10 md-ft] had the same trend but it was slightly lower than the higher values. In fact, the effective stress impact diminishes over-time for the higher conductivity values by having a slight no change, semi-constant change on the productivity of the well.

4.2.2 FRACTURE SPACING

In order to investigate the impact of the fracture spacing associated with the number of stages on the stimulated reservoir volume (SRV), three production profiles were generated for further analysis. The first production profile represents the early-production time of the well by selecting the first 30 days. On the other hand, the second production profile was chosen to be 5 years to investigate the effect over a longer period of production over time. Lastly, the third production profile was chosen to represent the 1-year. The figure below (Figure 42) represent a schematic of the fracture spacing, stages, and fracture half-length of a horizontal well and how each is related to the other. As can be observed, the more fracture stages in the wellbore reduces the fracture spacing in between. For the base model, initially, there were eight hydraulic fracture stages with a 300 ft hydraulically fractured spaces. For this study, testing higher values of the fracture stages to 12, and 16 stages to investigate the impact of the fracture spacing on the cumulative gas production of the multi-stage fractured horizontal well.

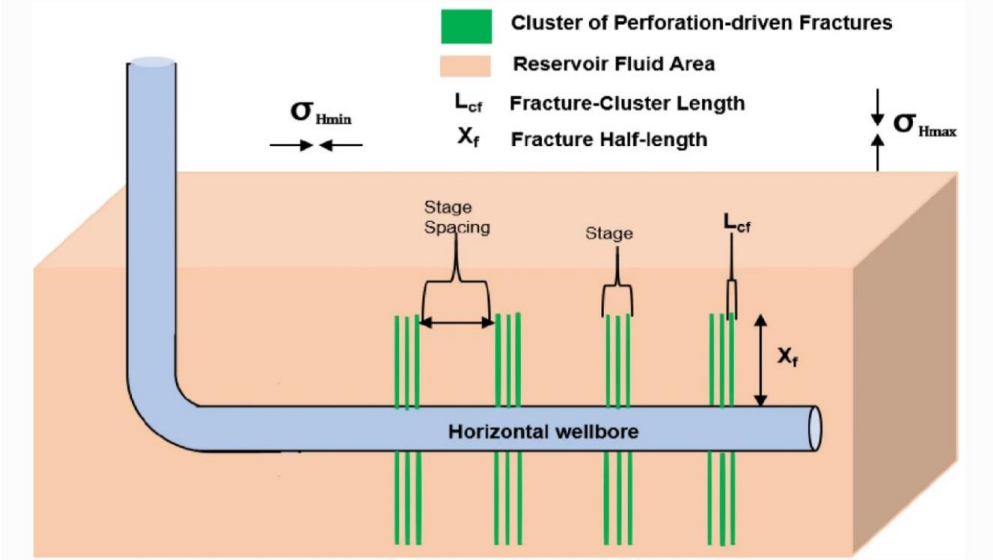

Figure 42: A Schematic of a horizontal well showing the fracture half-length and fracture spacing (Kolawole, O., Wigwe, M., Ispas, I. et al., 2020)

The tables below illustrate the results of the 30-days production profile for the different fracture stages values impact on the cumulative gas production with including and excluding the compressibility impacts as well as the percent reduction impact on the productivity of the well.

Table 13: 30-Days percent reduction of hydraulic fracture spacing on the cumulative gas production for well MIP-6H

% Reduction Change	30-Days Production Profile	
	Number of Stages	Total Reduction in Cumulative Gas Production
		%
	8	43.4862
	12	43.8309
	16	44.1832

Table 14: 30-Days hydraulic fracture spacing on the cumulative gas production with compressibility impacts

Compressibility Impact	30-Days Production Profile	
	Number of Stages	Cumulative Gas Production
		SC (MMSCF)
	8	86
	12	134
	16	175

Table 15: 30-Days hydraulic fracture spacing on the cumulative gas production with no compressibility impacts

No Compressibility Impact	30-Days Production Profile	
	Number of Stages	Cumulative Gas Production
		SC (MMSCF)
	8	152
	12	239
	16	314

It was observed that, Including the compressibility impacts resulted in reducing the cumulative gas production rates for the 8-stages case with a recorded value of 86 MMscf, unlike removing the compressibility impacts for the 8-stages resulted in a higher cumulative gas production of 152 MMscf. As the fracture stages increase, the cumulative gas production increases accordingly, for the lower stage spacing cases (higher fracture stages). To illustrate, the following figures represent the impact of the fracture spacing on the productivity of the well for each case study on the 30-days production profile, respectively.

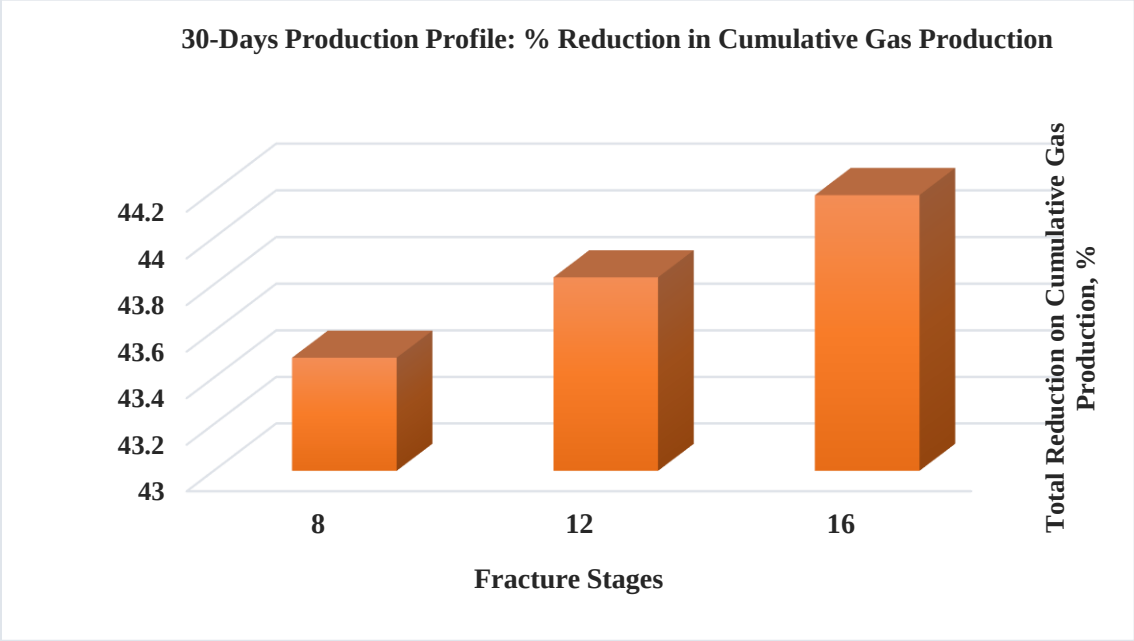

Figure 43: 30-Days percent Reduction hydraulic fracture stages impact on the cumulative gas production.

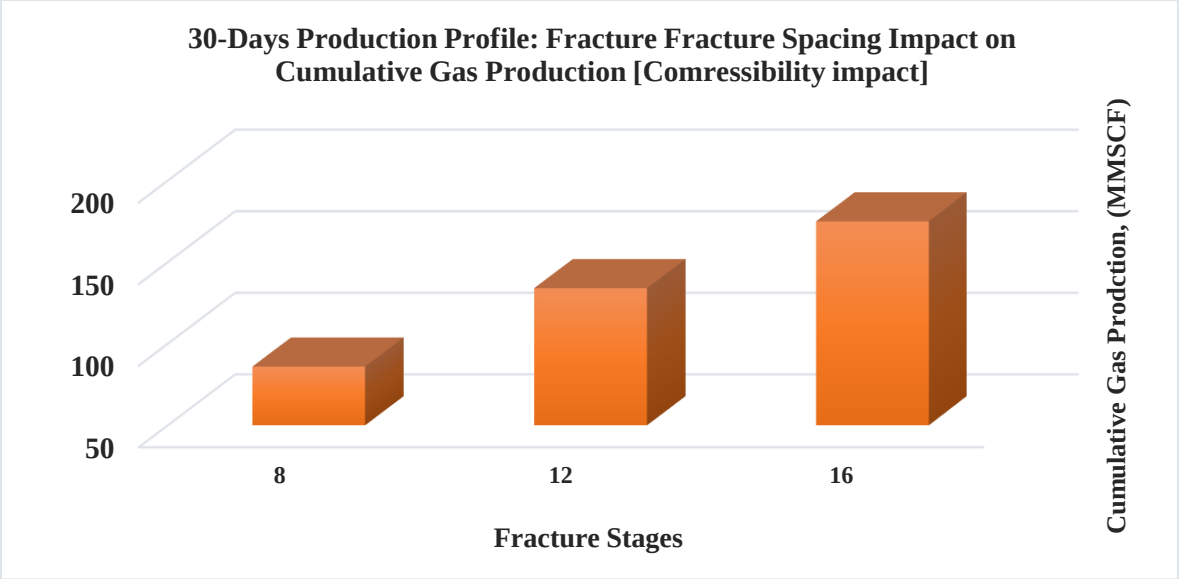

Figure 44: 30-Days hydraulic fracture stages impact on the cumulative gas production (compressibility effects)

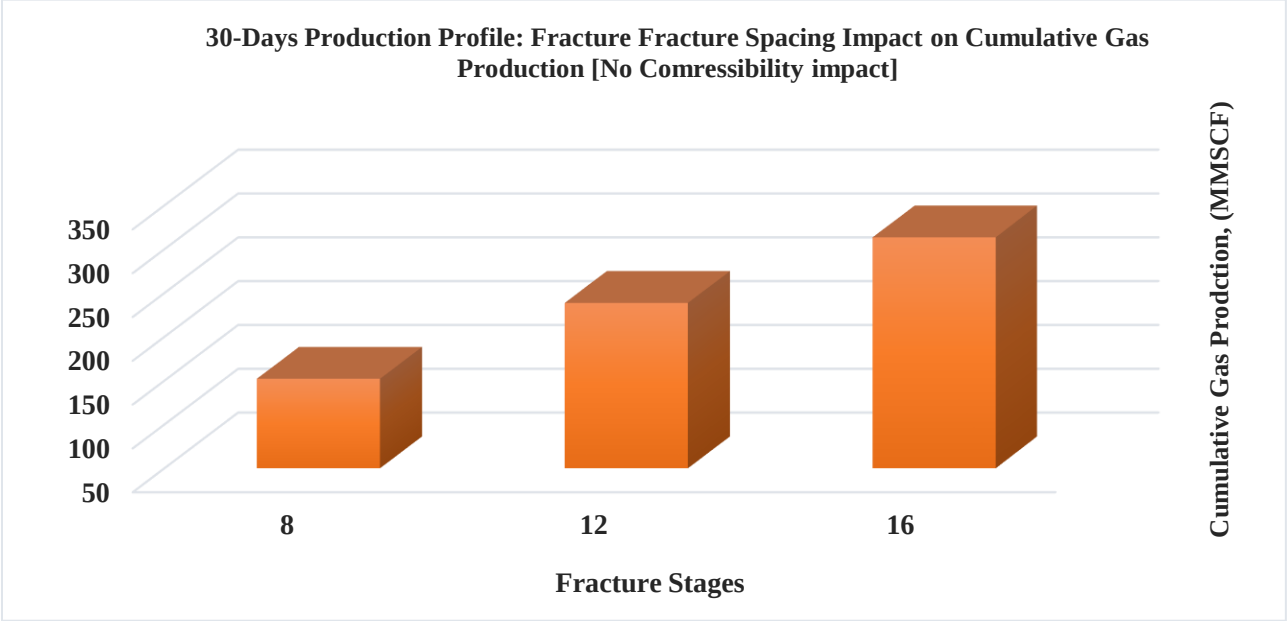

Figure 45: 30-Days hydraulic fracture stages impact on the cumulative gas production (no compressibility effects)

From the figures above, the higher the fracture stages (12, and 16 stages) the more gas rate from the well was produced by aligned with a decrease in the fracture spacing. As a result, this confirms the inverse relationship between the fracture spacing and the fracture stages in the wellbore and how it affects the production during the early fluid-flow phase.

On the other hand, the tables below illustrate the results of the 1-year production profile for the different fracture stages values impact on the cumulative gas production with including and excluding the compressibility impacts as well as the percent reduction impact on the productivity of the well.

Table 16: 1-year percent reduction of hydraulic fracture spacing on the cumulative gas production for well MIP-6H

% Reduction Change	1-Year Production Profile	
	Fracture Spacing	Total Reduction in Cumulative Gas Production
		%
	8	36.5697
	12	32.9587
	16	31.5144

Table 17: 1-year hydraulic fracture spacing on the cumulative gas production with compressibility impacts

Compressibility Impact	1-Year Production Profile	
	Fracture Spacing	Cumulative Gas Production
		SC (MMSCF)
	8	437
	12	616
	16	759

Table 18: 1-year hydraulic fracture spacing on the cumulative gas production with no compressibility impacts

No Compressibility Impact	1-Year Production Profile	
	Fracture Spacing	Cumulative Gas Production
		SC (MMSCF)
	8	689
	12	919
	16	1108

It was observed that, Including the compressibility impacts resulted in reducing the cumulative gas production rates for the 8-stages case with a recorded value of 437 MMscf, unlike removing the compressibility impacts for the 8-stages resulted in a higher cumulative gas production of 689 MMscf. As the fracture stages increase, the cumulative gas production increases

accordingly, for the lower stage spacing cases (higher fracture stages). To illustrate, the following figures represent the impact of the fracture spacing on the productivity of the well for each case study on the 1-year production profile, respectively.

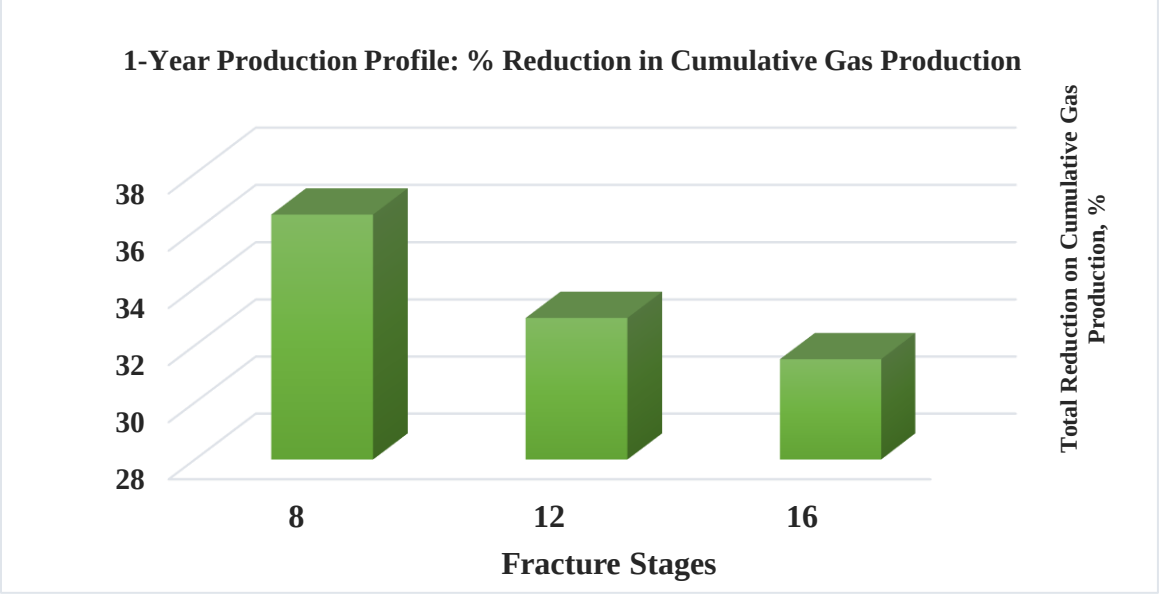

Figure 46: First-year percent reduction hydraulic fracture stages impact on the cumulative gas production.

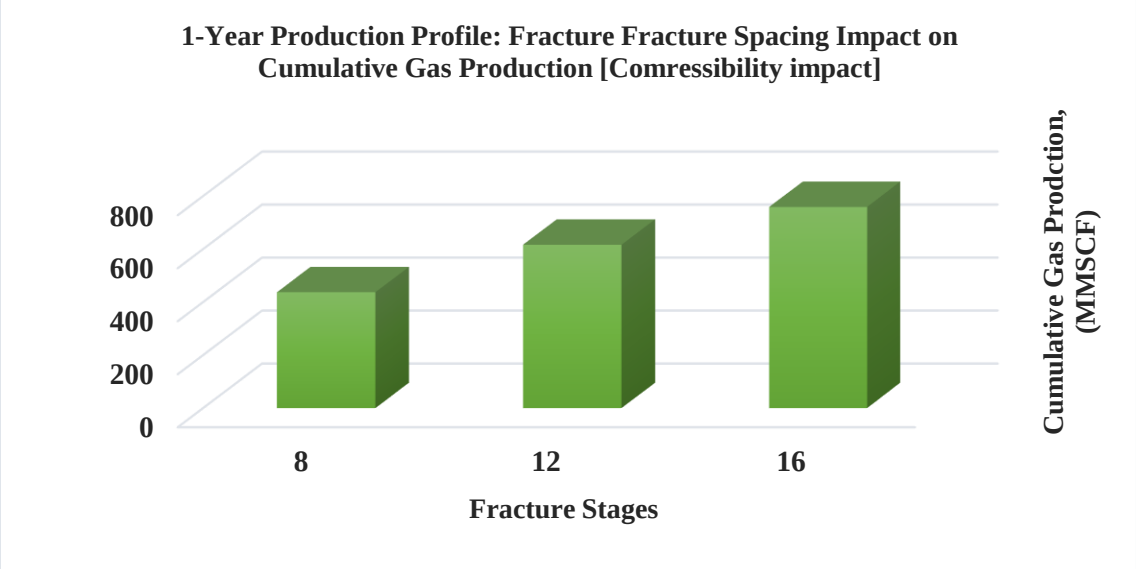

Figure 47: First-year hydraulic fracture stages impact on the cumulative gas production (with compressibility effects)

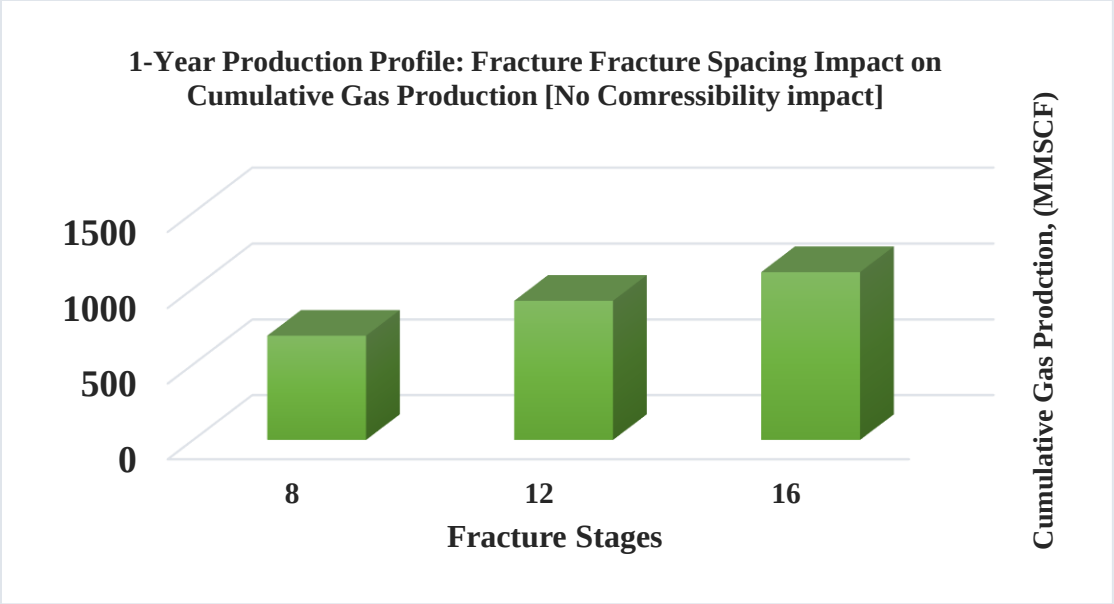

Figure 48: First-year hydraulic fracture stages impact on the cumulative gas production (without compressibility effects)

On the other hand, the tables below illustrate the results of the 5-years production profile for the different fracture stages values impact on the cumulative gas production with including and excluding the compressibility impacts as well as the percent reduction impact on the productivity of the well. For the 5-year production profile, the analysis was the opposite of the 30-days production profile impact of the fracture stages on the productivity of the well, where these will be illustrated below.

Table 19: 5-Years percent reduction of hydraulic fracture spacing on the cumulative gas production for well MIP-6H

% Reduction Change	5-Year Production Profile	
	Number of Stages	Total Reduction in Cumulative Gas Production
	-	%
	8	24.7945
	12	19.4719
	16	17.2122

Table 20: 5-Years hydraulic fracture spacing on the cumulative gas production with compressibility impacts

Compressibility Impact	5-Year Production Profile	
	Number of Stages	Cumulative Gas Production
	-	SC (MMSCF)
	8	1098
	12	1275
	16	1462

Table 21: 5-Years hydraulic fracture spacing on the cumulative gas production with no compressibility impacts

No Compressibility Impact	5-Year Production Profile	
	Number of Stages	Cumulative Gas Production
	-	SC (MMSCF)
	8	1460
	12	1583
	16	1766

It was observed that, Including the compressibility impacts resulted in reducing the cumulative gas production rates for the 8-stages which was the lowest with a recorded value of 1098 MMscf, unlike removing the compressibility impacts for the 8-stages resulted in a higher cumulative gas production of 1460 MMscf, which concludes a difference of 362 MMscf. As the fracture stages increase, the cumulative gas production increases accordingly, for the lower stage spacing cases (higher fracture stages).

To illustrate, the following figures below represent the impact of the fracture spacing on the productivity of the well for each case study on the 5-years production profile, respectively. As a matter of fact, both production profiles had the opposite impact as the lowest fracture stages had the lowest gas rate in the 30-days production, then the opposite occurred for the 5-year production profile as the fracture stages were increasing, the gas production rate started to decrease. From the figures below, the 16 stages showed the highest positive impact on the gas production unlike the low base case with 8 stages. Whereas the percent reduction in the cumulative gas production showed the highest percent change in the 8 stages (base case).

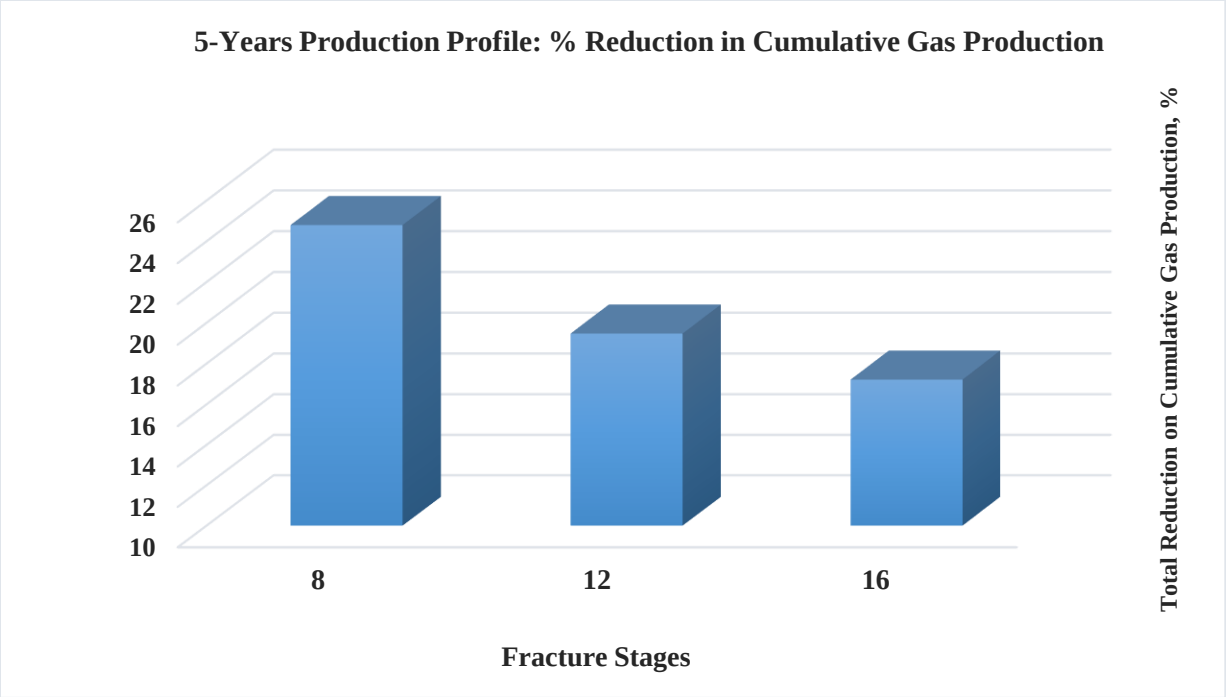

Figure 49: 5-Years percent Reduction hydraulic fracture stages impact on the cumulative gas production.

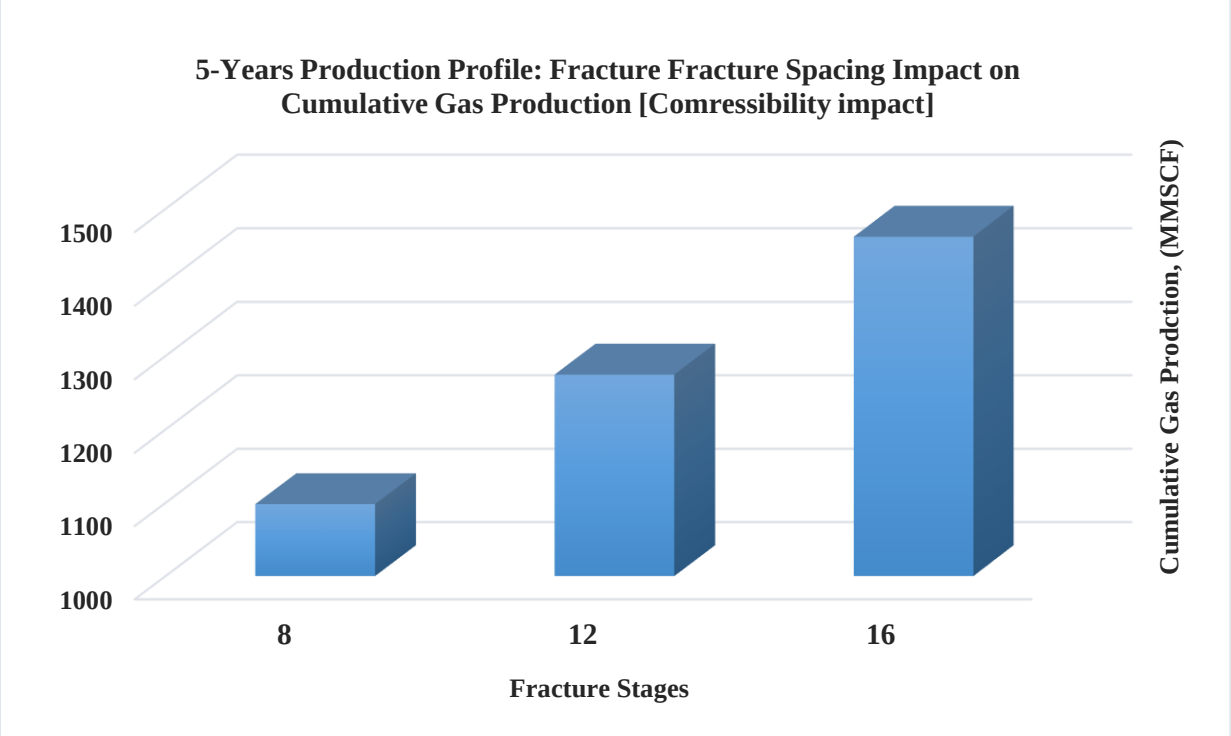

Figure 50: 5-Years hydraulic fracture stages impact on the cumulative gas production (compressibility effects)

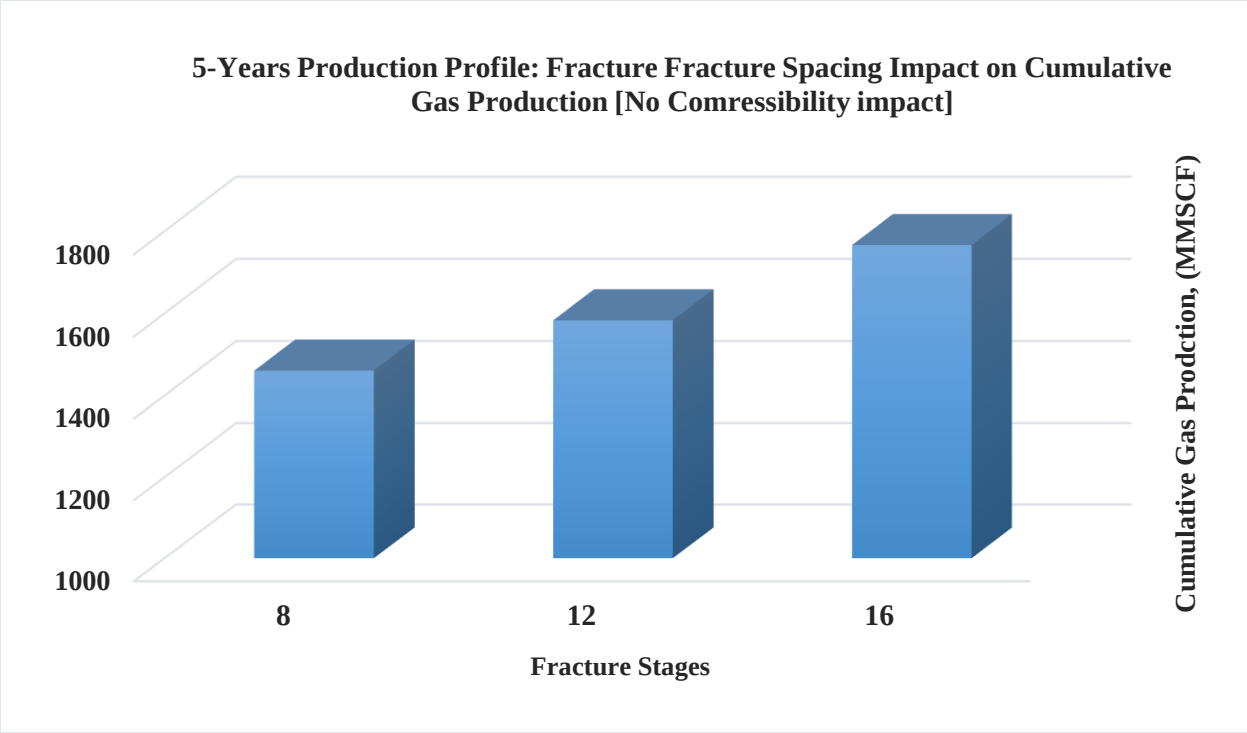

Figure 51: 5-Years hydraulic fracture stages impact on the cumulative gas production (no compressibility effects)

The figure below (Figure 52), illustrates a combination percent change in the cumulative gas production of the two production profiles (30-days, and 5-years) and their total impact on the productivity of the MIP-6H well. Generally, due to an increased production at the early stages of the well lowers the porosity, permeability of both the matrix and the natural fractures inducing the fluid to flow out of the wellbore.

As a result, the 30-days production profile illustrated this phenomenon as it showed an increased yet diminishing effect of the different fracture stages on the gas production, unlike both the 1-year and 5-year production profile which showed a decrease in all of the fracture stages due to decreased production rates throughout the remaining life of the well. Additionally, the 30-days production profile mimic the early stages of production whereas from the years 1-5 the gas production rates are lower and declining.

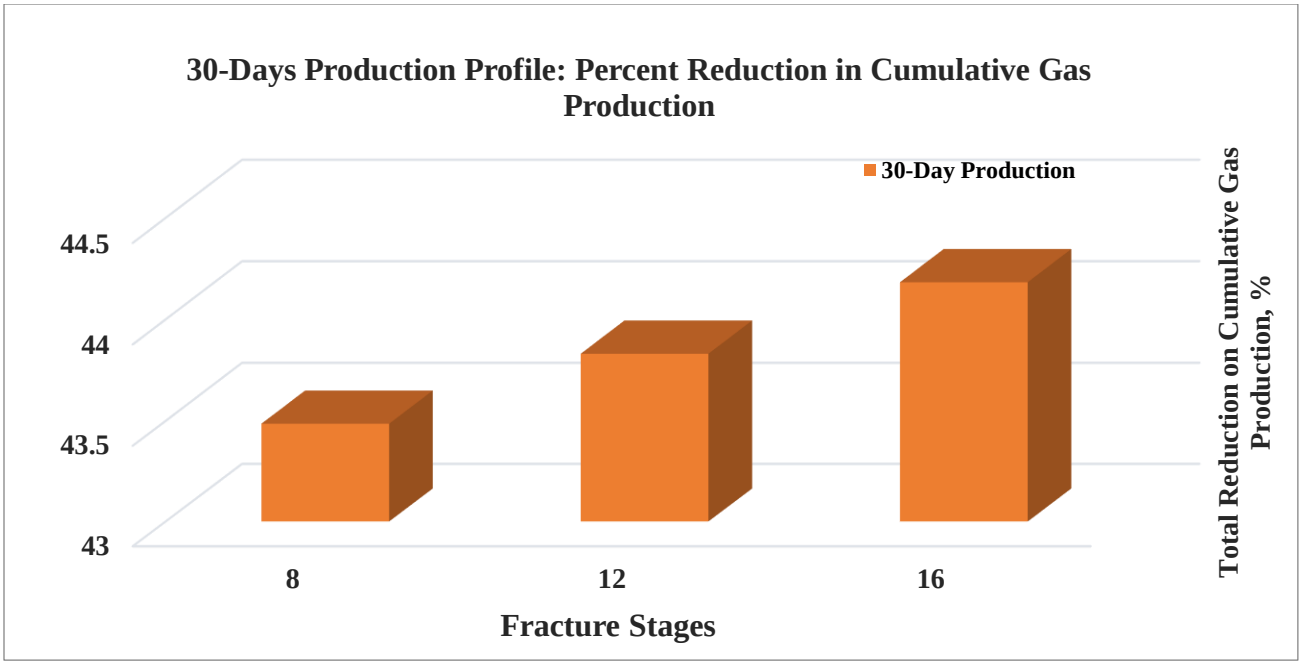

Figure 52: The percent reduction in the cumulative gas production of the 30-days production profile for well MIP-6H for the different fracture stages.

Additionally, the figure below (Figure 53), illustrates a combination percent change in the cumulative gas production of the two production profiles (1-year, and 5-years) and their total impact on the productivity of the MIP-6H well.

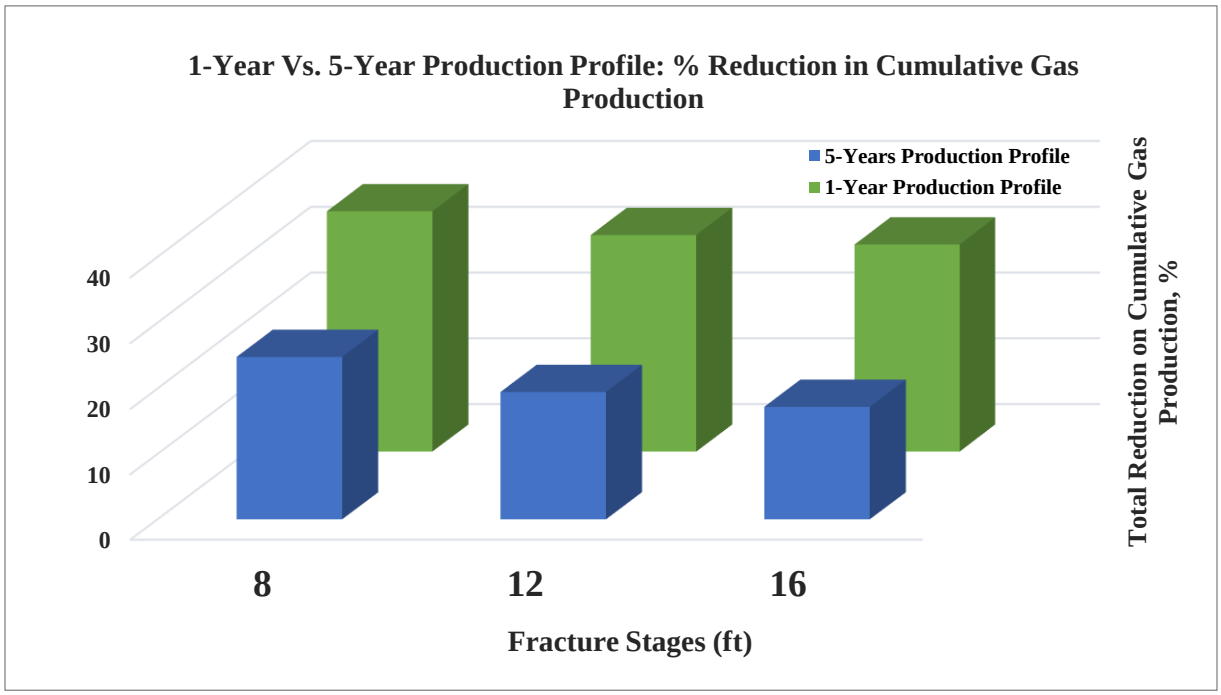

Figure 53: The percent reduction in the cumulative gas production of the 1-year versus the 5-year production profile for well MIP-6H for the different fracture stages.

Lastly, the impact of the different fracture stages had a noticeable impact on the effective stress which confirms the claims of this study. The figure below (Figure 54), illustrate the impact of the effective stress on the fracture spacing for the MIP-6H for a time window of 15 years having the same increasing trend for the previous parametric studies which confirms that including the compressibility impacts could alter the effective stress acting on the stimulated reservoir volume for the well.

Although the difference in the effective stress is not large, this increasing trend diminishes over-time due to the low production gas rates. The adverse compressibility impacts are usually more pronounced during the early production times, compaction which aid in the reduction of the permeability, porosity and hydraulic fracture conductivity causing an enhancement for the fluid-flow in the formation.

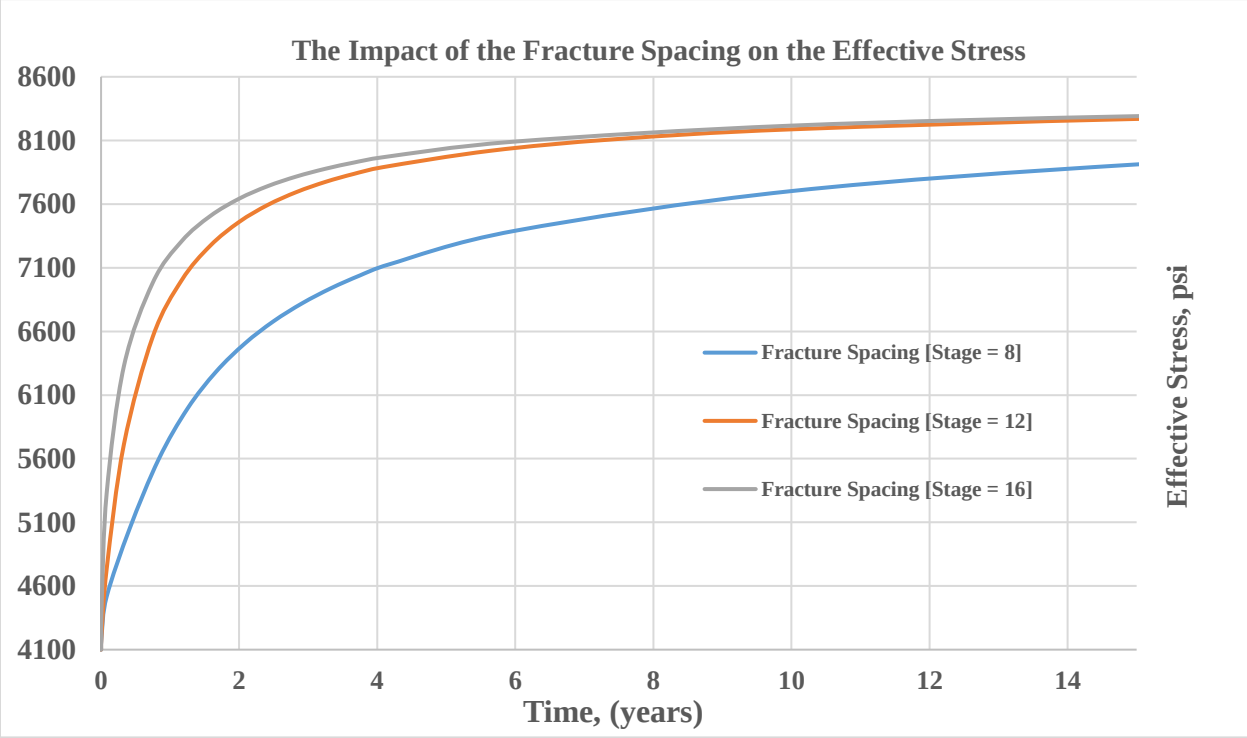

Figure 54: The impact of the hydraulic fractures spacing and fractures on the effective stress for well MIP-6H

As can be observed from the figure above (Figure 54), the effective stress increases rapidly for the higher stages' values (12, and 16) which means there is less fracture spacing compared to the lower fracture stage case (the base case), which remains almost constant throughout the remaining life of the well. In addition, this is due to the high volume of the gas recovery in the early stages of the production phase. After 15 years, the lowest fracture spacing with the highest

fracture stages (16 stages) had a total effective stress of 8291 psi whereas the lower fracture spacing had a lower effective stress of 7912 psi.

4.2.3 FRACTURE HALF-LENGTH

In order to investigate the impact of the hydraulic fracture half-length on the inside and outside stimulated reservoir volume (SRV), two production profiles were generated for further analysis. The first production profile represents the early-production time of the well by selecting 1 year. On the other hand, the second production profile was chosen to be 5 years to investigate the effect over a longer period of production over time. Additionally, the compressibility impacts have been included to the model and act as a geomechanical barrier in comparison to the results with no compressibility impact.

This approach was used in the study in order to provide a more realistic simulated production profile to limit the over-estimation or under-estimation of the gas reserves production. The tables below illustrate the results obtained from the 1-year production profile including the compressibility impacts and without.

Table 22: First-Year percent reduction of hydraulic fracture half-length on the cumulative gas production for well MIP-6H

% Reduction Change	First-Year Production Profile	
	Fracture Half-Length	Total Reduction in Cumulative Gas Production
	ft	%
	100	32.8021
	200	34.1512
	300	36.5697
	400	39.0113

Table 23: First-Year hydraulic fracture half-length on the cumulative gas production with compressibility impacts

Compressibility Impact	First-Year Production Profile	
	Fracture Half-Length	Cumulative Gas Production
	ft	SC (MMSCF)
	100	214
	200	335
	300	437
	400	518

Table 24: First-Year hydraulic fracture half-length on the cumulative gas production with no compressibility impacts

No Compressibility Impact	First-Year Production Profile	
	Fracture Half-Length	Cumulative Gas Production
	ft	SC (MMSCF)
	100	318
	200	509
	300	689
	400	850

During the 1-year production profile, as the fracture half-length increases, the cumulative gas production increases accordingly. The inclusion of the compressibility impacts lowered the cumulative gas production for this study which supports the claim.

As a result, with the highest fracture half-length of 400 ft, for the case including the compressibility impacts it recorded 518 MMscf of cumulative gas rate. Whereas the exclusion of the compressibility impacts for the same half-length recorded 850 MMscf which is higher by 332 MMscf. The percent reduction of the base case with 300 ft fracture half-length illustrated a 36.56% whereas the lowest case with 100 ft of fracture half-length showed the lowest reduction of 32.8%. The figures below demonstrate the 1-year production profile for the fracture half-length impact on the cumulative gas production of the well.

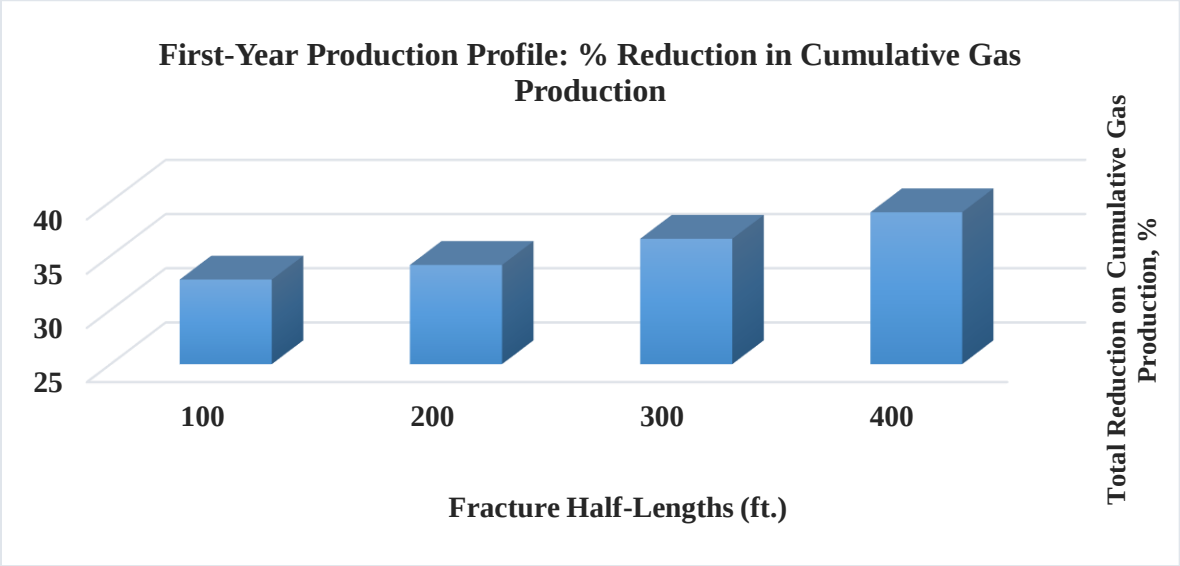

Figure 55: 1-Year % Reduction hydraulic fracture half-length impact on the cumulative gas production.

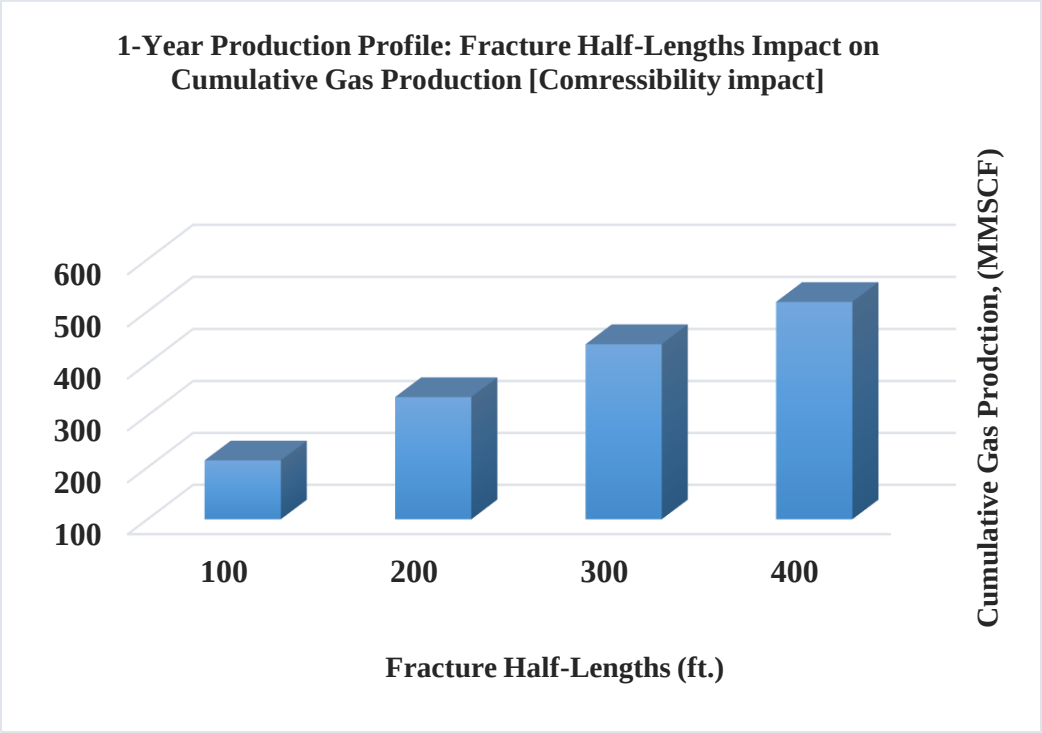

Figure 56: 1-Year hydraulic fracture half-length impact on the cumulative gas production (compressibility effects)

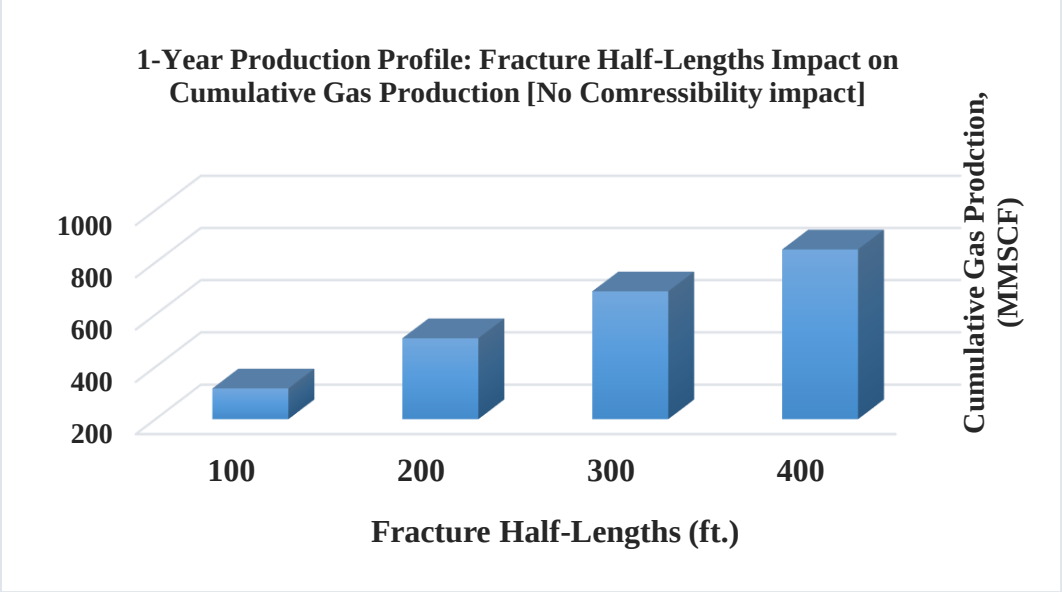

Figure 57: 1-Year hydraulic fracture half-length impact on the cumulative gas production (no compressibility effects)

On the other hand, during the 5-year production profile, as the fracture half-length increases, the cumulative gas production increases accordingly. However, the cumulative gas rate

is reduced due to a reduced production since the pore pressure is lowered after a while of producing. The inclusion of the compressibility impacts lowered the cumulative gas production for this study which supports the claim as well. Consequently, the production rates are higher due to an increase in the effective stress causing the fluid-flow mechanism to take place.

As a result, with the highest fracture half-length of 400 ft, for the case including the compressibility impacts it recorded 1279 MMscf of cumulative gas rate. Whereas the exclusion of the compressibility impacts for the same half-length recorded 1685 MMscf which is higher by 406 MMscf. The percent reduction of the base case with 300 ft fracture half-length illustrated a 24.48% whereas the lowest case with 100 ft of fracture half-length showed the highest reduction of 26.48%.

Table 25: 5-Years % reduction of hydraulic fracture half-length on the cumulative gas production for well MIP-6H

% Reduction Change	5-Year Production Profile	
	Fracture Half-Length	Total Reduction in Cumulative Gas Production
	ft	%
	100	26.4890
	200	25.4126
	300	24.7945
	400	24.1082

Table 26: 5-Years hydraulic fracture half-length on the cumulative gas production with compressibility impacts

Compressibility Impact	5-Year Production Profile	
	Fracture Half-Length	Cumulative Gas Production
	ft	SC (MMSCF)
	100	601
	200	867
	300	1098
	400	1279

Table 27: 5-Years hydraulic fracture half-length on the cumulative gas production with no compressibility impacts

No Compressibility Impact	5-Year Production Profile	
	Fracture Half-Length	Cumulative Gas Production

	ft	SC (MMSCF)
	100	818
	200	1162
	300	1460
	400	1685

The figures below demonstrate the 5-year production profile for the fracture half-length impact on the cumulative gas production of the well. It has been observed that the 5-year production profile does not exhibit significant differences for the various hydraulic fracture half-lengths. Consequently, from year 2 to year 5 the production rates of the well started to decline leading the effective stress to have a diminishing impact on the stimulated reservoir volume as can be shown in the graphs below.

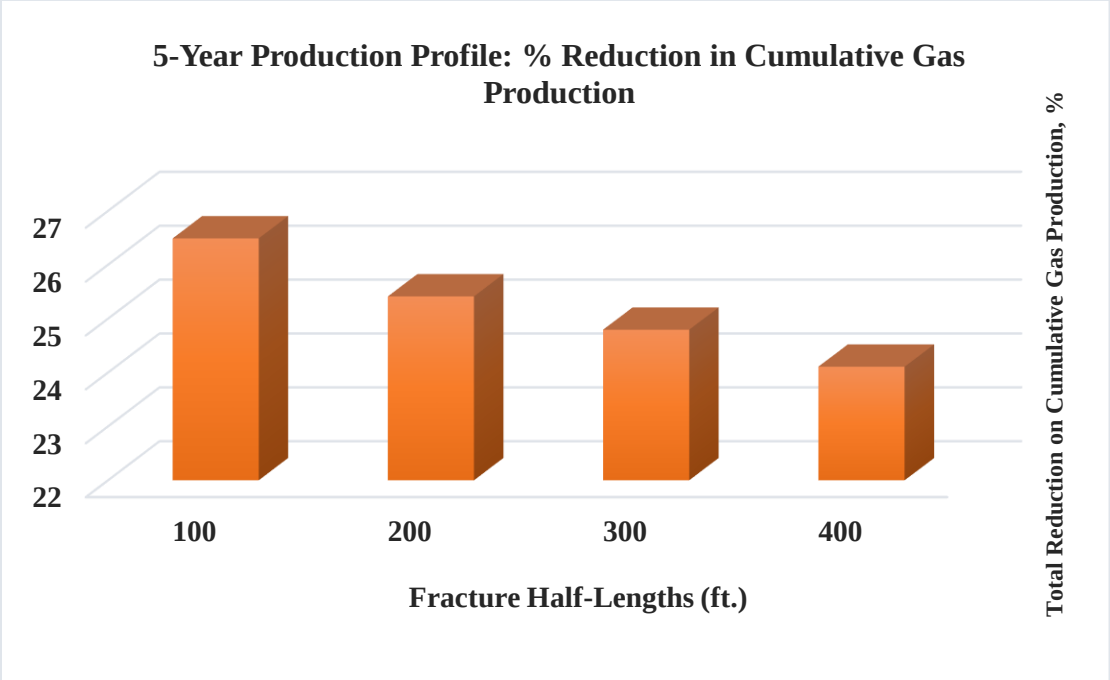

Figure 58: 5-Years Percent Reduction hydraulic fracture half-length impact on the cumulative gas production.

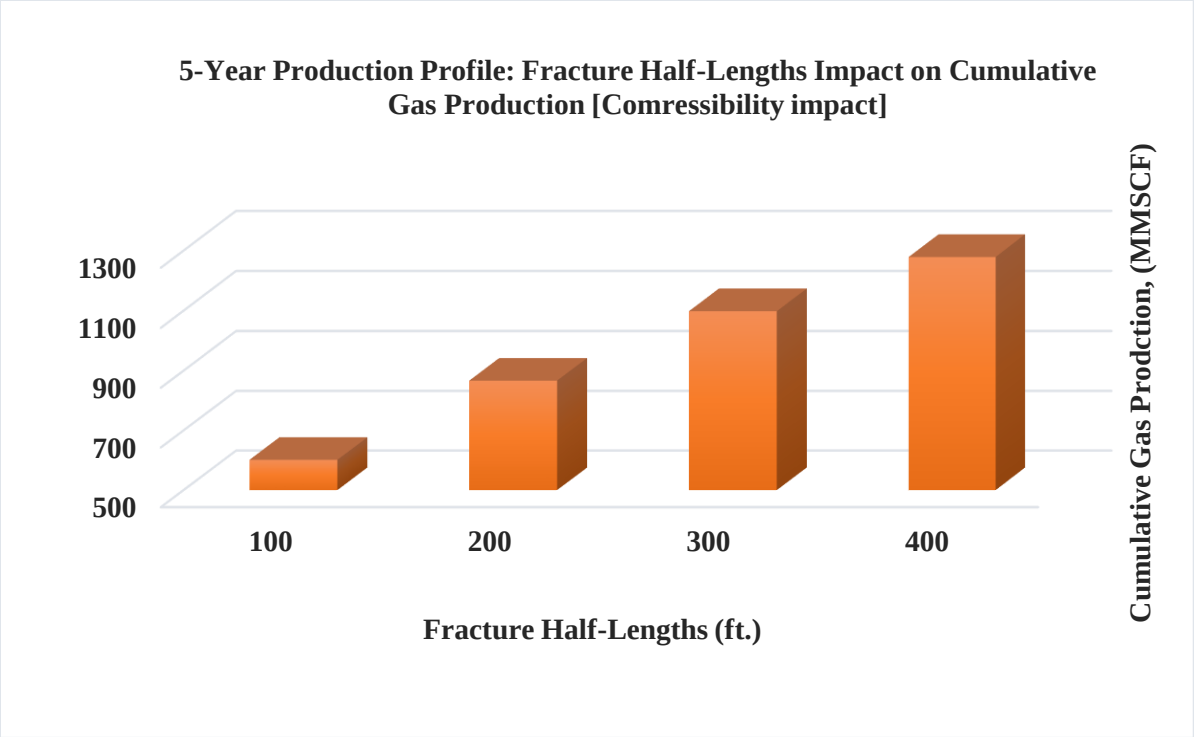

Figure 59: 5-Years hydraulic fracture half-length impact on the cumulative gas production (compressibility effects)

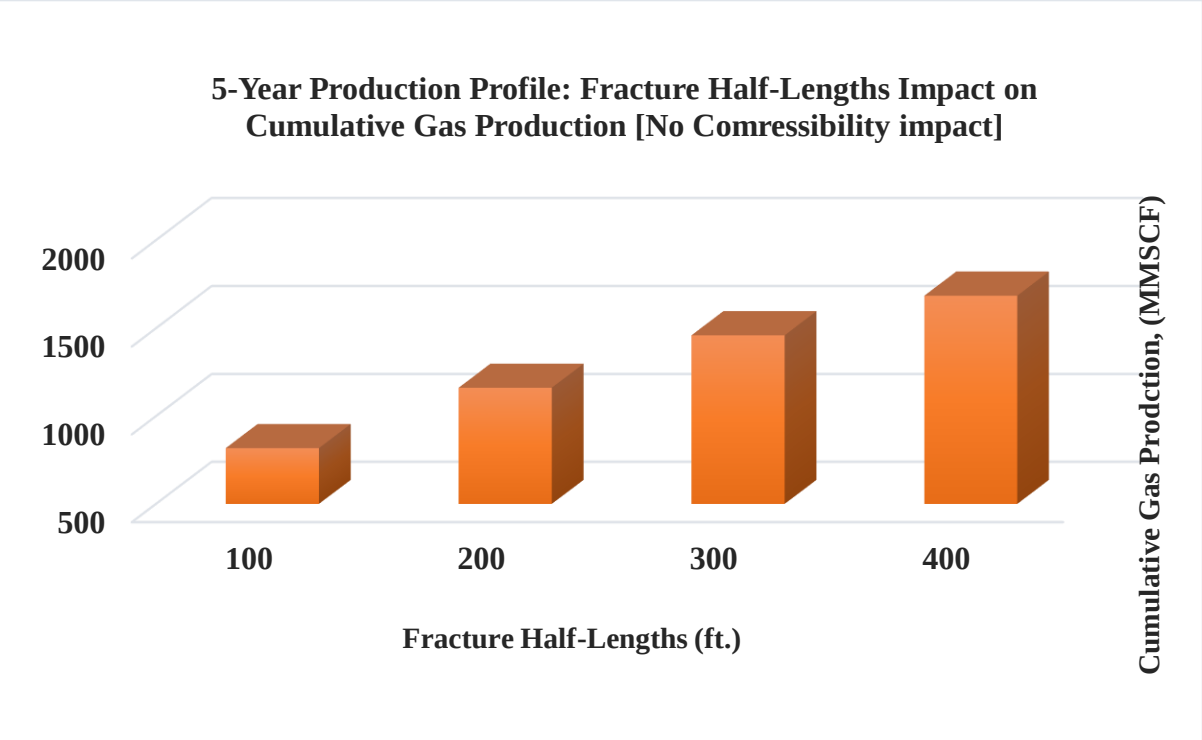

Figure 60: 5-Years hydraulic fracture half-length impact on the cumulative gas production (no compressibility effects)

The figure below (Figure 61), illustrates a combination of the percent change in the cumulative gas production of the two production profiles both 1-year and 5-year. The percent change was observed on the impact of productivity of the MIP-6H well. Generally, due to an increased production at the early stages of the well it lowered the porosity, permeability of both the matrix and the natural fractures inducing the fluid to flow out of the wellbore.

As a result, the 1-year production profile illustrated this phenomenon as it showed an increased yet diminishing effect of the different hydraulic fracture half-lengths on the gas production, unlike the 5-years production profile which showed a decrease in all of the hydraulic fracture half-length due to decreased production rate throughout the remaining life of the well.

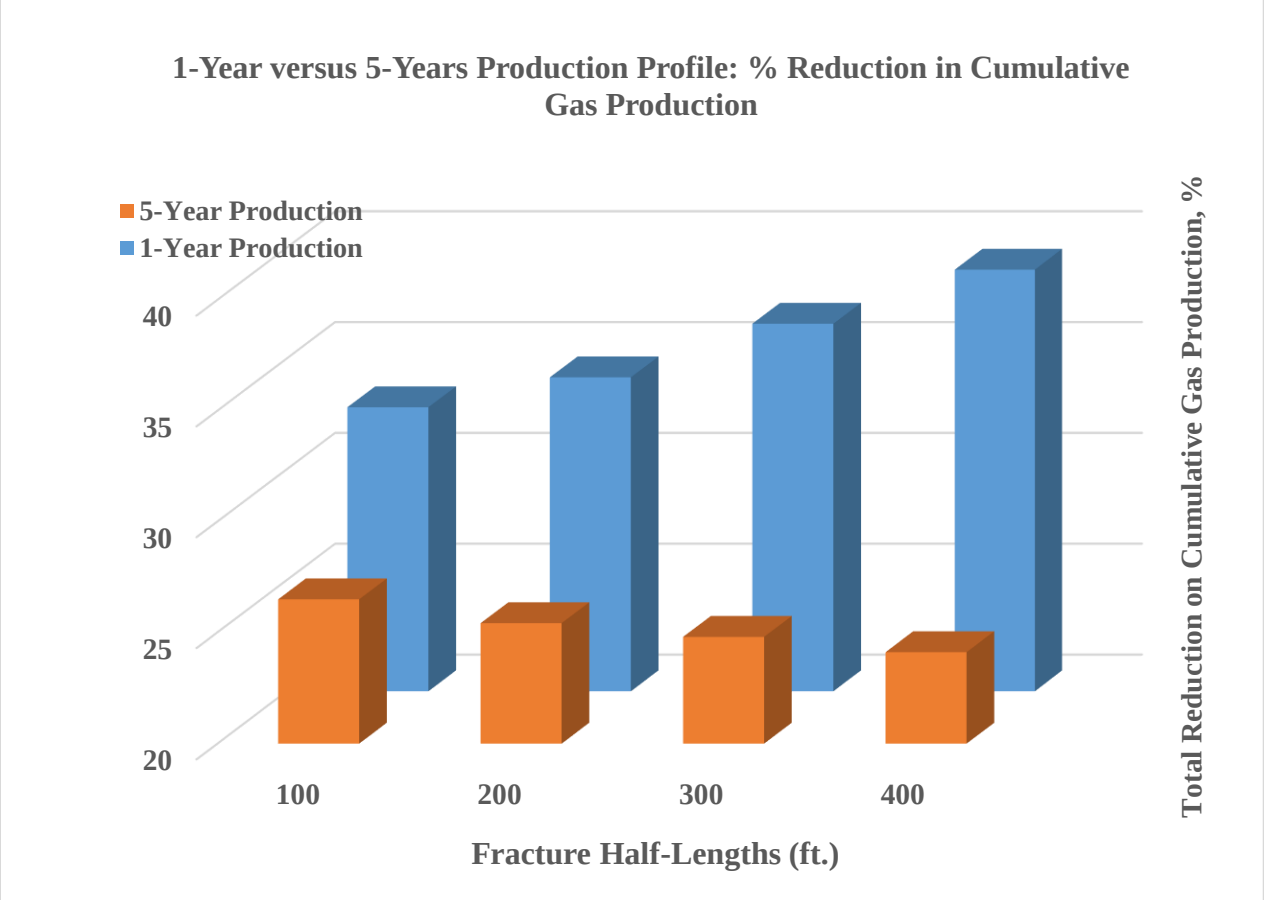

Figure 61: The percent reduction in the cumulative gas production of the 30-days versus the 5-year production profile for well MIP-6H for the different hydraulic fracture half-lengths.

In summary of the three parametric studies done on the hydraulic fracture properties, initial hydraulic fracture conductivity, hydraulic fracture spacing and stages, and lastly, hydraulic fracture half-length. Each case generated two production profiles during the early time and a later time for the well, with inclusion and exclusion of the compressibility impacts of the productivity

of the well as well as the effective stress. The two figures below have a significant value since the impact of the hydraulic fracture half-length was investigated not only inside the stimulated reservoir volume, but also from the outside to distinguish the difference.

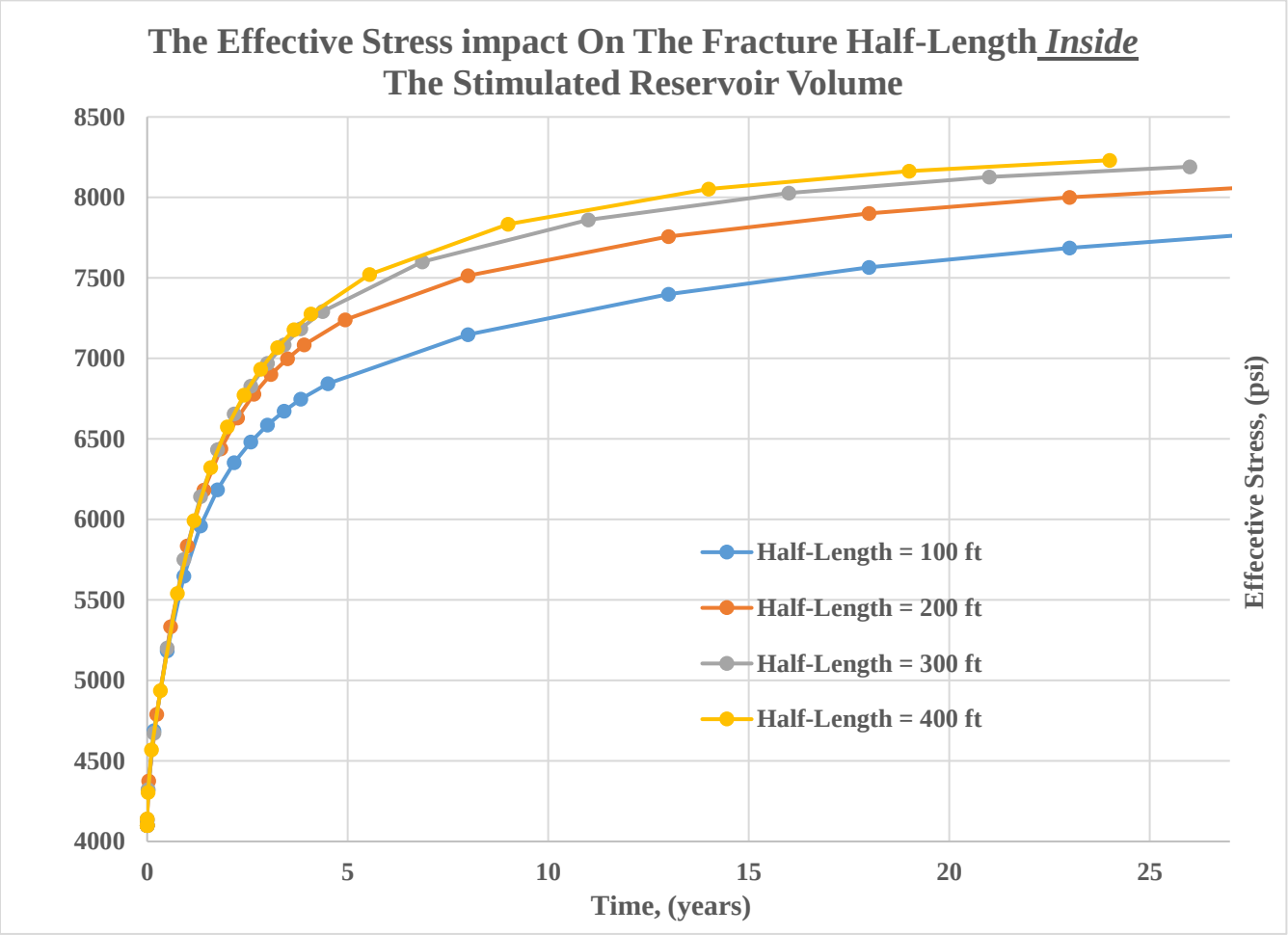

Figure 62: The impact of the hydraulic fracture half-length on the effective stress inside the stimulated reservoir volume for well MIP-6H

From the Figure above (Figure 62), the effective stress started to increase dramatically in the first 5-years and then showed a diminished impact later. As can be observed, as the fracture half-length increases throughout the life of the well, the effective stress increase accordingly. As the fracture half-length increases (xf = 400 ft.), the effective stress increases which showed the highest effective stress value at 8231 psi after 23 years. On the other hand, the lowest half-length of 100 ft had an effective stress of 7687 psi in the same year which results in a total reduction of 544 psi in effective stress.

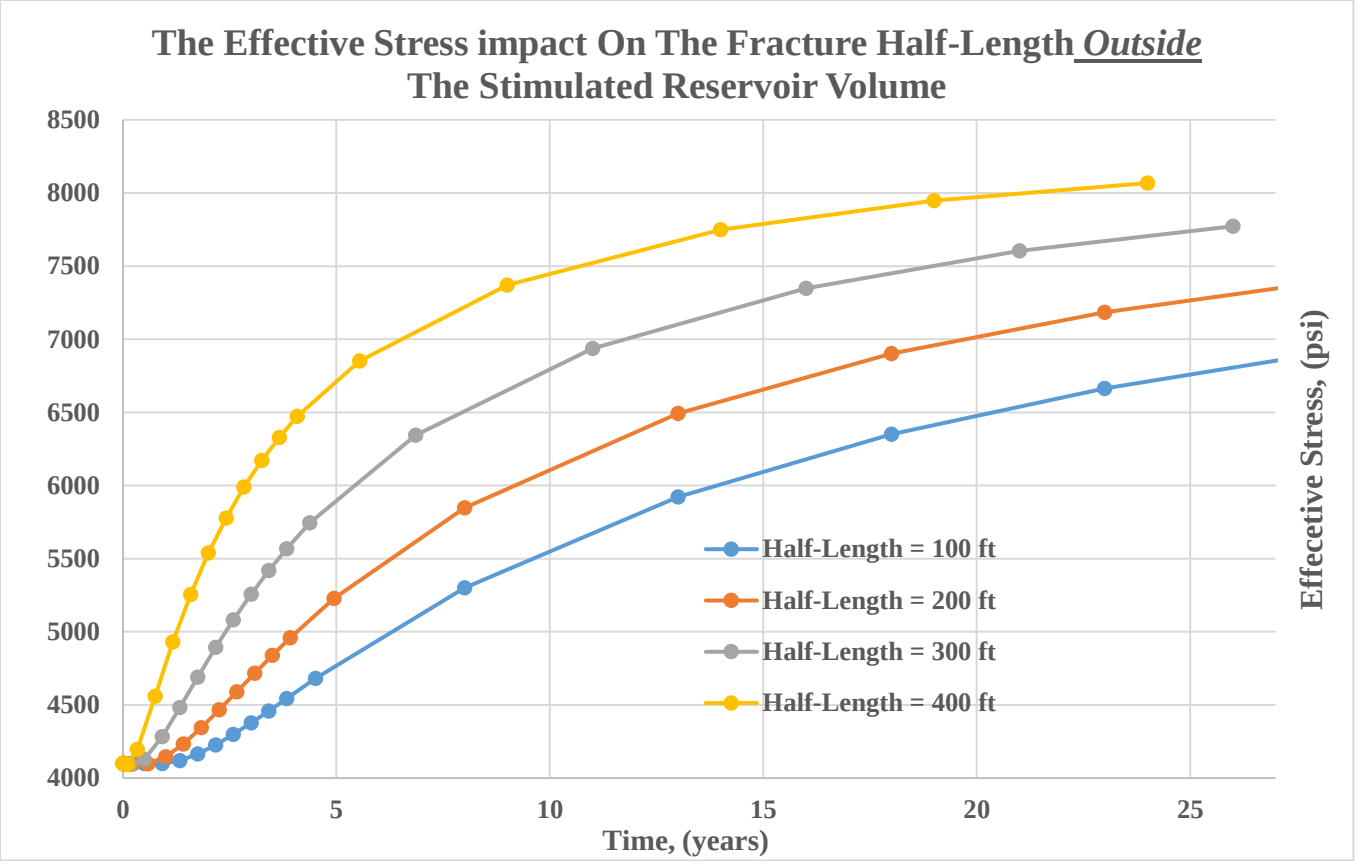

Figure 63: The impact of the hydraulic fracture half-length on the effective stress outside the stimulated reservoir volume for well MIP-6H

From the Figure above (Figure 63), the effective stress started to increase in the first 5-years and then showed a diminished impact later. As can be observed, as the fracture half-length increases throughout the life of the well, the effective stress decrease accordingly in comparison to the inside SRV. As the fracture half-length increases (xf = 400 ft.), the effective stress showed a decrease 8068 after 24 years. On the other hand, the lowest half-length of 100 ft had an effective stress of 6664 psi in the same year which results in a higher total reduction of 1404 psi in effective stress compared to the inside SRV.

4.3 THE IMPACT OF THE OPERATING CONDITIONS

For this study, there was only parameter to investigate for the operating conditions of the multi-stage fractured horizontal well, wellbore pressure. The wellbore pressure is often referred to as the pore pressure of the formation. In addition, wellbore pressure is directly affected by the effective stress distribution and the increase of the cumulative gas production. The table below (Table 28) represent the parameters used for the parametric studies of the wellbore pressure aligned with the base model initial. These values have been chosen specifically based on the Marcellus shale characteristics. The base model resulted in a wellbore pressure of 400 psi which was calculated from the difference between the constant overburden pressure acting on the SRV 8800 psi and the initial reservoir pressure of 4800 psi.

Table 28: The operating conditions properties for well MIP-6H

Operating Conditions Properties			
Parameters	**Base Model**	**Range Values**	**Unit**
Wellbore Pressure	**400**	**600, 800, and 1000**	**psi**

4.3.1 WELLBORE PRESSURE

When it comes to drilling a Marcellus shale formation, the wellbore pressure (P_{wf}) one of the main aspects to be focused on since it is associated with wellbore instability. Such that, when the well was under compaction the overburden pressure was recorded 8800 psi in the simulated reservoir volume. Initially, the reservoir pressure was 4800 psi which is less than the overburden pressure, this difference is what is called wellbore pressure. The productivity of the MIP-6H in this study was affected by the different values of the wellbore pressure to illustrate the fluid-flow in the formation under compaction and deformations.

Two production profiles were generated for the impact of the wellbore pressure on the cumulative gas production of both 1-year and 5-years. The tables below will illustrate how including and excluding the compressibility impacts for the 5-year production profile in the reservoir model had a noticeable impact on the gas production rates. Such that, including the compressibility impacts resulted in decreasing the cumulative gas production rates to illustrate an accurate production profile. On the other hand, excluding the compressibility impacts gave an over-estimate of the gas production rate in comparison to the actual field data. The percent reduction of the cumulative gas production was recorded for each case study. It was observed that as the wellbore pressure increases, the percent reduction in the cumulative gas production decrease.

The tables below will illustrate how including and excluding the compressibility impacts for the 1-year production profile in the reservoir model had a noticeable impact on the gas production rates.

Table 29: 1-Year percent reduction of wellbore pressure impact on the total cumulative gas production

% Reduction Change in Cumulative Gas Production	1-Year Production Profile	
	Wellbore Pressure	Total Reduction in Cumulative Gas Production
	psi	%
	400	36.5747
	600	35.8304
	800	34.8261
	1000	33.6243

Table 30: 1-Year wellbore pressure impact on the cumulative gas production (with compressibility effects)

Compressibility Impact	1-Year Production Profile	
	Wellbore Pressure	Cumulative Gas Production
	psi	SC (MMSCF)
	400	437
	600	432
	800	426
	1000	419

Table 31: 1-Year wellbore pressure impact on the cumulative gas production (without compressibility effects)

No Compressibility Impact	1-Year Production Profile	
	Wellbore Pressure	Cumulative Gas Production
	psi	SC (MMSCF)
	400	689
	600	673
	800	654
	1000	631

It has been observed that as the wellbore pressure increases for the 1-year production profile the cumulative gas production decreases which confirms the inverse relationship between the wellbore pressure and the gas rate for the Marcellus shale formation. Consequently, the

wellbore pressure decreases over-time since the fluid capacity decreases which causes the decrease in the gas rate.

To illustrate, the inclusion of the compressibility impacts at 400 psi the gas rate was 437 MMscf which is lowered compared to 689 MMscf when the compressibility impacts were included. As a result, this is for the early production time where the effective stress is very high causing an increase in the gas production rates.

For this reason, the increase in the wellbore pressure showed an increase on the total reduction on the cumulative gas production. The figures below (Figure 64) will illustrate each case with the four different wellbore pressure values on the cumulative gas production for the 1-year production profile.

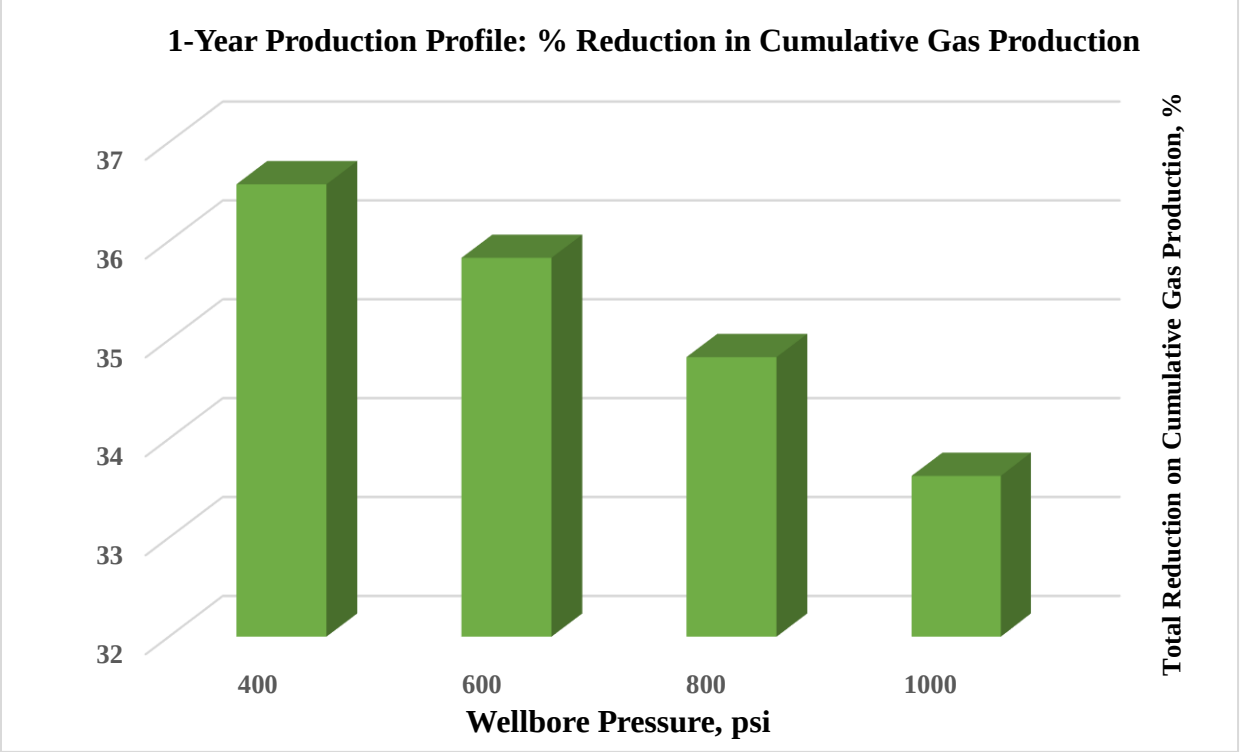

Figure 64: 1-Year Percent Reduction in wellbore pressure impact on the cumulative gas production.

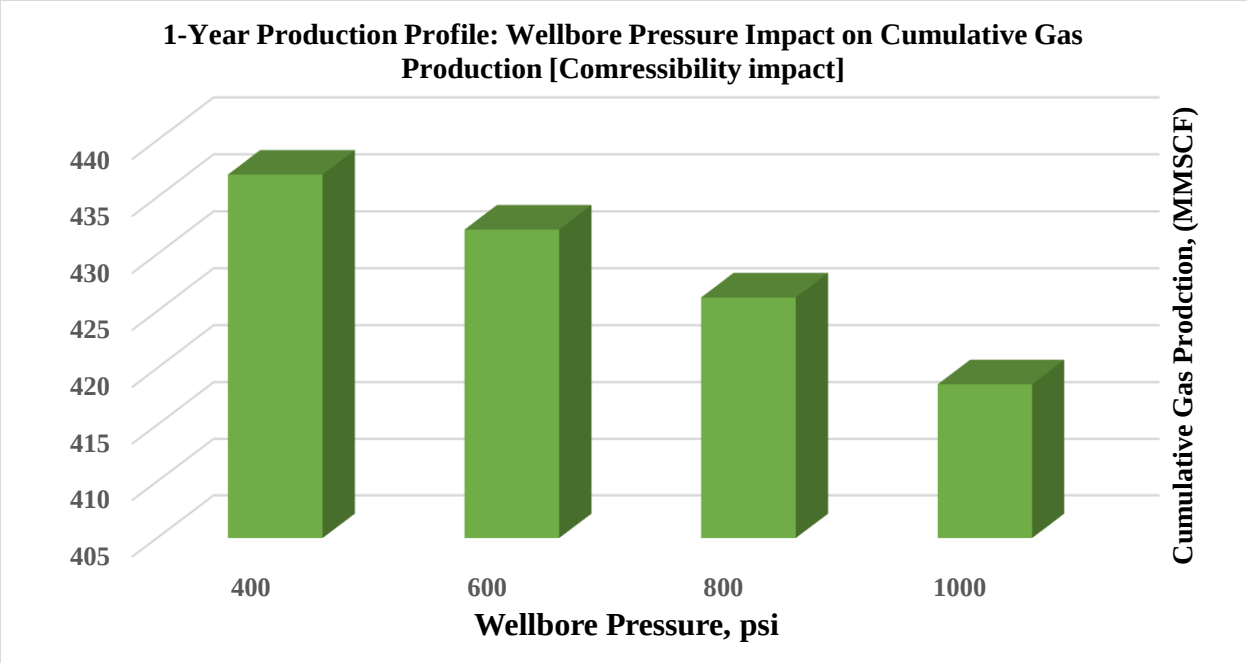

Figure 65: 1-Year Wellbore pressure impact on the cumulative gas production (with compressibility effects)

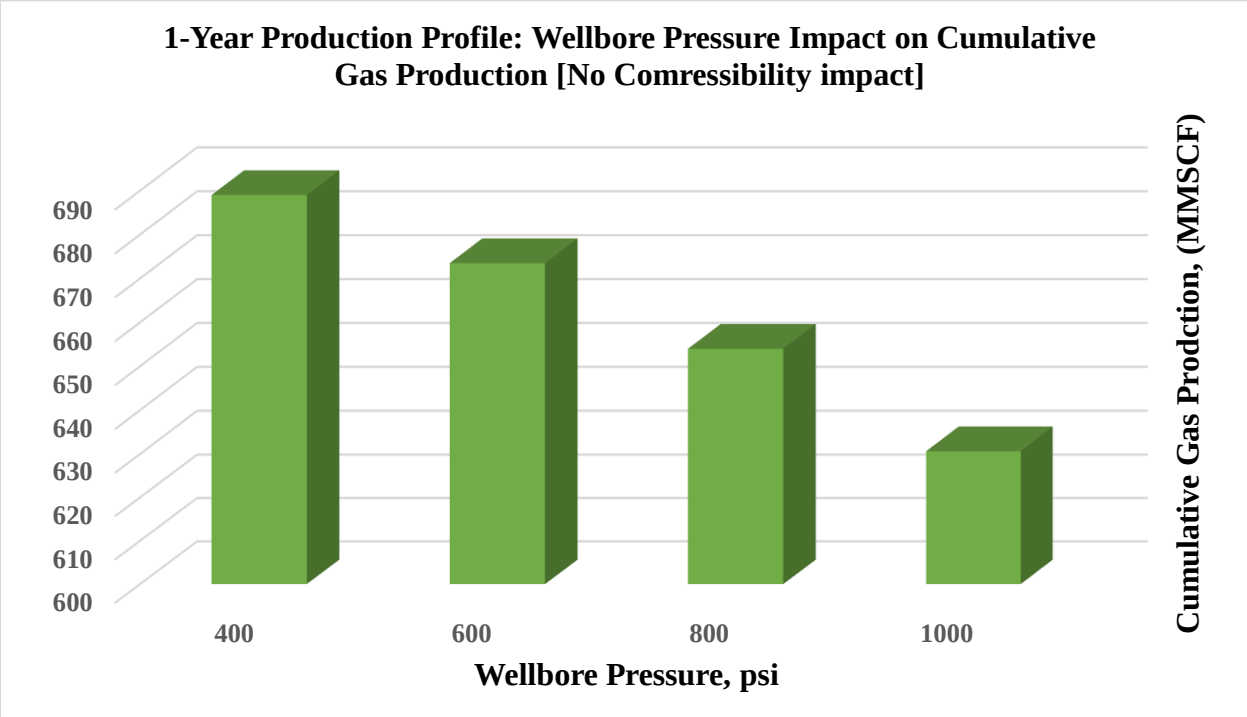

Figure 66: 1-Year Wellbore pressure impact on the cumulative gas production (without compressibility effects)

On the other hand, the tables below will illustrate how including and excluding the compressibility impacts for the 5-year production profile in the reservoir model had a noticeable impact on the gas production rates.

Table 32: 5-Year percent reduction of wellbore pressure impact on the total cumulative gas production

% Reduction Change in Cumulative Gas Production	5-Year Production Profile	
	Wellbore Pressure	Total Reduction in Cumulative Gas Production
	psi	%
	400	24.7945
	600	23.7222
	800	22.3332
	1000	20.9989

Table 33: 5-Year wellbore pressure impact on the cumulative gas production (compressibility effects)

Compressibility Impact	5-Year Production Profile	
	Wellbore Pressure	Cumulative Gas Production
	psi	SC (MMSCF)
	400	1460.231323
	600	1422.134399
	800	1374.306519
	1000	1319.173584

Table 34: 5-Year wellbore pressure impact on the cumulative gas production (no compressibility effects)

No Compressibility Impact	5-Year Production Profile	
	Wellbore Pressure	Cumulative Gas Production
	psi	SC (MMSCF)
	400	1098.173584
	600	1084.772583
	800	1067.379639
	1000	1042.161987

It has been observed that as the wellbore pressure increases for the 5-year production profile the cumulative gas production decreases which confirms the inverse relationship between the wellbore pressure and the gas rate for the Marcellus shale formation. Consequently, the wellbore pressure decreases over-time since the fluid capacity decreases which causes the decrease in the gas rate. When the wellbore pressure for the base model was 400 psi, the cumulative gas

production rate was at its peak due to early production. To illustrate, the inclusion of the compressibility impacts at 400 psi the gas rate was 1460.23 MMscf which is higher compared to 1098.17 MMscf when the compressibility impacts were included. The figures below will illustrate each case with the four different wellbore pressure values.

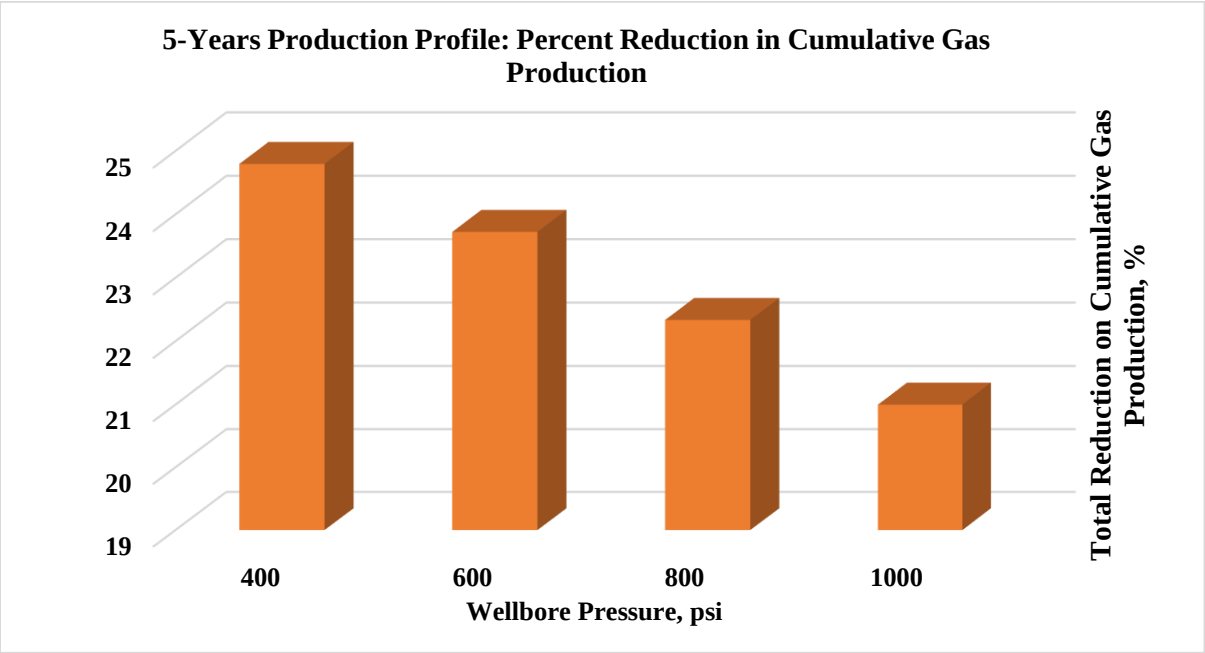

Figure 67: 5-Year percent reduction in wellbore pressure impact on the cumulative gas production.

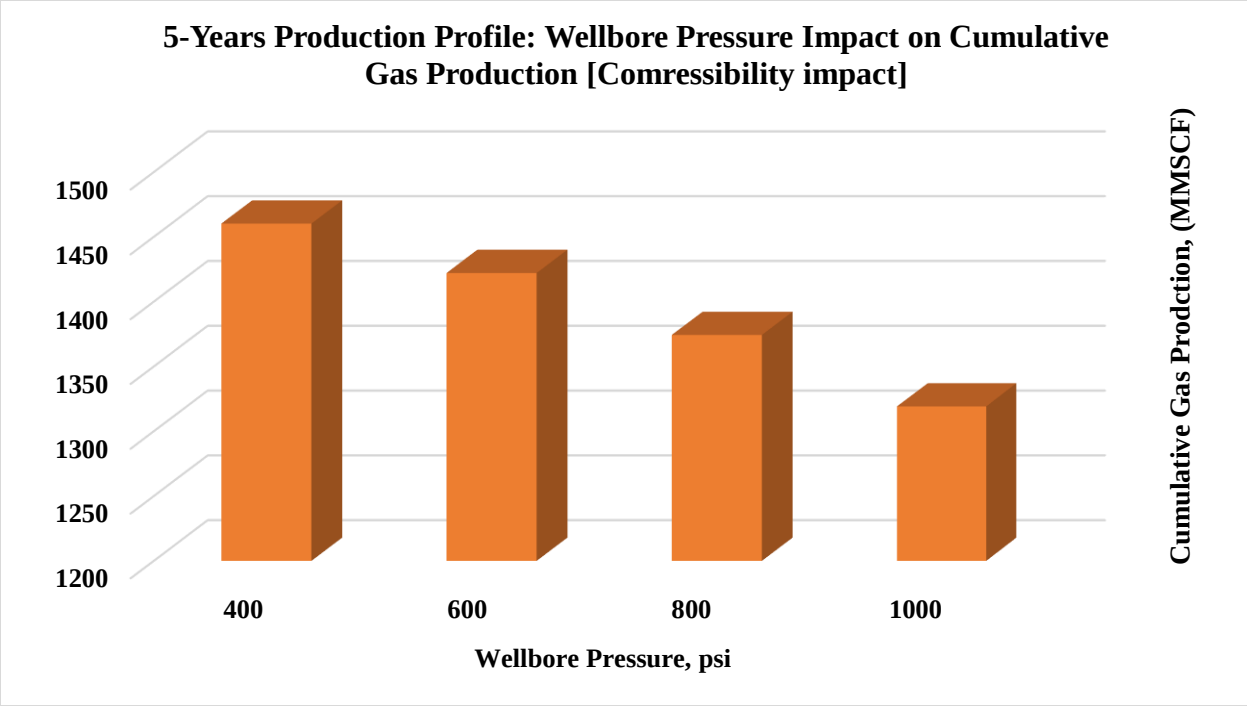

Figure 68: 5-Year Wellbore pressure impact on the cumulative gas production (with compressibility effects)

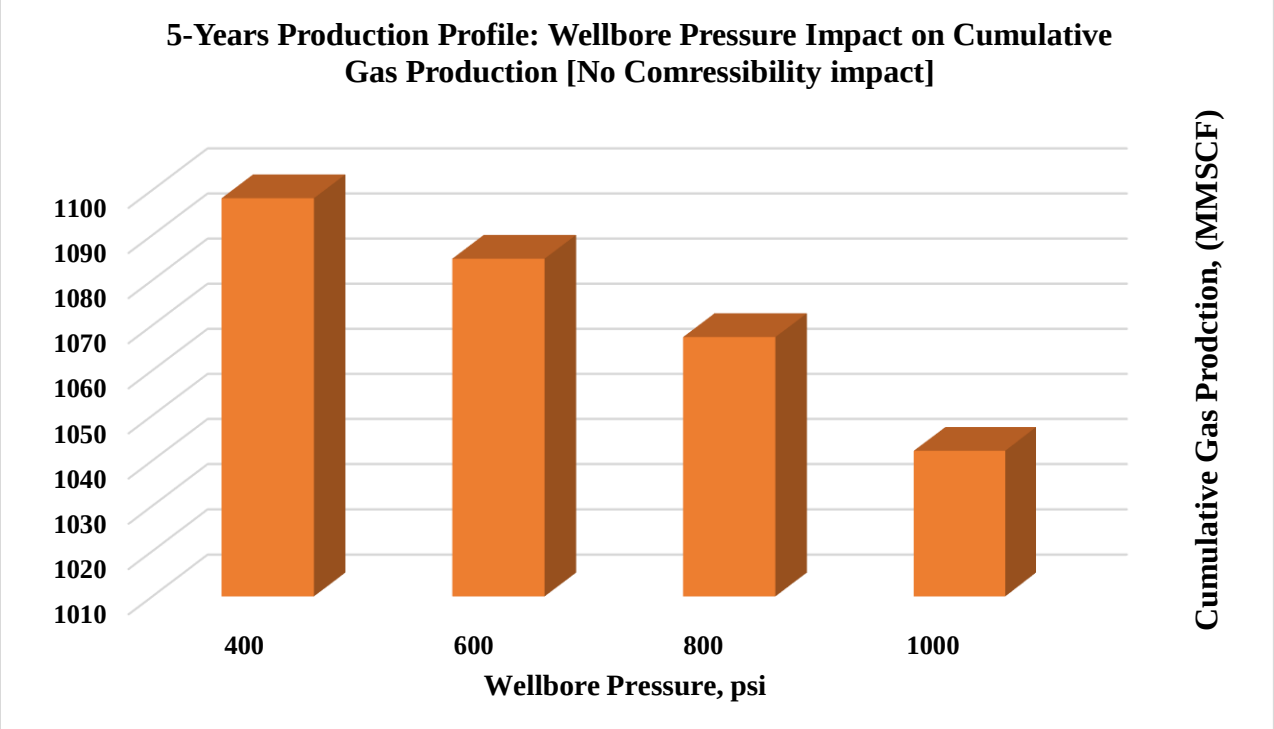

Figure 69: 5-Year Wellbore pressure impact on the cumulative gas production (without compressibility effects)

The compaction of the reservoir is often associated with an increase in the effective stress causing the pore pressure to decrease in the formation. Consequently, porosity in this case acts as the drive mechanism for the fluid-flow in the stimulated reservoir volume. The wellbore pressure then decreases as the well is producing causing the gas production to decrease throughout the remaining life of the well. The figure below (Figure 70), represent the different set of values for the wellbore pressure acting on the stimulated reservoir volume (SRV) relative to the impact of the effective stress on well MIP-6H.

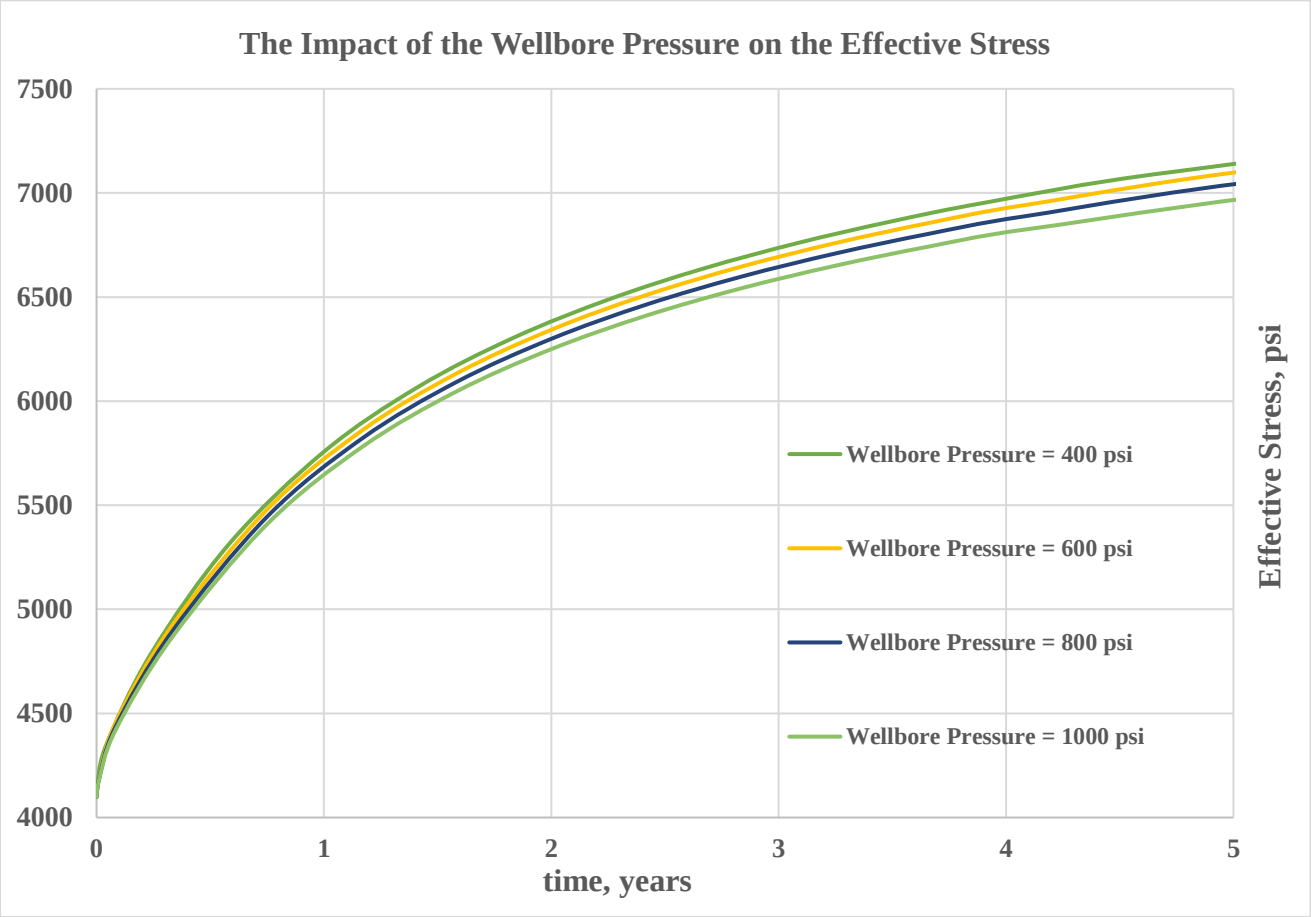

Figure 70: The impact of the wellbore pressure on the effective stress for well MIP-6H

As can be observed from the figure above, the lowest wellbore pressure had the highest impact on the effective stress with a recorded value of 8104 psi, in comparison to the highest wellbore pressure of 1000 psi which resulted in a lower effective stress of 7693.78 psi. The impact of the wellbore pressure starts to increase initially then diminishes overtime since most of the fluid is no longer in the wellbore and moving upward to the surface. In addition, the effective stress increases slowly when the gas production rates decreasing due to low porosity and permeability

for the well to produce under compaction. Lastly, lower draw-down pressure can mitigate the increase of the effective stress impact on the gas production rates for the multi-stage fractured Marcellus shale horizontal well.

4.4 CASE STUDY

After the investigation of all the parametric studies for this research i.e., mechanical properties (Young's modulus and Poisson's ratio), hydraulic fracture properties (initial fracture conductivity, fracture half-length, and fracture spacing), and lastly, operating conditions (wellbore pressure). It has been observed that the initial fracture conductivity had the highest impact on the gas recovery for the well. The lower the initial fracture conductivity, the higher the impact is on the cumulative gas rate. Consequently, the 10 md-ft of initial fracture conductivity was incorporated to the model and run with the different fracture spacing (8, 12, and 16 stages) to implement the enhancement of the gas recovery for the week MIP-6H. The table below (Table 36), illustrates the 5-year production profile of the percent reduction change on the different fracture stages with the 10- md-ft fracture conductivity.

It was observed that with the lower fracture stage of 8 (base case), the gas recovery percent change was 30.5% which is higher than the base case of 20 md-ft with a total reduction of 24.79%. As a result, the 5-year production profile showed a diminishing effect of the cumulative gas production over time yet was chosen to provide accurate estimate of the gas recovery of the well MIP-6H.

The first production profile was generated for the 1-year, the tables below will illustrate the impact of the fracture stages with a lower initial fracture conductivity on the cumulative gas production of the well.

Table 35: The 1-year production profile of the percent reduction change in cumulative production of fracture stages and 10 md-ft conductivity [case study]

% Reduction Change	1-Year Production Profile	
	Number of stages	Total Reduction in Cumulative Gas Production
	-	%
	8	41.9753
	12	34.6082
	16	33.9458

Table 36: The 1-year production profile of the of fracture stages and 10 md-ft conductivity on the cumulative gas production with compressibility impacts [case study]

Compressibility Impact	1-Year Production Profile	
	Number of Stages	Cumulative Gas Production
	-	SC (MMSCF)
	8	376
	12	744
	16	876

Table 37: The 1-year production profile of the of fracture stages and 10 md-ft conductivity on the cumulative gas production with no compressibility impacts [case study]

No Compressibility Impact	1-Year Production Profile	
	Number of Stages	Cumulative Gas Production
	-	SC (MMSCF)
	8	648
	12	1138
	16	1326

From the tables above, the inclusion of the compressibility impacts lowered the percent reduction in gas recovery of the well as the fracture stages decrease. On the other hand, removal of the compressibility factors increased the cumulative gas production rates as the fracture stages increase (lower fracture spacing) causing the matrix porosity to act as a driving mechanism for the fluid-flow.

The figures below illustrate the 1-year production profile for this case study with the inclusion and exclusion of the compressibility impacts as well as the percent reduction in the cumulative gas production for well MIP-6H. As a result, the 8-fracture stage showed the highest percent reduction in gas recovery of 41% unlike the 12 and 16 fracture stages with a diminishing impact over-time.

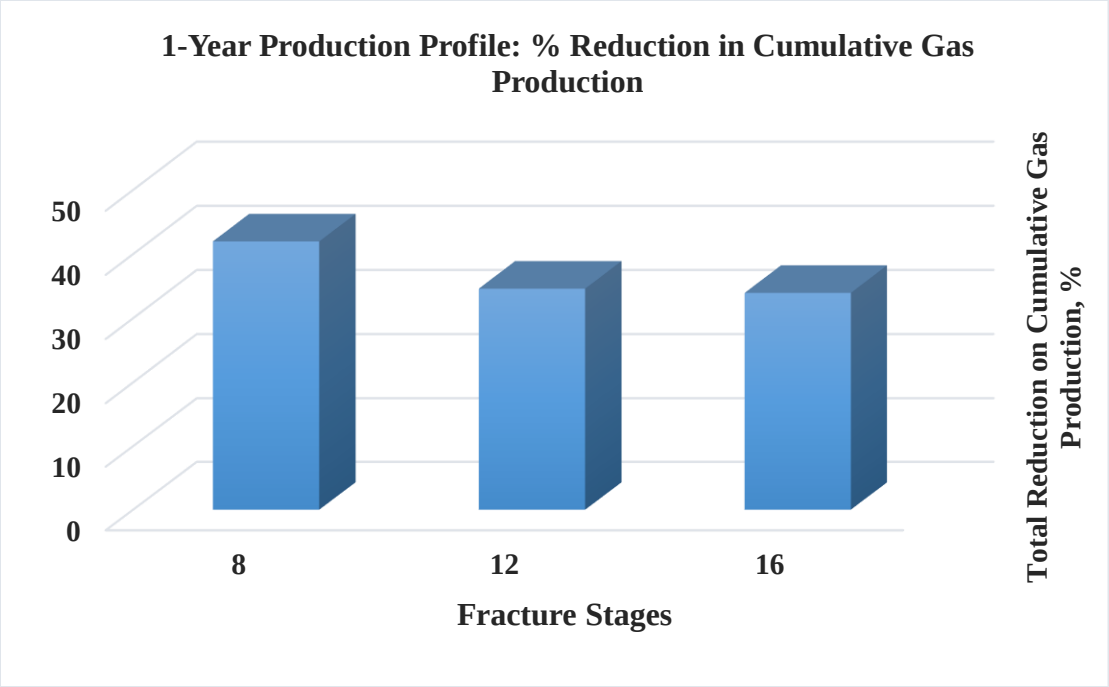

Figure 71: The 1-year production profile of the percent reduction change in cumulative production of fracture stages and 10 md-ft conductivity [case study]

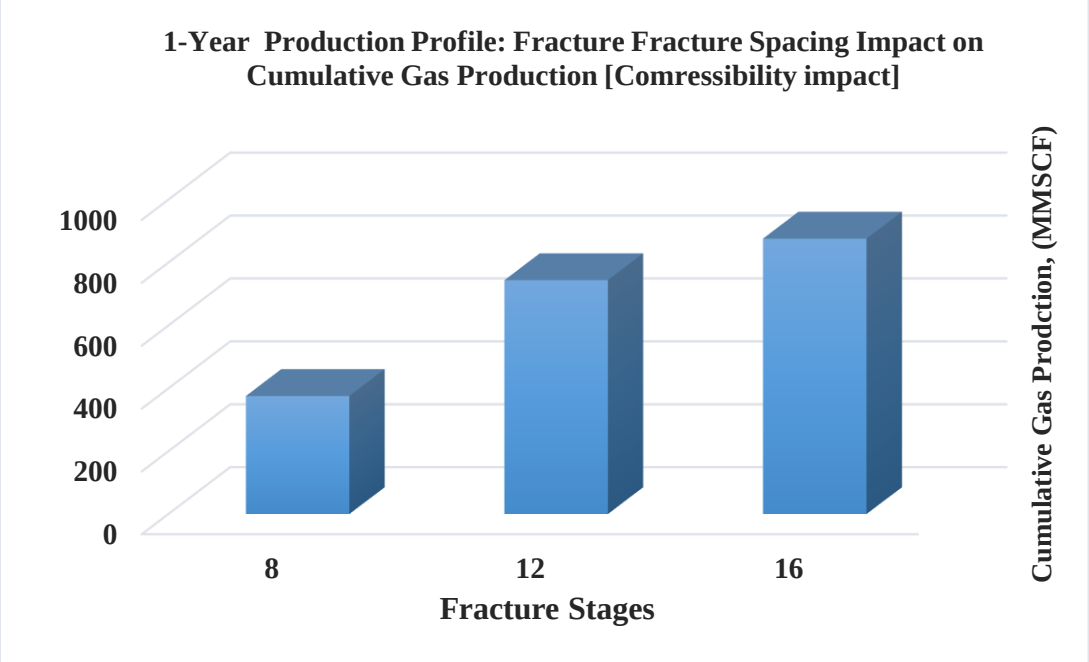

Figure 72: The 1-year production profile of the fracture stages and 10 md-ft conductivity on the cumulative gas production with compressibility impacts [case study]

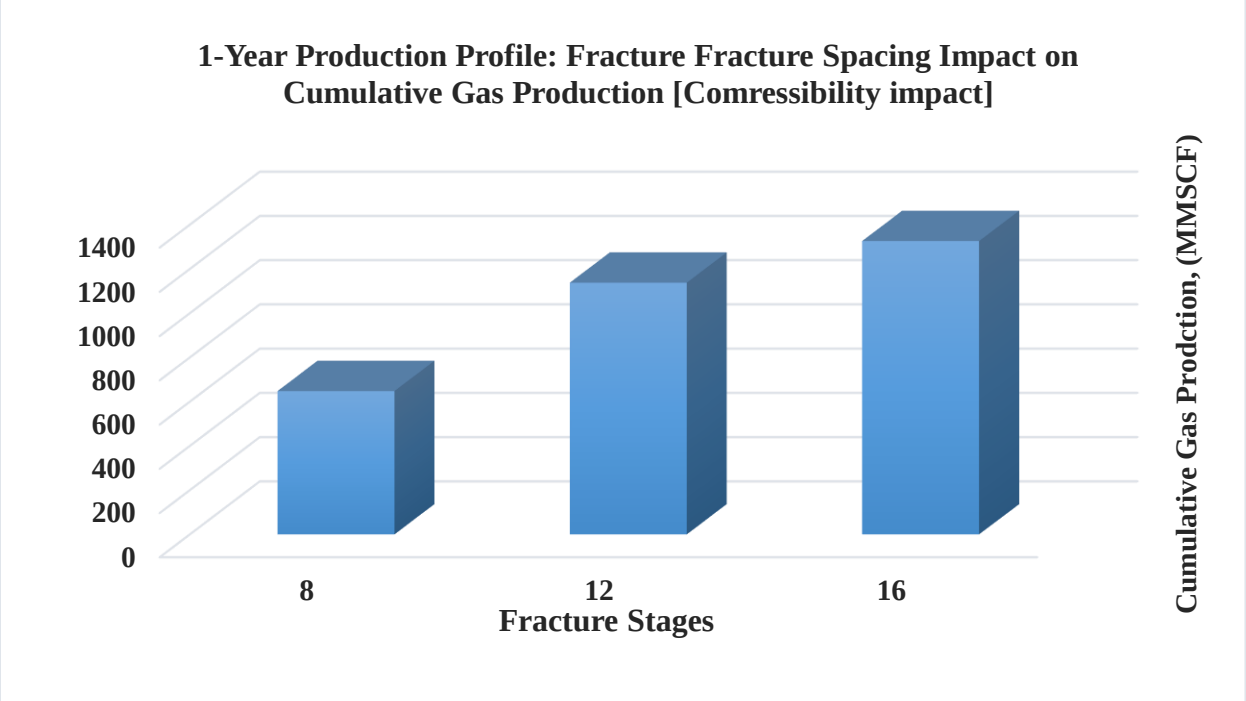

Figure 73: The 1-year production profile of the fracture stages and 10 md-ft conductivity on the cumulative gas production with no compressibility impacts [case study]

The second production profile was generated for the 5-year, the tables below will illustrate the impact of the fracture stages with a lower initial fracture conductivity on the cumulative gas production of the well.

Table 38: The 5-year production profile of the percent reduction change in cumulative production of fracture stages and 10 md-ft conductivity [case study]

% Reduction Change	5-Year Production Profile	
	Number of Stages	Total Reduction in Cumulative Gas Production
	-	%
	8	30.5634
	12	25.0968
	16	23.4853

Table 39: The 5-year production profile of the of fracture stages and 10 md-ft conductivity on the cumulative gas production with compressibility impacts [case study]

Compressibility Impact	5-Year Production Profile	
	Number of Stages	Cumulative Gas Production
	-	SC (MMSCF)
	8	986
	12	1161
	16	1326

Table 40: The 5-year production profile of the of fracture stages and 10 md-ft conductivity on the cumulative gas production with no compressibility impacts [case study]

No Compressibility Impact	5-Year Production Profile	
	Number of Stages	Cumulative Gas Production
	-	SC (MMSCF)
	8	1420
	12	1550
	16	1733

From the tables above, the inclusion of the compressibility impacts lowered the gas recovery of the well as the fracture stages decrease. On the other hand, removal of the compressibility factors increased the cumulative gas production rates as the fracture stages increase (lower fracture spacing) causing the matrix porosity to act as a driving mechanism for the fluid-flow. However, this is confirmed by the percent change in the total reduction of the gas production for this case study with a 5.71% total increase in difference.

The figures below illustrate the 5-year production profile for this case study with the inclusion and exclusion of the compressibility impacts as well as the percent reduction in the cumulative gas production for well MIP-6H. As a result, the 8-fracture stage showed the highest percent reduction in gas recovery of 30.5% unlike the 12 and 16 fracture stages with a diminishing impact over-time with an average of 24.45% percent reduction in the gas recovery.

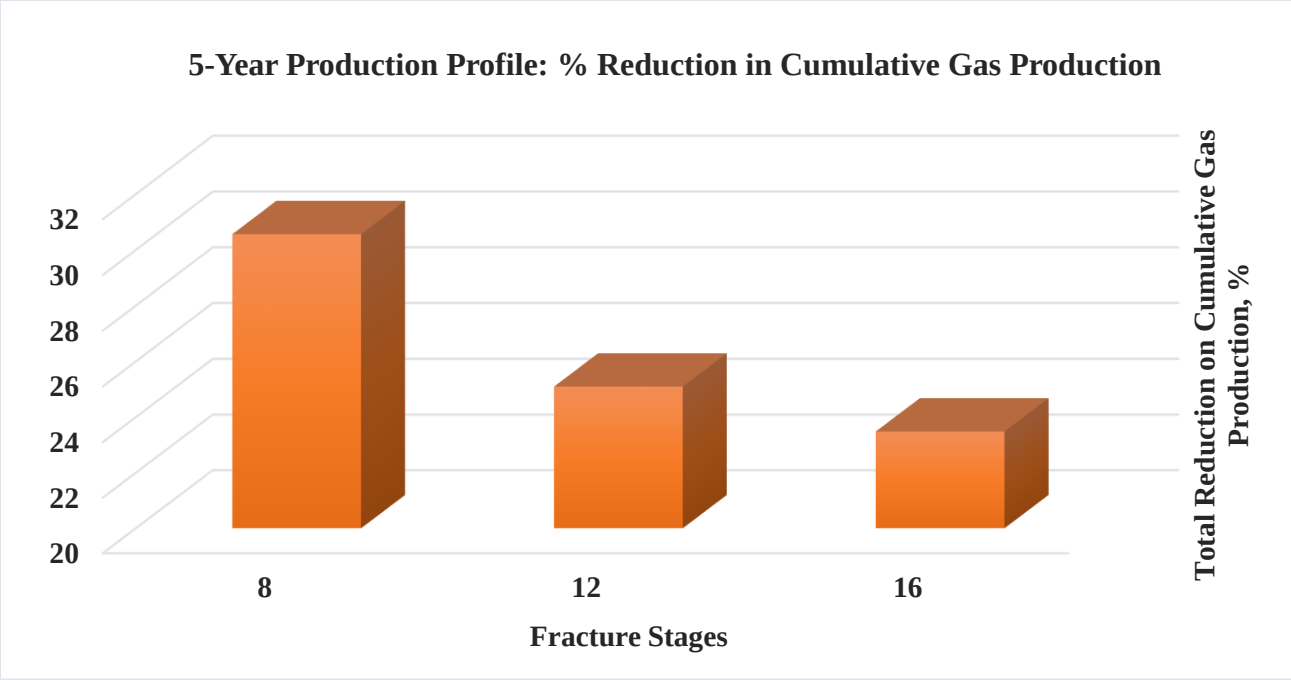

Figure 74: The 5-year production profile of the percent reduction change in cumulative production of fracture stages and 10 md-ft conductivity [case study]

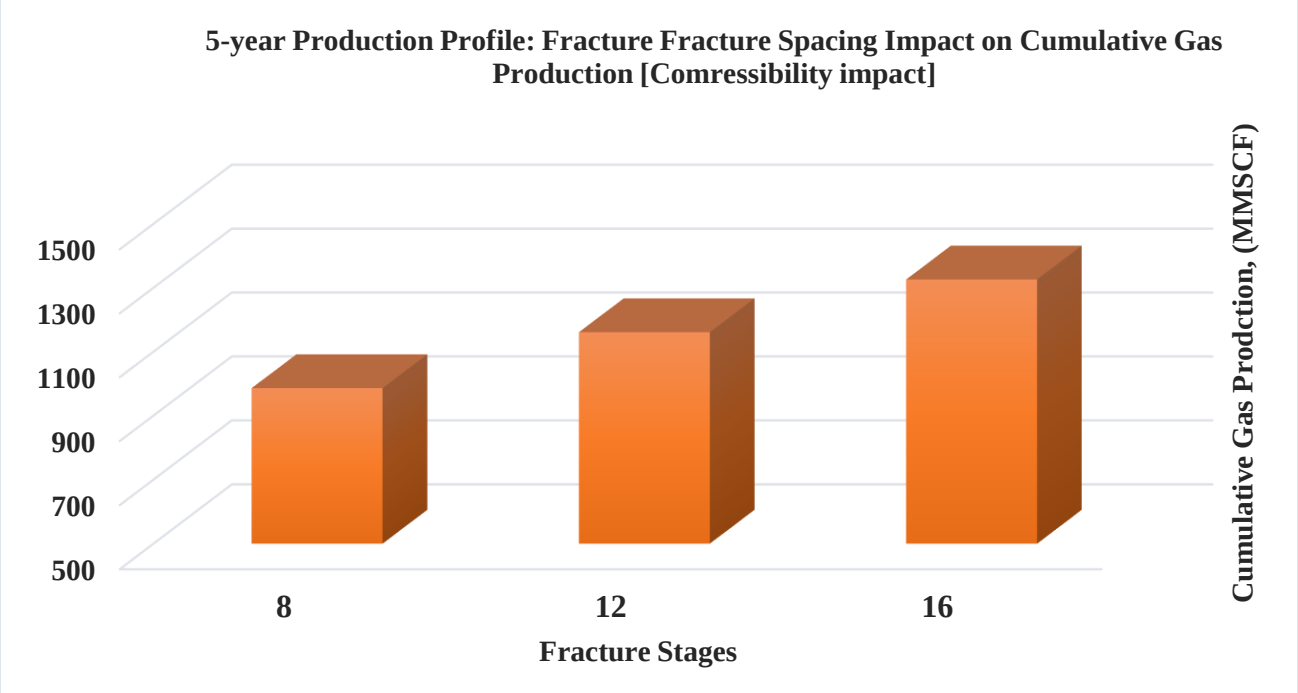

Figure 75: The 5-year production profile of the fracture stages and 10 md-ft conductivity on the cumulative gas production with compressibility impacts [case study]

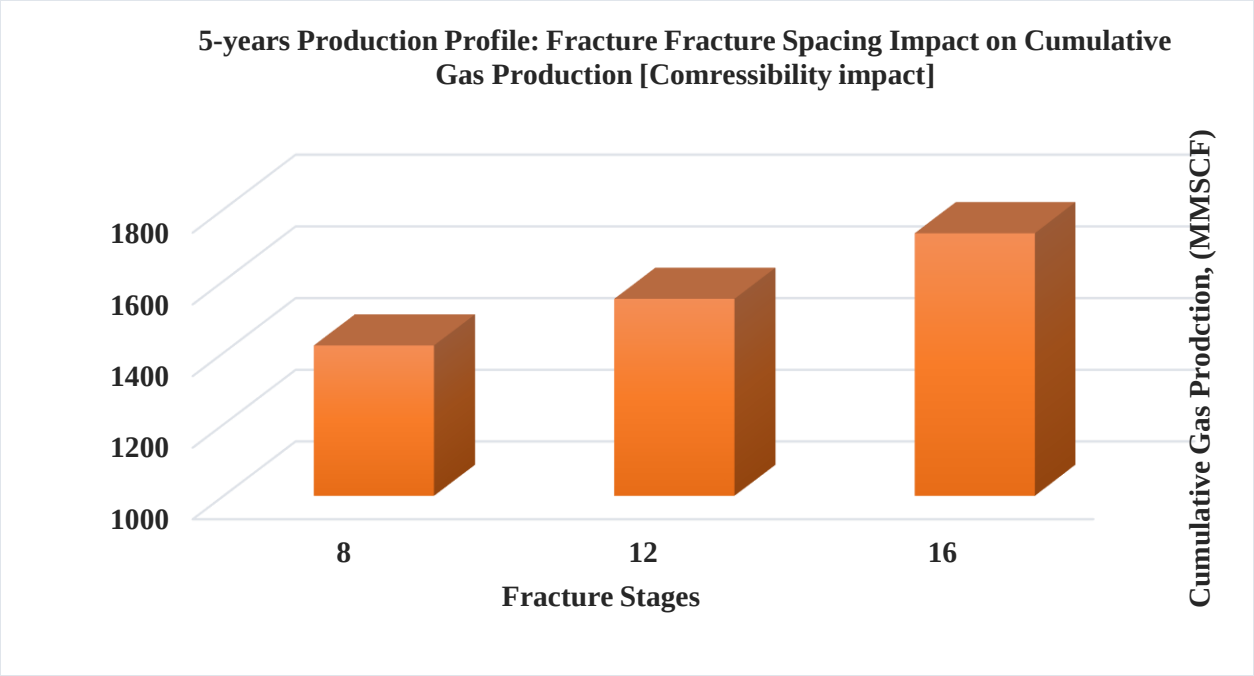

Figure 76: The 5-year production profile of the fracture stages and 10 md-ft conductivity on the cumulative gas production with no compressibility impacts [case study]

Similarly, the exclusion of the compressibility impacts increases the gas recovery rates noticeably unlike the inclusion of the compressibility impacts with an adverse impact on the 16-ft fracture stage with a total cumulative gas production of 1733 MMscf. Moreover, the 12-fracture stage gave an average effect on the gas recovery for the well unlike the huge gap between the 8 and 16 fracture stage impacts acting on the stimulated reservoir volume.

Lastly, the impact of the different fracture stages had a noticeable impact on the effective stress which confirms the claims of this study. The figure above (Figure 76), illustrate the impact of the effective stress on the fracture spacing for the MIP-6H for a time window of 15 years having the same increasing trend for the previous parametric studies which confirms that including the compressibility impacts could alter the effective stress acting on the stimulated reservoir volume for the well.

Although the difference in the effective stress is not large, this increasing trend diminishes over-time due to the low production gas rates. The adverse compressibility impacts are usually more pronounced during the early production times, compaction which aid in the reduction of the permeability, porosity and hydraulic fracture conductivity causing an enhancement for the fluid-flow in the formation.

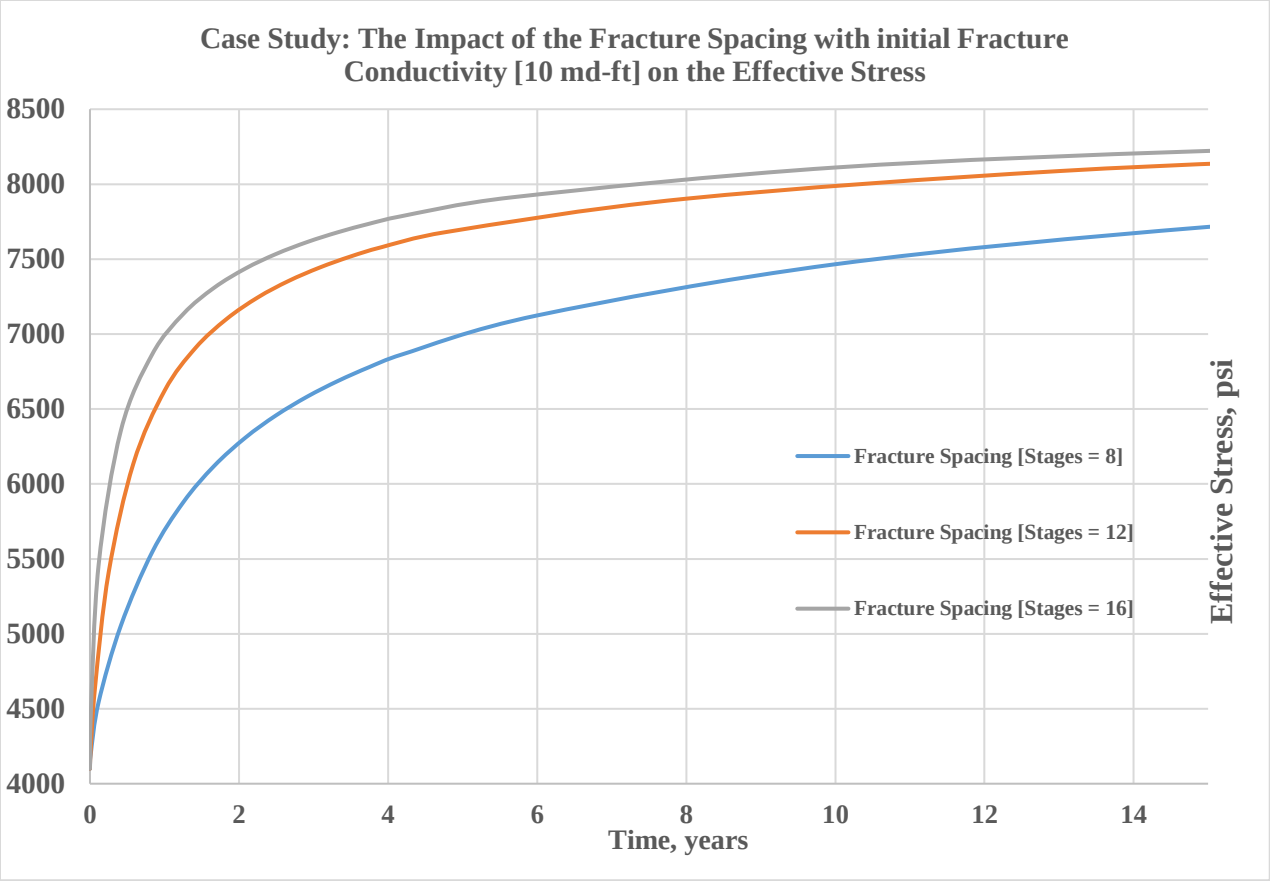

Figure 77: [case study]: The impact of the hydraulic fracture spacing with initial fracture conductivity [10 md-ft] on the effective stress for well MIP-6H

the effective stress increases rapidly for the higher stages' values (12, and 16) which means there is less fracture spacing compared to the lower fracture stage case (the base case), which remains almost constant throughout the remaining life of the well. In addition, this is due to the high volume of the percent reduction in gas recovery in the early stages of the production phase. After 15 years, the lowest fracture spacing with the highest fracture stages (16 stages) had a total effective stress of 8222 psi whereas the lower fracture spacing had a lower effective stress of 7715 psi.

As has been demonstrated, the inclusion of the lower initial hydraulic fracture conductivity increased the total percent reduction in cumulative gas production on the fracture spacing by 5.71% in comparison to the base case. Additionally, the 5 md-ft showed a higher reduction on the cumulative gas production but could be used for future studies if required as well as the different grade of the sand to be injected into the formation to keep the fracture open for more production.

CHAPTER 5
CONCLUSIONS AND RECOMMENDATIONS

Based on the various steps taken to investigate the impact of the hydraulic fracture properties and formation mechanical properties alternations on the productivity of the Marcellus shale gas well with multi-stage hydraulic fractures. Consequently, many conclusions towards the completion this study were summarized below, and all led to support the claim of this study towards the impact of both the effective stress and the compaction effects on the productivity of the stimulated reservoir volume.

1- The understanding of the shale formation reservoir characteristics was an essential step towards the completion of this study.
2- This study focused on how the different categories of hydraulic fracture properties (initial fracture conductivity, fracture half-length, and fracture spacing), formation mechanical properties (Young's modulus and Poisson's ratio), and the operating conditions (wellbore pressure) could alter the productivity of the multi-stage hydraulically fractured horizontal wells.
3- During the reservoir compaction, the degree of the effective stress increases on the stimulated reservoir volume causing adverse effects on the reduction of matrix porosity, matrix permeability, natural fractures permeability, and the hydraulic fracture conductivity.
4- The gas recovery of a Marcellus shale gas well (MIP-6H) was adversely affected by the increase in the effective stress during the compaction of the reservoir which decreases the pore pressure in the formation.
5- The importance of iterative coupling (two-way coupling) for a 3-Dimensional reservoir model with a geomechanical module provides an accurate prediction profile for the gas production of a Marcellus shale gas well with multi-stage hydraulic fractures.
6- The reservoir simulation and coupling methods are crucial to a better understanding of the reservoir characteristic such as: pressure, porosity, permeability, stress, strain, displacement and hydraulic fracture properties.
7- During the early production stages of the well, the adverse compressibility impacts are more pronounced due to greater gas production rates which diminish over an increased production time.

8- The reduction in the hydraulic fracture conductivity had the highest adverse impact yet negative on the gas recovery from the Marcellus shale due to an increase in effective stress.
9- Consequently, the reduction in the matrix porosity had a positive yet small impact on the gas recovery since it acts as the drive mechanism of the Marcellus shale reservoir.
10- The Marcellus shale is a brittle formation due to a low Poisson's ratio and a moderate Young's modulus which makes it susceptible to the adverse compressibility impacts due to the increase in the effective stress.
11- The higher values of the formation mechanical properties (Young's modulus & Poisson's ratio) can dampen the adverse gas recovery impacts due to an increase in the effective stress.
12- The decrease of the Poisson's ration and Young's modulus can improve the gas recovery of a Marcellus shale well, especially on the hydraulic fracture properties.
13- For the hydraulic fracture properties, the higher hydraulic fracture half-length and a lower fracture spacing (more stages) during the early production time can amplify the adverse compressibility impacts on the cumulative gas production.
14- Additionally, the lower values of the initial hydraulic fracture conductivity can nourish the gas recovery for the horizontal Marcellus shale gas well.
15- As fracture stage spacing start to decrease, the number of fracture stages increase which confirms the inverse relationship between the two parameters which could lower the impact of the hydraulic fracture conductivity and the geomechanical properties.
16- The operating conditions impact was minor on the cumulative gas production since the higher-pressure draw-down amplify the adverse compressibility impacts of the gas well.
17- The impact of the geomechanical decreases as the operating conditions (wellbore pressure) increase during the early production of the horizontal well.

The following is the list of recommendations to improve and use this study in the oil and gas industry by professional and researchers:

1- Investigate this study on the other wells and pads available in the reservoir from the published MSEEL data base.

2- Incorporate different sand grades to inject during the hydraulic fracturing process and how it would impact the gas production rate.
3- The inclusion of more parametric studies such as how would different pore pressure values alter the productivity of the well.

REFERENCES

"Hydraulic Fracturing." *Wikipedia*, Wikimedia Foundation, 6 July 2022, https://en.wikipedia.org/wiki/Hydraulic_fracturing

Alramahi, B., and Sundberg, M.I. 2012. Proppant embedment and conductivity of hydraulic fractures in shales. The 46th US Rock Mechanics/Geomechanics Symposium, 24-27 June 2012, Chicago, IL. ARMA 12-291.

Apga.org. n.d. *A Brief History of Natural Gas - American Public Gas Association*. [online] Available at: https://www.apga.org/apgamainsite/aboutus/facts/history-of-natural-gas#:~:text=In%201821%2C%20William%20Hart%20dug,American%20natural%20gas%20distribution%20company.

Api.org. n.d. *Marcellus Shale*. [online] Available at: https://www.api.org/oil-and-natural-gas/energy-primers/hydraulic-fracturing/marcellus-shale

Belyadi, Hoss, et al. *Hydraulic Fracturing in Unconventional Reservoirs: Theories, Operations, and Economic Analysis*. Second ed., Gulf Professional Publishing, an Imprint of Elsevier, 2019. doi: https://doi.org/10.1016/C2018-0-01643-6

Bentek: August Nat Gas Production Nearly as High as July Record | Marcellus Drilling News. (2015,

Biot, M.A., 1941. General Theory of Three-Dimensional Consolidation, J. Applied Physics, 12, 155–164.

Britannica, the Editors of Encyclopaedia. "fracking". Encyclopedia Britannica, 3 Feb. 2022, https://www.britannica.com/technology/fracking.

CMG: GEM User's guide. Computer Modeling Group Ltd., 2020.

Columbia.edu.n.d. *Stress and Strain - Rock Deformation*. [Online] Available at: http://www.columbia.edu/~vjd1/stress-strain_basic.htm

Dey, A., n.d. *Poisson's Ratio-Formula, Significance, Equation, Example (With PDF) – What Is Piping*. [Online] Whatispiping.com. Available at: https://whatispiping.com/poissons-ratio/

Economides, M. J., & Nolte, K.G., 2000. Reservoir stimulation. John Wiley & Sons, Ltd., 3rd Ed., 1- 1 to 20-13 pp.

Eia.gov. 2017. [Online] Available at: https://www.eia.gov/maps/pdf/MarcellusPlayUpdate_Jan2017.pdf

Eia.gov. 2019. *EIA adds new play production data to shale gas and tight oil reports*. [Online] Available at: https://www.eia.gov/todayinenergy/detail.php?id=38372

Eia.gov. 2021. *Natural gas explained - U.S. Energy Information Administration (EIA)*. [Online] Available at: https://www.eia.gov/energyexplained/natural-gas/

Eia.gov. 2021. *Three producing regions drove U.S. natural gas production in 2021*. [online] Available at: https://www.eia.gov/todayinenergy/detail.php?id=52198

Eia.gov. 2022. *Frequently Asked Questions (FAQs) - U.S. Energy Information Administration (EIA)*. [Online] Available at: https://www.eia.gov/tools/faqs/faq.php?id=907&t=8

Eia.gov. 2022. *Where our natural gas comes from - U.S. Energy Information Administration (EIA)*. [online] Available at: https://www.eia.gov/energyexplained/natural-gas/where-our-natural-gas-comes-from.php

El Sgher, Mohamed, Aminian, Kashy , and Samuel Ameri. "Geomechanical Impact on Gas Recovery from Marcellus Shale." Paper presented at the SPE Western Regional Meeting, Garden Grove, California, USA, April 2018. doi: https://doi.org/10.2118/190054-MS

El Sgher, Mohamed, Aminian, Kashy, Aldbayan, Dalal, Sattari, Arya Maher, and Samuel Ameri. "The Impact of Formation and Fracture Properties Alterations on the Productivity of the Multi-Stage Fractured Marcellus Shale Horizontal Wells." Paper presented at the SPE Eastern Regional Meeting, Wheeling, West Virginia, USA, October 2022. doi: https://doi.org/10.2118/211892-MS

El Sgher, Mohamed, Aminian, Kashy, and Samuel Ameri. "Evaluation of Stresses Alteration on the Productivity of Marcellus Shale Horizontal Well." Paper presented at the SPE Western Regional Meeting, Bakersfield, California, USA, April 2022. doi: https://doi.org/10.2118/209303-MS

Elsaig, M., Aminian, K., Ameri, S., and Zamirian, M. 2016. Accurate Evaluation of Marcellus Shale Petrophysical Properties. Presented at the SPE Eastern Regional Meeting, Canton, Ohio, USA, 13-15 September 2016. SPE-184042-MS

En.wikipedia.org. n.d. *Shale gas - Wikipedia*. [Online] Available at: https://en.wikipedia.org/wiki/Shale_gas

En.wikipedia.org. n.d. *Stress–strain curve - Wikipedia*. [Online] Available at: https://en.wikipedia.org/wiki/Stress%E2%80%93strain_curve

En.wikipedia.org. n.d. *Thomas Young (scientist) - Wikipedia*. [Online] Available at: https://en.wikipedia.org/wiki/Thomas_Young_(scientist)

En.wikipedia.org. n.d. *Wilmington Oil Field - Wikipedia*. [Online] Available at: https://en.wikipedia.org/wiki/Wilmington_Oil_Field

Geertsma, J.,:"The Effect of Pressure Decline on Volumetric Changes of Porous Rocks," Trans. AIME, Vol. 201, pp. 331-340, 1957.

Helmenstine, A., n.d. *Young's Modulus Formula and Example*. [Online] Science Notes and Projects. Available at: https://sciencenotes.org/youngs-modulus-formula-and-example/

https://doi.org/10.1306/13321465M973491

Institute for Energy Research, n.d. *Marcellus Shale Fact Sheet*. [online] Instituteforenergyresearch.org. Available at: https://instituteforenergyresearch.org/wp-content/uploads/2012/08/Marcellus-Fact-Sheet.pdf

Jalali, M.R., and M.B. Dusseault "Coupled Fluid-Flow And Geomechanics In Naturally Fractured Reservoirs." Paper presented at the ISRM International Symposium - 5th Asian Rock Mechanics Symposium, Tehran, Iran, November 2008.

Jalili, Sajjad & Ahangari, Kaveh. (2017). Effects of different stress regimes on hydraulic fracture geometry: a particle flow code approach. Innovative Infrastructure Solutions. 2. 10.1007/s41062-017-0096-1.

Kelly, PA. Mechanics *Lecture Notes: An introduction to Solid Mechanics*. Available from http://homepages.engineering.auckland.ac.nz/~pkel015/SolidMechanicsBooks/index.html

Khaled, M. 1980. Infiltration of a Two-state Compressible Fluid through a Linearly Deformed, Porous, Elastic, Fissured rock, Ph.D. Thesis, Univ. of Illinois, Urbana, Illinois.

King, H., n.d. *Shale: Sedimentary Rock - Pictures, Definition & More*. [online] Geology.com. Available at: https://geology.com/rocks/shale.shtml

Kolawole, O., Wigwe, M., Ispas, I. *et al.* How will treatment parameters impact the optimization of hydraulic fracturing process in unconventional reservoirs? *SN Appl. Sci.* **2**, 1865 (2020). https://doi.org/10.1007/s42452-020-03707-w

Lacy, Lewis L. "Dynamic Rock Mechanics Testing for Optimized Fracture Designs." Paper presented at the SPE Annual Technical Conference and Exhibition, San Antonio, Texas, October 1997. doi: https://doi.org/10.2118/38716-MS

Madhusha, 2018. *Difference between Elastic and Plastic Deformation | Definition, Effect on Chemical Bonding, Stress-Strain Curve, Differences*. [Online] Pediaa.Com. Available at: https://pediaa.com/difference-between-elastic-and-plastic-deformation/#:~:text=Elastic%20deformation%20is%20the%20deformation,action%20of%20a%20sustained%20force.

Markou, Nikolaos , and Panos Papanastasiou. "Geomechanics of Compartmentalized Reservoirs with Finite Element Analysis: Field Case Study from the Eastern Mediterranean." Paper presented at the SPE Annual Technical Conference and Exhibition, Virtual, October 2020. doi: https://doi.org/10.2118/201642-MS

McGinley, M., Zhu, D., Hill, A.D 2015. The effects of fracture orientation and anisotropy on hydraulic fracture conductivity in the Marcellus Shale. Presented at the SPE Annual Technical Conference and Exhibition, Houston, Texas, USA, 28–30 September 2015. SPE-174870-MS.

McGinley, Mark, Zhu, Ding, and A. Daniel Hill. "The Effects of Fracture Orientation and Elastic Property Anisotropy on Hydraulic Fracture Conductivity in the Marcellus Shale." Paper presented at the SPE Annual Technical Conference and Exhibition, Houston, Texas, USA, September 2015. doi: https://doi.org/10.2118/174870-MS

New York, March 24, 2022 (GLOBE NEWSWIRE) -- Reportlinker.com announces the release of the report "Shale Gas Global Market Report 2022" https://www.reportlinker.com/p06247580/?utm_source=GNW

Nicoguaro, n.d. *Stress–strain curve - Wikipedia*. [Online] En.wikipedia.org. Available at: https://en.wikipedia.org/wiki/Stress%E2%80%93strain_curve#/media/File:Stress_strain_ductile.svg

OilField Geomechanics. n.d. *Reservoir Compaction & subsidence*. [Online] Available at: https://ofgeomech.com/ofg20/reservoir-compaction-subsidence/

PetroWiki. 2017. *Fracture mechanics*. [online] Available at: https://petrowiki.spe.org/Fracture_mechanics

Pierce, R., 1970. Reducing Land Subsidence in the Wilmington Oil Field by Use of Saline Waters. *Water Resources Research*, 6(5), pp.1505-1514.

Ranter, M. and Tiemann, M., 2015. *An Overview of Unconventional Oil and Natural Gas; Resources and Federal Actions*.

Roodhart, L.P., Kulper, T.O.H., and Davies, D.R.: "Proppant-Pack and Formation Impairment During Gaswell Hydraulic Fracturing," SPEPE (November 1988) 438.

Schlumberger. n.d. *Poisson's ratio - Energy Glossary*. [Online] Available at: https://glossary.oilfield.slb.com/en/terms/p/poissons_ratio

Schlumberger. n.d. Strain *Energy Glossary*. [Online] Available at: https://glossary.oilfield.slb.com/en/terms/s/strain

Schlumberger. n.d. *Young's modulus - Energy Glossary*. [Online] Available at: https://glossary.oilfield.slb.com/en/terms/y/youngs_modulus

SEG, 2018. *Unconventional reservoir - SEG Wiki*. [online] Wiki.seg.org. Available at: https://wiki.seg.org/wiki/Unconventional_reservoir#:~:text=An%20unconventional%20reservoir%20consists%20of,reached%20thermal%20maturity%20without%20migration.

September 10). https://marcellusdrilling.com/2015/09/bentek-august-natgas-productionnearly-as-high-as-july-record/

Settari, A. "Reservoir Compaction." *J Pet Technol* 54 (2002): 62–69. Doi: https://doi.org/10.2118/76805-JPT

Settari, A. and F.M. Mourits, 1998. A Coupled Reservoir and Geomechanical Modeling System, SPEJ, SPE 50939, 219-226.

Shales. Ph.D. Dissertation, West Virginia University, Morgantown, WV (2015)

Skempton, A.W.,: "Terzaghi's Discovery of Effective Stress," in From Theory to Practice in Soil Mechanics, edited by Bjerrum, L., Casagrande, A., Peck, R.B. and Skempton, A.W., John Wiley, New York, pp. 42-53, 1960.

Sönnichsen, N., 2022. *Global natural gas production by country 2021 | Statista*. [online] Statista. Available at: https://www.statista.com/statistics/264101/world-natural-gas-production-by-country/#:~:text=As%20of%202021%2C%20the%20United,the%20second%20biggest%20producer%20%2D%20Russia.

Su, Kai & Li, Yin & Cheng, Dan. (2016). Slope Stability Analysis under Combined Failure Criteria. The Open Civil Engineering Journal. 10. 125-131. 10.2174/1874149501610010125.

Temizel, Cenk , Kirmaci, Harun , Inceisci, Turgay , Wijaya, Zein , Balaji, Karthik , Suhag, Anuj , Ranjith, Rahul , Tran, Minh , Al-Otaibi, Basel , AlKouh, Ahmad , Zhu, Ying , and Cengiz Yegin. "An Approach to Mitigate Subsidence in Soft Rocks through Coupling Surface Tiltmeter and Injection/Production Data." Paper presented at the SPE Heavy Oil Conference and Exhibition, Kuwait City, Kuwait, December 2016. doi: https://doi.org/10.2118/184107-MS

Tran, David, Settari, Antonin, and Long Nghiem. "New Iterative Coupling between a Reservoir Simulator and a Geomechanics Module." Paper presented at the SPE/ISRM Rock Mechanics Conference, Irving, Texas, October 2002. doi: https://doi.org/10.2118/78192-MS

Walsh, J.B. 1981. Effect of pore pressure and confining pressure on fracture permeability. International Journal of Rock Mechanics and Mining Sciences& Geomechanics Abstracts 18 (5): 429-435.

Wells, B., n.d. *Shooters - A "Fracking" History*. [Online] American Oil & Gas Historical Society. Available at: https://aoghs.org/technology/hydraulic-fracturing/

Wpowerproducts.com. n.d. *10 Biggest Shale Plays in the US - New & Used Generators, Ends and Engines | Houston, TX | Worldwide Power Products*. [online] Available at: https://www.wpowerproducts.com/news/10-biggest-shale-plays-in-the-us-revised/

Yang, Fen , Britt, Larry K., and Shari Dunn-Norman. "Performance Comparison of Transversely and Longitudinally Fractured Horizontal Wells Over Varied Reservoir Permeability." *SPE J.* 21 (2016): 1537–1553. doi: https://doi.org/10.2118/173331-PA

Zagorski, W. A., Wrightstone, G. R., & Bowman, D. C. (2012). The Appalachian Basin Marcellus Gas PlayIts History of Development, Geologic Controls on Production, and Future Potential as a World-class Reservoir. In J. A. Breyer, Shale Reservoirs—Giant Resources for the 21st Century. American Association of Petroleum Geologists.

Zamirian. M, 2015. New Experimental Approach to Measure Petrophysical Properties of Organic Rich

Zhan, J.. , Seetahal, S.. , Cao, J.. , Hejazi, H.. , Alexander, D.. , He, R.. , Zhang, K.. , and Z.. Chen. "An Integrated Method to Characterize Shale Gas Reservoir Performance." Paper presented at the SPE Trinidad and Tobago Section Energy Resources Conference, Port of Spain, Trinidad and Tobago, June 2016. doi: https://doi.org/10.2118/180884-MS

APPENDIX

APPENDIX A: The Individual compressibility impacts on the cumulative gas production

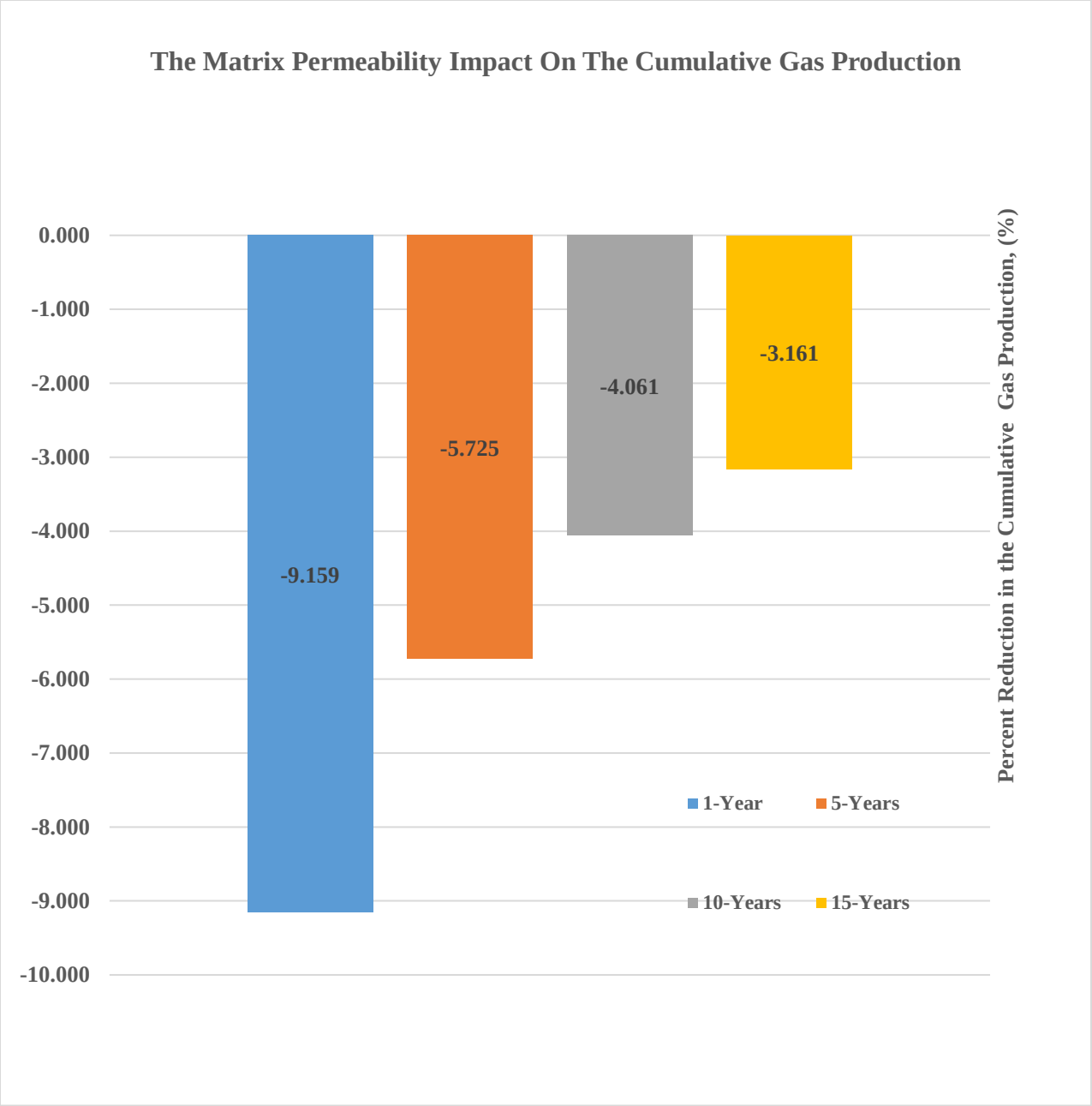

Figure 78: The impact of the matrix permeability on the cumulative gas production

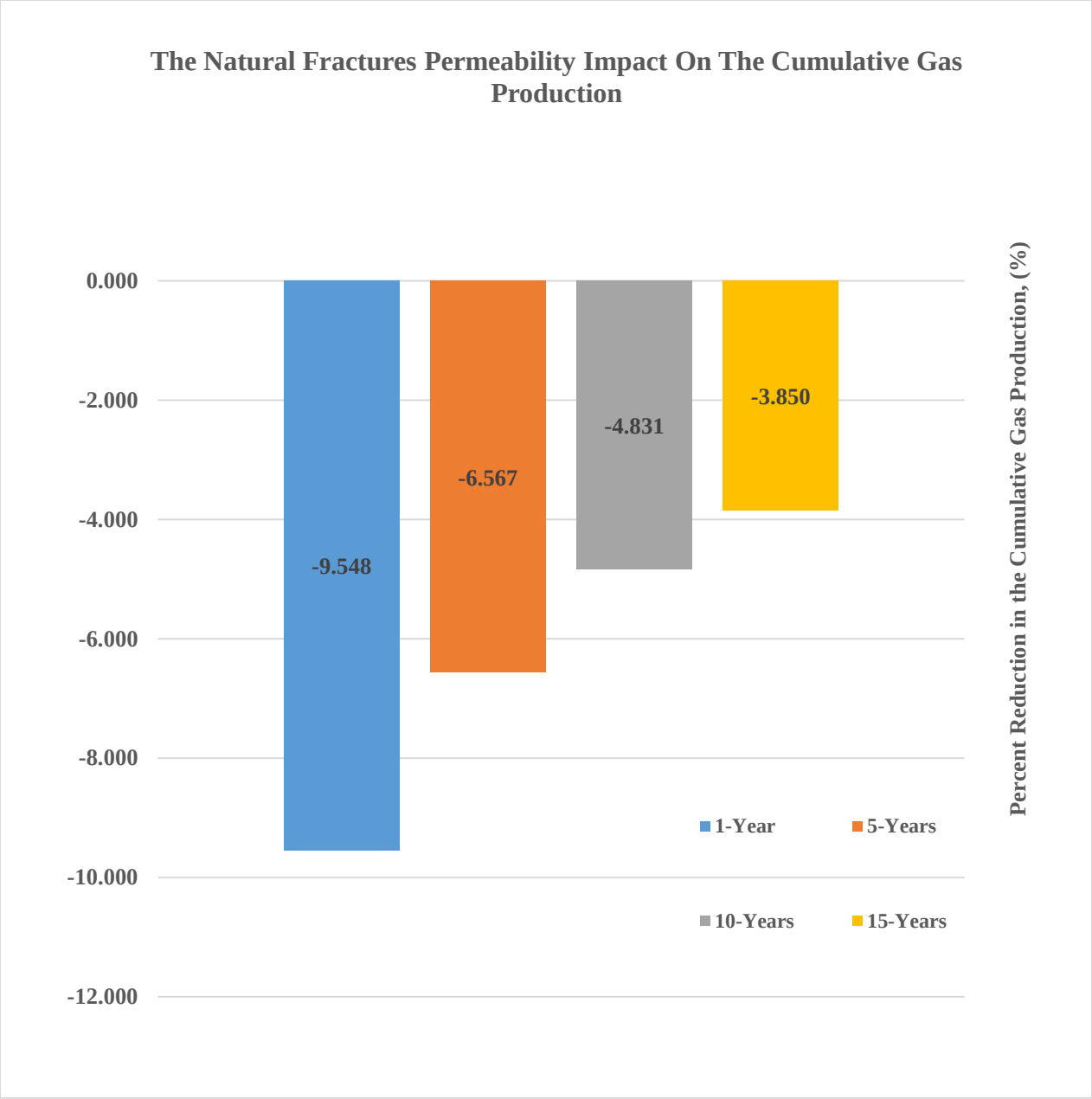

Figure 79: The impact of the natural fractures (fissure) permeability on the cumulative gas production for well MIP-6H

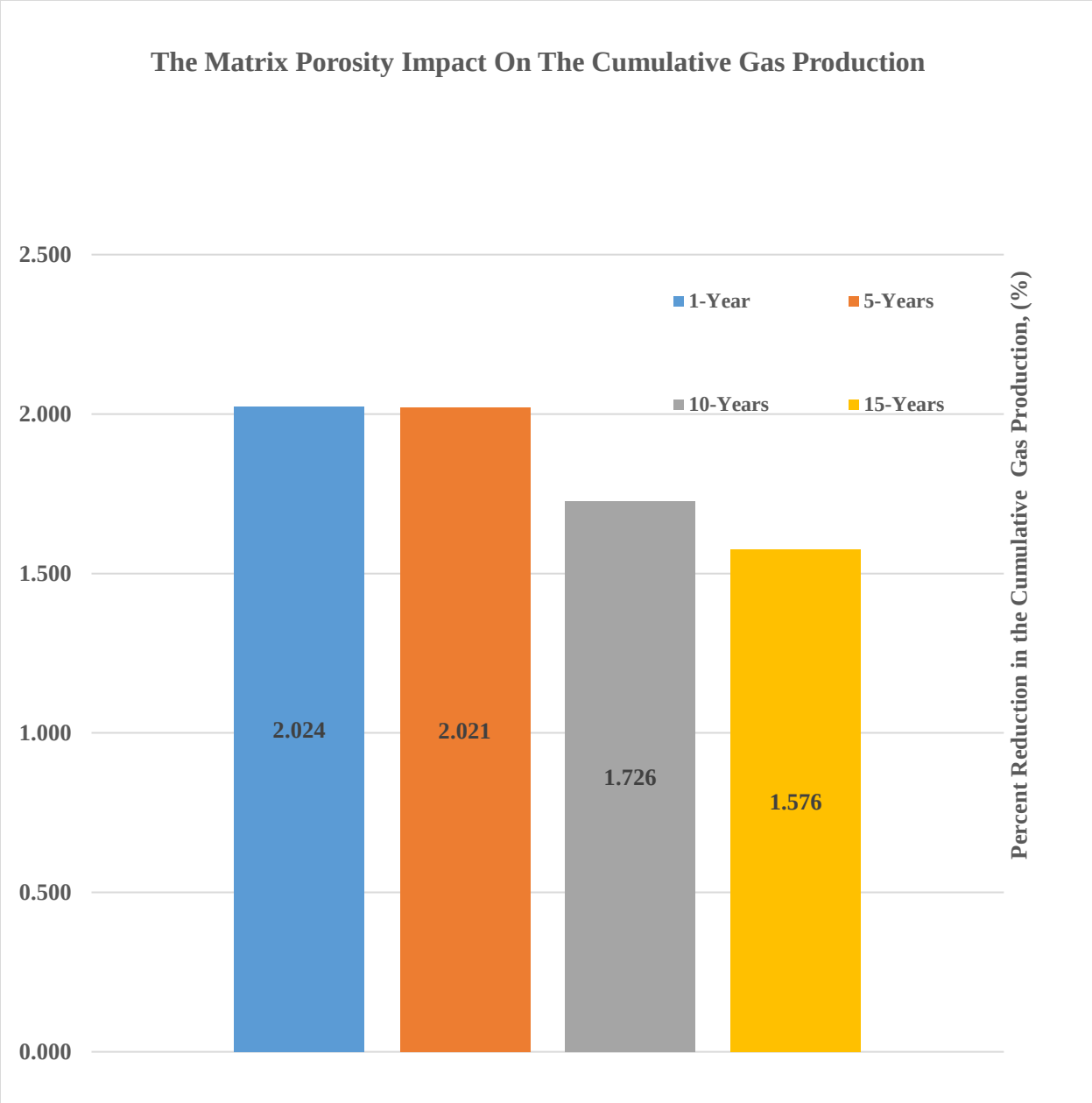

Figure 80: The impact of the matrix porosity on the cumulative gas production for well MIP-6H

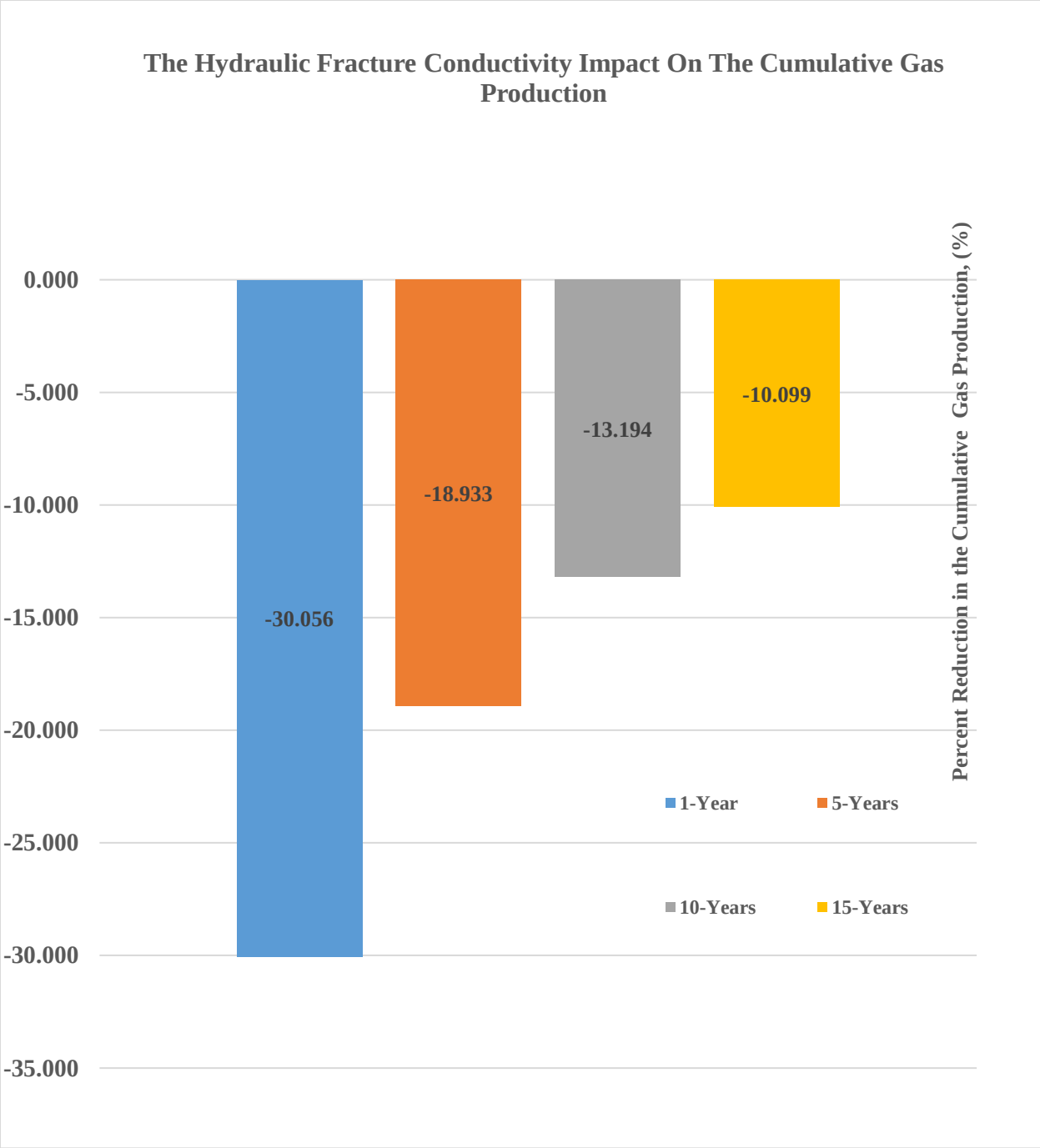

Figure 81: The impact of the hydraulic fracture conductivity on the cumulative gas production for well MIP-6H